Testing and Analysis of Building-Integrated Photovoltaics in Southern Norway

SIMEN OMMUNDSEN

SUPERVISORS
Anne Gerd Imenes
Basant Raj Paudyal
Muhammad Bilal

University of Agder, 2019
Faculty of Engineering and Science
Department of Engineering Science

Abstract

The goal of this thesis is to test and analyse building-integrated photovoltaics roof tiles in Grimstad, Norway. This is done to figure out if the BIPV roof tiles can compete with today's PV technology. The different analysis performed includes performance analysis, temperature analysis, and four economic cases. In order to get as realistic results as possible, an experimental setup is built, including a demo roof, where 16 BIPV modules are mounted. To analyse the performance of the modules efficiency, performance ratio and specific yield are calculated, as well as an I-V curve analysis is done. The results are then compared to today's PV technology. The temperature analysis is done by using data from Pt100 temperature sensors, along with an IR camera. It is found that the BIPV roof tiles still has room for improvement both in regards to performance and price.

Individual/group Mandatory Declaration

1.	I/We hereby declare that my/our report is my/our own work and that I/We have not used any other sources or have received any other help than mentioned in the report.	☒
2.	I/we further declare that this report: - has not been used for another exam at another department/university/university college in Norway or abroad; - does not refer to the work of others without it being stated; - does not refer to own previous work without it being stated; - have all the references given in the literature list; - is not a copy, duplicate or copy of another's work or manuscript.	☒
3.	I/we am/are aware that violation of the above is regarded as cheating and may result in cancellation of exams and exclusion from universities and colleges in Norway, see Universitets- og høgskoleloven §§4-7 og 4-8 og Forskrift om eksamen §§ 31.	☒
4.	I/we am/are aware that all submitted reports may be checked for plagiarism.	☒
5.	I/we am/are aware that the University of Agder will deal with all cases where there is suspicion of cheating according to the university's guidelines for dealing with cases of cheating.	☒
6.	I/we have incorporated the rules and guidelines in the use of sources and references on the library's web pages.	☒

Publishing Agreement

Authorization for electronic publishing of the report.

Author(s) have copyrights of the report. This means, among other things, the exclusive right to make the work available to the general public (Åndsverkloven. §2).

All theses that fulfill the criteria will be registered and published in Brage Aura and on UiA's web pages with author's approval.

Reports that are not public or are confidential will not be published.

I hereby give the University of Agder a free right to

make the task available for electronic publishing: ☐JA ☒NEI

Is the report confidential? ☐JA ☒NEI

(confidential agreement must be completed and signed by the Head of the Department)

- If yes:

Can the report be published when the confidentiality period is over? ☐JA ☐NEI

Is the task except for public disclosure? ☐JA ☐NEI

(contains confidential information. see Offl. §13/Fvl. §13)

Contents

List of Figures

List of Tables

1 Introduction

The sun is the source of all life on earth. The amount of energy that hits the earth's surface every year is several thousands times larger than the worlds yearly energy consumption. This energy has been harvested and used for thousands of years. In recent years, the focus on greenhouse gasses has increased as well as the global energy demand is growing rapidly. This has lead to an explosive growth in the renewable energy sector. renewable-based electricity generation increased by 4% from 2018 to 2019 and is now producing 25% of the global power [2]. Solar PV is the renewable energy source with the fastest growth in 2018 and has doubled the installed capacity worldwide since 2015. In Norway, the PV market is still in the early stages but has been growing fast the last years. At the start of 2018, there was an installed capacity of 35 MW_p in Norway, where 2/3 were installed in the last 2 years [3]. One thing that makes Norway stand out from the rest of the world is that most of the new installations are roof-based. In most cases, the PV modules are placed on top of the roof. This is called Building Attached Photovoltaics (BAPV). By introducing Building Integrated Photovoltaics (BIPV), one is able to have a power source that also acts as a part of the building. This leads to a reduction in building materials for buildings with PV. Not only can the BIPV modules reduce costs but it also offers a more aesthetically pleasing look than traditional BAPV modules. According to [4], out of the 60 GW of PV that was shipped in 2017, less than 2% were BIPV. This shows that BIPV is both a fairly new concept, but also new to the PV market. Groups like BIPVNO and PVSITES has been started to develop robust BIPV solutions and to drive BIPV technology to a larger market. To do so, the product that is already available on the market needs testing to see if they comply with the standards and regulations made for BIPV.

1.1 Problem Definition

The goal of this thesis is to install, test and analyze BIPV modules on an existing testing site on the rooftop of the University of Agder in Grimstad. The BIPV modules are made in Germany and distributed by a local Norwegian company called Sun-Net. The modules used in this thesis are BIPV roof tiles with monocrystalline silicon solar cells.

One aspect that is a concern when using BIPV modules is the module temperature. Most BIPV modules do not get the same natural cooling as BAPV modules and can thereby have a significantly higher module temperature. This will be investigated using four Pt100 temperature sensors to measure the module temperature on each of the rows of modules. An IR camera will also be used to analyze the temperature distribution in the string and to validate the data from the temperature sensors.

Last, an economic case will be presented. The base of the case is the building of a new roof with BIPV modules installed. LCOE calculations and down-payment time will be calculated for each of the cases. The data used in the cases are from Sun-Net both for system prices and estimated yearly production for each system.

The main objective of the thesis is to analyze the relatively new technology to see if it is an acceptable solution compared to today's PV technology. The research questions to be answered are: how do these new BIPV modules compare with today's PV technology and how will the temperature influence the power production. So to summarize, the goal of this thesis is:

- Build a demo roof to simulate realistic conditions for the BIPV modules.
- Analyze performance using logged data and I-V tracing.
- Investigate the temperature distribution in the modules and string of modules.
- Calculate LCOE and down payment time for four different system sizes.

1.2 Thesis Structure

The structure of this thesis starts with an introduction to PV in Norway, the research problem and thesis structure in Chapter 1, followed by General theory about solar radiation, solar cells, integration of photovoltaics and background for performance evaluation in Chapter 2. Next, in Chapter 3 the methodology is presented where the building of the demo roof, workings of the experimental setup, how the performance analysis and economic cases were done is explained. Chapter 4 presents the results for each of the different sections from the method chapter followed by chapter 5 where each of the sections is discussed. Finally, chapter 6 is the conclusion of the problems asked in the thesis and recommendations for further work.

2 Theoretical Background

2.1 Solar Radiation

The radiation from the sun is constantly hitting the earth's surface, but the intensity is varying. There are several factors which cause this variation. The first factor is the earth's atmosphere. Gasses, dust, and aerosols in the atmosphere absorb, scatters and reflects radiation from the sun and thereby reducing the amount of energy that hits the earth's surface by 30 % on a clear day [5].

2.1.1 The Radiation Components

The radiation from the sun can be divided into different components. First we have direct radiation. Direct radiation is the radiation that hits the earth's surface on clear days. The next component is diffuse radiation. This is everything that is not coming directly from the sun. This can be scattered radiation from clouds and reflected sunlight. These components is illustrated in Fig. 1.

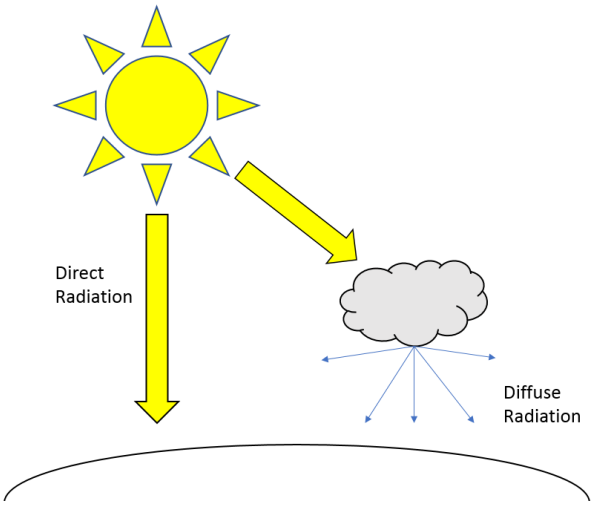

Figure 1: Shows the difference between direct and diffuse radiation

2.1.2 Air Mass

Geographical location and inclination is also a decisive factor. The shorter distance the light has to travel, the more radiation hits the earth. The length that the light has to travel can be approximated by using equation 1 . Equation 1 is an approximation where θ_z is the angle between the sun and a point directly above.

$$AM = 1/cos\theta_z \tag{1}$$

If the sun is directly above, the air mass is 1 (AM1). AM1.5 is commonly used as a standard for PV work, this is equal to an angle of 48.2°. The spectral power density of different air

masses is shown in Fig. 2, where a 5778K blackbody is a approximation of the radiation from the sun. AM0 is the air mass outside of the atmosphere. Here the radiation is not varying, and when integrating over the curve in Fig. 2, we get a spectral power density of 1366.1 W/m^2. This number is referred to as the solar constant [6]. The shape of these curves is due to absorption by the gases listed in Fig. 2.

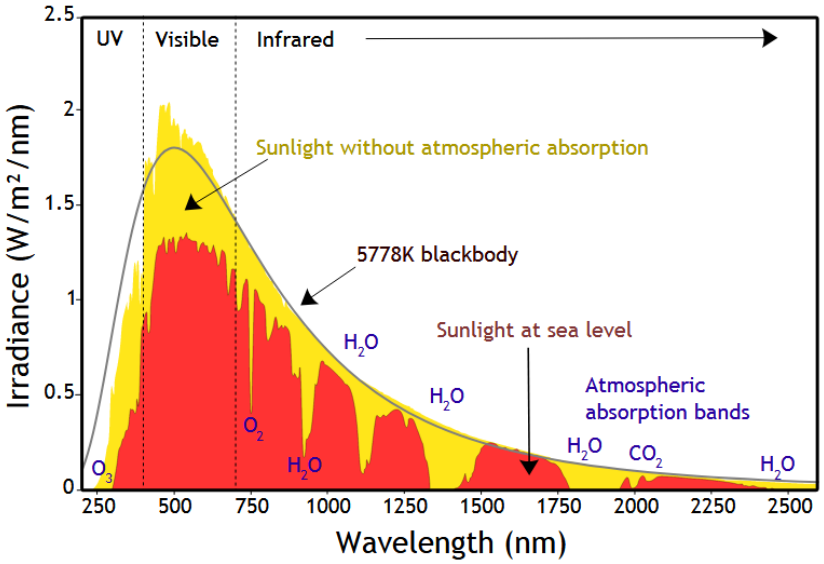

Figure 2: Spectral power density for different wavelengths [7]

2.1.3 Solar angles

PV modules are often mounted at a fixed location and angle. In order to absorb as much of the radiation from the sun as possible, the PV module needs to be perpendicular to the sunrays. This means that the tilt angle of the PV module is important for power production. Therefore it is important to know the movement of the sun at a given location. This is where the elevation angle is important. The elevation angle is the angular height of the sun in the sky measured from a horizontal surface. When the sun starts to rise it is 0°and 90°when the sun is directly above. The maximum elevation angle is at solar noon and depends on the geographical location and declination angle. The declination angle changes throughout the year.

2.2 Photovoltaic modules

PV modules convert radiation from the sun into electric current. This is known as the photovoltaic effect. When sunlight hits the solar cell, an electron is released inside of the cell material. This electron is then lifted up into the conduction band where it can move freely. By connecting it to an external circuit, the electrons can move through the loop and thereby create an electrical current and power. The power will vary with the intensity of the irradiance.

2.2.1 Cell material

The most common material used in PV modules is silicon. There are several reasons for this, but the most important is that silicon is a semiconductor material. A semiconductor only conducts current under certain conditions. By adding impurities into the semiconductor material one can change its characteristics. This is why this type of material are widely used in the world of electronics. Pure silicon has a stable structure at low temperatures. This is because of the bonding between the silicon atoms. Silicon is in group IV in the periodic table. This means that each atom has 4 electrons in the outer shell. By sharing these with 4 surrounding atoms, silicon forms a covalent bond, This is illustrated in Fig. 3.

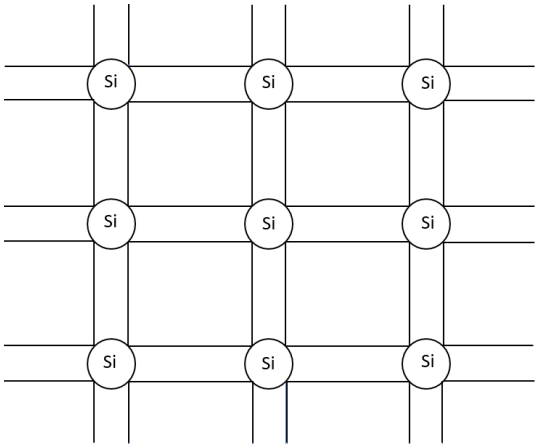

Figure 3: Shows an illustration of the bond model

In order to explain how the electrons move, the band model is used. When the electrons form covalent bonds, they have energy corresponding to the *valence band*. If the electrons get enough energy, they can break the bonds shown in Fig. 4 and move up to the *conduction band*. Here the electrons can move freely and can be used in an external circuit. Between the valence and conduction band is the band gap. The electrons need a certain amount of energy to get from the low energy valence band and up to the conduction band. For silicon, the amount of energy needed at room temperature is 1.11 eV [8]. The band model is shown in Fig. 4. When an electron leaves the valence band, a hole is created. To make it easier, this can be seen as a positively charged particle. When a hole is created, a new electron can fill

the hole and thereby creating a new hole in its place and so on. This combination of electrons and holes is called carriers.

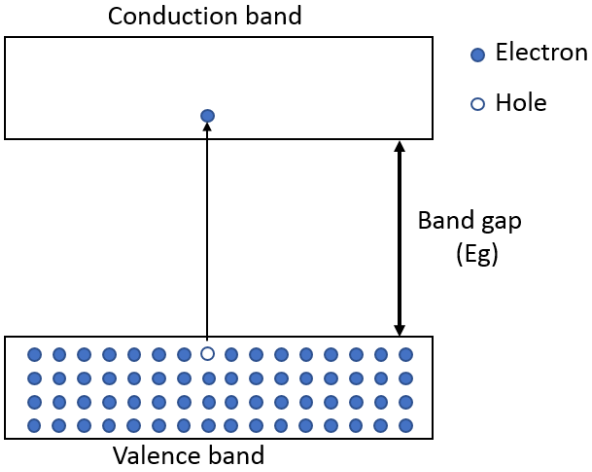

Figure 4: Shows an illustration of the band model

To increase the number of carriers in a semiconductor material, doping is introduced. Doping is adding impurities into the semiconductor material and thereby increasing the number of free electrons and holes. Elements from group III will give more holes and elements from group V gives more electrons [9]. This is called p-type and n-type semiconductors respectively. When combining these two types of semiconductors, we get a p-n junction [10]. This doping increases the number of carriers in the material and thereby creating an electric field. These materials can come in different structures. Each structure has its own characteristics. The most common type of structure used is crystalline and amorphous silicon, but also materials like Cadmium telluride (CdTe) and Copper indium gallium selenide (CIGS) are used [11].

Crystalline silicon

What characterizes crystalline silicon is that the atoms are in a crystal structure. For single-crystalline silicon (c-Si), the structure is one single crystal with every atom lying in perfect order. This type of structure has the highest efficiency but the process of making c-Si is slow and expensive [9]. Therefor multi-crystalline (m-Si) and polycrystalline silicon is introduced. The process of making these types of cell structure is less challenging and therefore also cheaper than for monocrystalline silicon. These structures consist of grains instead of one single crystal. The grain boundaries reduce the efficiency of the cell. The difference between multi- and polycrystalline silicon is the grain size. Cells with grains smaller than 1 mm are defined as polycrystalline while the grain size for multi-crystalline is less than 10 cm [12]. The difference between monocrystalline and poly/multi-crystalline is shown in Fig. 5

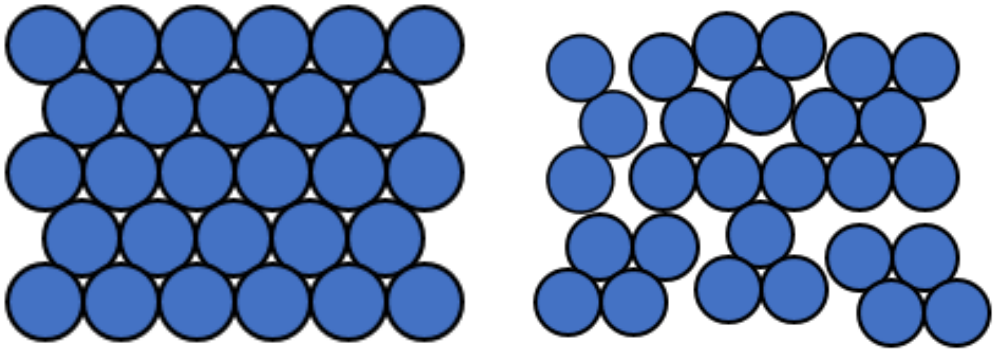

(a) Mono-crystalline silicon (b) Multi-crystalline silicon

Figure 5: Shows the differnce between mono- and multi-crystalline cell structure for silicon

Amorphous silicon

In amorphous silicon (a-Si), there is no long-range arrangement in the structure as there is in crystalline silicon. This results in a less delicate production process and even cheaper production costs than for multi- and polycrystalline silicon. When the structure has no long-range arrangements, some of the silicon atoms will have *dangling* bonds. What this means is that not all of the silicon atoms will have bonds with four other atoms. This is illustrated in Fig. 6.

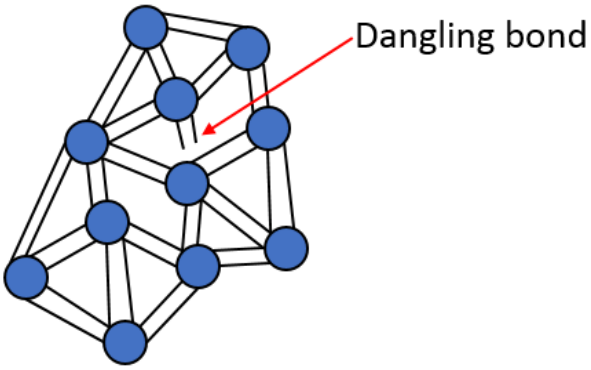

Figure 6: Shows Amorphous structure

Before a-Si can be used in PV modules, these dangling bonds need to be "removed". In order to do so, the material is saturated with 5-10% hydrogen atoms, and thereby improve the quality of the a-Si. One of the main advantages of a-Si is that the absorption coefficient is much higher than for mono- and multi-crystalline silicon. This means that a-Si cells are much thinner than mono- and multi-crystalline cells. In fact, the a-Si cells are only a few microns thick whereas crystalline silicon can vary between 200-500 μm. This is why a-Si is often used in thin film technologies. One of the main disadvantages of a-Si is that efficiency is lower than for crystalline silicon and also a higher degradation rate [13].

2.2.2 Cell design and module structure

In the previous chapters, the basics of PV technology has been explained. This chapter will focus on the actual cell and module design. The first and most important aspect is to collect the current generated by the solar cell. To do so, metal contacts are placed on top of the module. There are two types of metal contacts, *fingers* and *busbars*. These can be seen in Fig. 7.

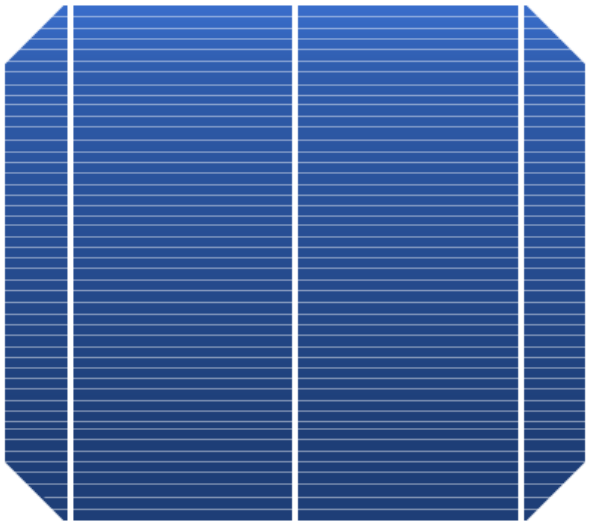

Figure 7: Shows a typical solar cell

The three vertical lines are busbars, and the horizontal lines are fingers. The fingers transfer current from the cell to the busbars. The busbars then transfer the current to a junction box or wires. The goal when designing the top contacts is to optimize current collection vs losses. These cells are then connected together in series and parallel to form a PV module. As mentioned in the previous chapters, PV modules are used in all kinds of environments. Therefore a safe housing is needed to protect the cells from weather and external damage. Fig. 8 shows a typical module structure. The top layer has to bee some form of transparent protection covers such as low-iron glass, or plastics. One of the most important characteristics for the front cover is that it has high transmission in the waveband between 350 and 1200 nm [9] as this is the wavelength that silicon can absorb.

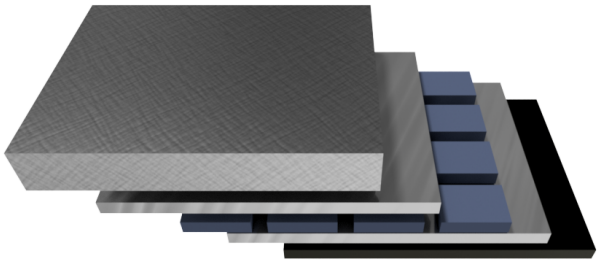

Figure 8: Shows a typical module structure

The next layer works as a protection against moisture and condensation between the glass and PV cells. The way that this layer is applied is by adhesion. The most common material used for this layer is ethylene vinylacetate copolymer (EVA) [14]. The last layer is the back layer. The important characteristics of the back sheet material are low thermal resistance and preventing water and water vapor entering the module. One of the most common types of material for this purpose is polyvinyl fluoride (Tedlar) [15]. A junction box on the back of the module provides electrical connections. The last part of the module is the frame which holds all the other parts together.

2.2.3 Interconnection of PV

The number of cells in series and parallel determines the amount of voltage and current module outputs. One silicon cell has a maximum voltage of approximately 0.6 V, and at AM1.5, optimal tilt and peak sunlight (100mW/cm^2) a current of 30mA/cm^2 [9]. Series connected cells increase the voltage and cells connected in parallel increase the current.

2.3 Solar Cell characteristics

A silicon solar cell can be described as a diode formed by a p-n junction. The circuit in Fig. 9 is called the one-diode model and can be used as an equivalent circuit of a silicon solar cell. The circuit consists of two parasitic resistances, a series resistance, R_s and shunt resistance in parallel R_{sh} with a diode. I_D is the current going through the diode and I_L is the light-generated current [9].

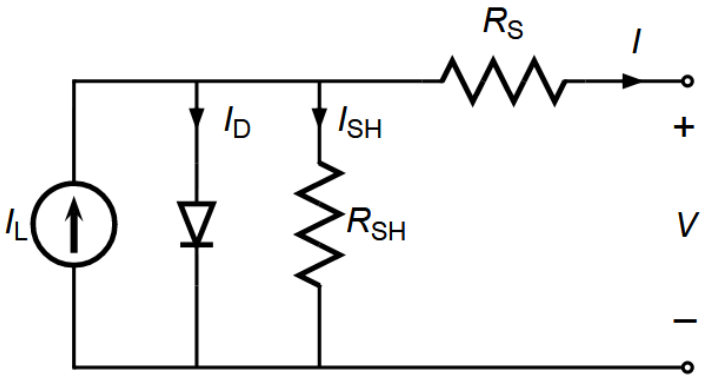

Figure 9: Shows the equivalent circuit of a solar cell [16]

Eq. 2 is derived from the circuit in Fig. 9 and can be used to describe the I-V curve and the effect of the two parasitic resistors.

$$I = I_L - I_0 \left[exp\left(\frac{V + IR_s}{nkT/q} \right) - 1 \right] - \frac{V + IR_s}{R_{sh}} \tag{2}$$

In Eq.2, I is the cell current, I_L is the light-generated current, I_0 is the dark saturation current, V is the cell potential, n is the ideality factor, k is the Boltzmann's constant, and q is the electron charge. The I-V curve of a solar cell or module can tell a lot about its characteristics. Fig. 10 shows a typical I-V and P-V curve. A P-V curve is the power voltage characteristics of a solar cell. Several describing factors can be derived from the I-V curve, such as the open circuit voltage (V_{oc}), short circuit current (I_{sc}) and the voltage (V_{mp}) and current (I_{mp}) for the maximum power point P_{mp}.

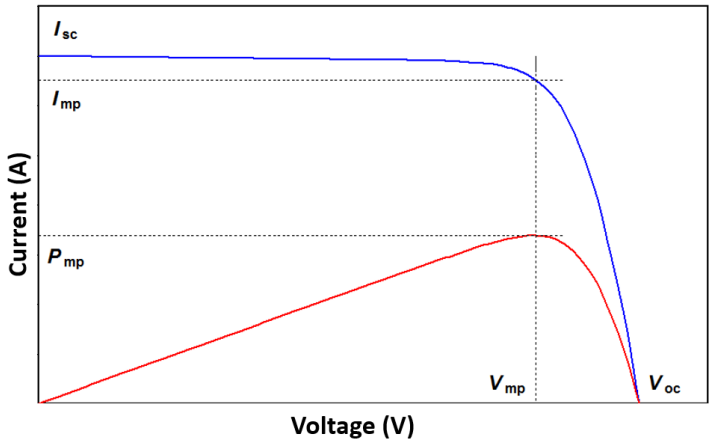

Figure 10: I-V curve for a silicon solar cell [17]

Fill factor (FF) is often used to measure the quality of a silicon solar cell. Ideally, the area under the I-V curve should be a perfect rectangle, the fill factor describes how close the I-V curve comes to this perfect rectangle [18]. The equation used to calculate the fill factor is presented in Eq. 3.

$$FF = \frac{V_{mpp} I_{mpp}}{V_{oc} I_{sc}} \tag{3}$$

When current is flowing through the internal resistance of the cell, the efficiency will be reduced. Ideally, R_{sh} from Fig. 9 should be infinitely large to prevent current passing through, while R_s should be zero to reduce the voltage drop before the load. R_s can, for example, be resistance in soldering bonds or in the output cables of the junction box. R_{sh} comes from impurities and damage to the crystal structure near the p-n junction [19]. The effect of series and shunt resistance in a solar cell can be seen in Fig. 11 .

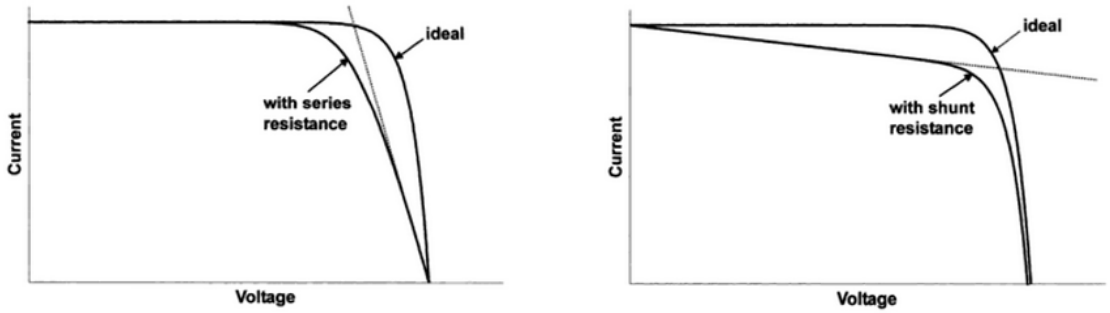

(a) Effect of series resistance [20]

(b) Effect of shunt resistance [20]

Figure 11: Shows the effect of parasitic resistance in a solar cell

2.3.1 Temperature effect on solar cells

One thing that is a disadvantage of using semiconductor materials is that is sensitive to temperature. A rise in temperature will result reduce the band gap and thereby affect several of the PV parameters. When the band gap is decreased, less energy is needed to free the electrons and a higher concentration of carriers in the conduction band. This results in a slight increase in short circuit current since more electrons now can move freely in the conduction band. While the short circuit current rises, the open circuit voltage decreases significantly. The reason for a drop in open circuit voltage is the rise in dark saturation current. The dark saturation current increases with temperature. The reason for this is that it is dependent on the concentration of intrinsic carrier. This will have the opposite effect at lower temperatures. The effect of temperature can easily be seen on the IV-curve of a PV module [21]. An example of this can be seen in Fig. 12.

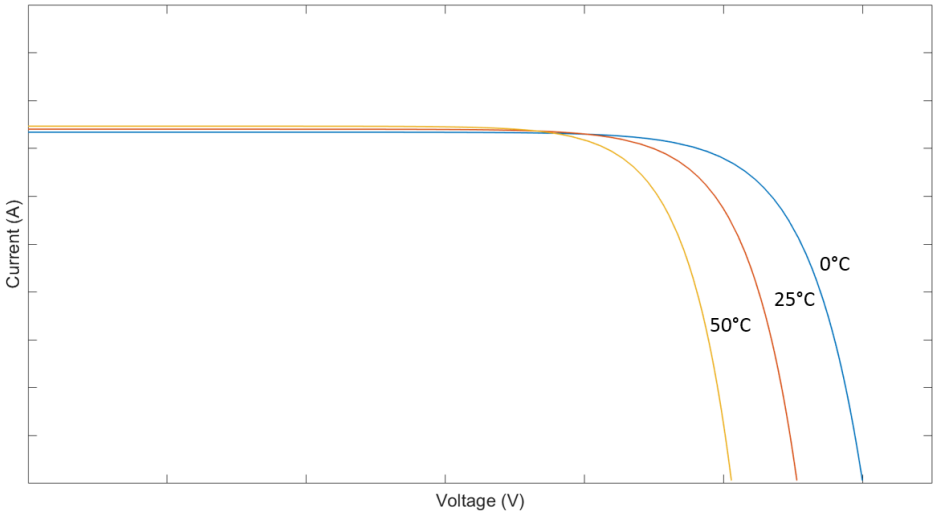

Figure 12: Shows the effect of temperature on the IV-curve

Here we can see that the decrease in V_{oc} is considerably larger than the rise in I_{sc}, this results in a drop in power as the temperature rises. This temperature coefficient is often listed in the datasheet of PV modules with the symbol γ for power and the unit is often %/°C. The decrease in power will also affect the efficiency of the PV module. Equation 4 shows how the efficiency will vary with change in temperature, where η_{ref} is module efficiency at STC and T_c is cell temperature.

$$\eta_T = \eta_{ref} \frac{(1 + \gamma(T_c - 25°C)}{100} \tag{4}$$

2.4 Integration of photovoltaics

The previous chapters has explained the working principals of solar cells. This next chapter will focus on the integration of photovoltaics into building. Building integrated photovoltaics (BIPV) are solar cell modules that are integrated into a building. The advantage of this concept is that the solar cells are not only just a source of energy but also replaces the traditional building materials and thereby reducing the installation costs. The advantage of BIPV compared to traditional PV systems is that a traditional PV system is placed on top of or above already existing building structures and acts as a building attached photovoltaic system (BAPV), while BIPV is a part of the construction. This leads to a cost reduction in building materials compared to BAPV systems and at the same time reduce the electricity bill. When designing BIPV, several aspects have to be considered. The product has to meet the requirements of the building material it is replacing. One factor that affects the power production of PV modules is temperature, so an air gap between the module and building is needed for good air flow to ensure ventilation and cooling. Inclination and direction also need to be considered both in regard to the building structure and the energy production of the photovoltaic (PV) module. When talking about BIPV products, there are often two big aspects to consider, aesthetics vs power production. This is because not only does a BIPV module produce power, but it also has the ability to blend naturally in with the building and can, therefore, give a more appealing facade than BAPV products. BIPV products can come in all shapes and sizes. Some come in the form of roof tiles while others are modules that is made to replace building envelope materials. One example of a BIPV product is shown in Fig. 13. Here we see solar cells integrated into roof tiles combined with regular roof tiles.

Figure 13: Shows a roof with both regular and PV roof tiles [22]

2.5 PV/BIPV standards

Since there are so many different manufacturers and technologies in the PV world, there is a need for a standard in regards to testing. This is to make a comparison of modules easier and to have an accurate test despite different test locations and external factors affecting the modules. The standard is defined by IEC 60891 and is called standard test conditions (STC). STC is an industrial standard for PV worldwide and is used to determine the system output performance. The parameters listed in datasheets such as efficiency, maximum power point, open circuit voltage, short circuit current and temperature coefficient are all tested under STC. However, when modules are mounted outside, both the module temperature and irradiance will vary. Since both temperature and irradiance are important for the output performance, it is important to look at the expected operating conditions for PV modules. Nominal Operating Cell Temperature (NOCT) is defined as the temperature a module can reach under the conditions listed in table 1 and gives a more realistic condition for testing than STC.

Table 1: Shows STC and NOCT [1]

STC	NOCT
• 1000 W/m^2	• 800 W/m^2
• 25°C cell temperature	• Ambient air temperature of 20°C
• AM 1.5	• Windspeed 1 m/s

There have been some difficulties when trying to determine test methods and international standards for BIPV products. This is because the modules have to comply with both the international standards and test methods that are already established for PV systems and also have the same properties and functionalities as the material that the BIPV product is replacing. The standards and regulations regarding the building material that is being replaced can also vary from country to country. IEA PVPS task 15 has been and is currently working on improving these standards to ensure high quality products on the market. The tests and standards for PV systems are already well established, and according to literature reviews the most common PV modules used is IEC 61215 "Crystalline silicon terrestrial photovoltaic modules-design qualification and type approval" [23], IEC 61646 "Thin-film terrestrial photovoltaic (PV) module-design qualification and type approval" [24], IEC 61730-1 "Photovoltaic module safety qualification-part-1: requirements for construction" [25], IEC 61730-2 "Photovoltaic module safety qualification-part-2: requirements for construction" [26], UL 1703 "UL standard for safety flat-plate photovoltaic modules and panels" [27], EN 50583:2016 "Photovoltaics in buildings" [28]. The last standard is the one that is most relevant for this thesis and will be looked into more thoroughly.

2.5.1 EN 50583:2016 - Photovoltaics in buildings

The EN 50583:2016 is divided into two separate parts, EN 50583-1 "Photovoltaics in buildings – Part 1: BIPV modules" and EN 50583-2 "Photovoltaics in buildings – Part 2: BIPV systems". The requirements for these standards is most often dependent on the country of application because of different regulations. Therefore a manufacturer of BIPV products may have to follow several regulations and standards. The first part applies to BIPV modules used as building materials and focuses on the properties of the modules compared to the product that is going to be replaced in regards to the Construction Product Regulation CPR 305/2011 and Low Voltage Directive (LVD) 2006/95/EC. By definition of EN 50583-1, "BIPV modules are considered to be building-integrated if the PV modules form a construction product providing a function as defined in CPR 305/2011. Thus, the BIPV module is a prerequisite for the integrity of the building's functionality" [28]. Because the requirements are from both the construction and electrical sector, EN 50583 is divided into three levels to make it easier to define the different requirements. The first level states that "the electrical requirements are relevant for all kinds of BIPV modules regardless of their technology and composition" but the building related requirements depends whether the product contains glass or not regardless the technology. The second level divides the products into whether the product contains glass or not regardless of where in the building the product is placed. The regulations in level three are only for products containing glass and add additional requirements relative to where the modules are placed on the building. The different locations for level three are presented in Fig. 14.

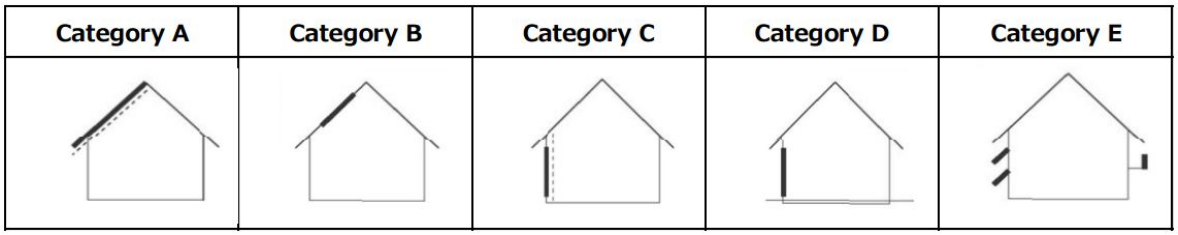

Figure 14: Different locations for level three regulations [28].

Part 2 of EN 50583:2016 describes PV systems instead of modules. As long as the modules used in the system meets the requirements of part 1, the PV system is considered building integrated. Part 2 follows the same levels and regulations as part 1 [28].

2.6 Performance evaluation

When evaluating the performance of a PV system there are several parameters that can be considered, such as performance ratio, efficiency and specific yield. The parameters that are important to evaluate is the power production of the system and irradiance, along with environmental factors such as temperature in particular. The efficiency tells us how much of the solar radiation is converted into electrical energy for a given area.

$$\eta_{sys} = \frac{P}{G * A} \tag{5}$$

Equation 5 shows the calculation of efficiency, where P is the output power of the PV system most commonly AC, G is the irradiance and A is the system area. The problem with comparing different system efficiencies and specific yield is that external factors such as module temperature and geographical location will affect the result. Because of this, other methods have been developed to make a comparison of different PV systems easier. A number of factors will affect the performance of a PV system. In [29], it is stated that factors such as temperature, dirt and dust, mismatch and wiring losses and DC to AC conversion losses is the main causes of reduced performance of a PV system.

2.6.1 Performance ratio

The performance ratio (PR) is a way of evaluating the quality of a PV system and has become one of the most important variables in regards to performance evaluation. The PR is a unitless number between zero and one, and it is the relation between theoretical and actual energy output of a PV system. According to [30], should a good PV system has a PR above 0.8. Equation 6 shows how the PR is calculated where Y_F is the final yield and Y_R is the reference yield [18].

$$PR = \frac{Y_f}{Y_r} = \frac{\text{Actual power output of PV system (kWh)}}{\text{Theoretical output of PV system (kWh)}} \tag{6}$$

The final yield is the energy output of a PV system divided by the nominal power from the datasheet [31]. This is shown in equation 7, where E is net energy output and P_o is the nominal power.

$$Y_f = \frac{E \text{ (kWh)}}{P_o \text{ (kW)}} \tag{7}$$

The reference yield (Y_r) describes the theoretical energy output of a PV system and is calculated by taking the total in-plane irradiance divided by the reference irradiance of the PV. At STC the reference irradiance is 1000 W/m^2. The reference yield is calculated by using equation 8, where H is the total in-plane irradiance and G is the reference irradiance.

$$Y_r = \frac{H \text{ (kWh/m}^2\text{)}}{G \text{ (kW/m}^2\text{)}} \tag{8}$$

Fig. 15 is a block schematic of a grid-connected PV system made by the IEA [30]. It describes the losses and factors affecting the energy output from the system. Here EA is the DC energy

from the array, EIO is the AC energy after the inverter and ETU is the energy fed into the grid and Ls is the difference between array yield and final yield.

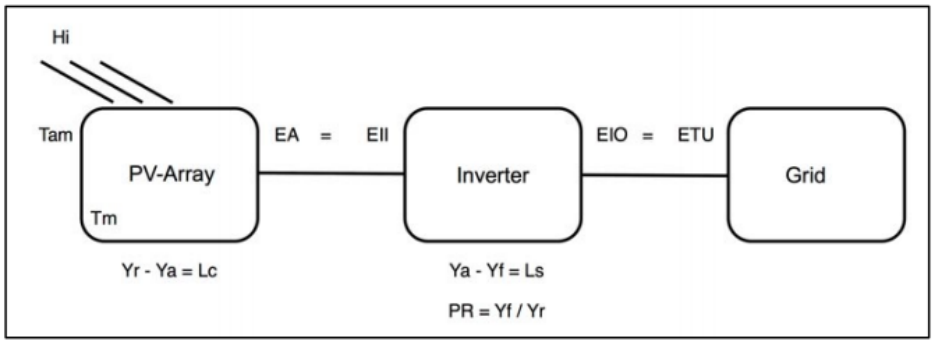

Figure 15: Block schematic for a grid-connected PV system [30]

Also, the module and ambient temperature are included, as this has a significant impact on the power production of a PV module. Both reference yield and final yield has been explained previously, but in this model also the array yield is listed. This parameter is also used in [29] to describe the performance of a PV array. The difference between array performance and system performance is that this is based on the array yield instead of the system yield. Equation 9 describes the performance ratio of an array, where Y_A is the array yield and Y_r is the reference yield.

$$PR_A = \frac{Y_A}{Y_r} \tag{9}$$

The array yield is related to the DC power of the system instead of the AC power. The array yield is presented in equation 10, where E_{DC} is the array output energy and P_o is nominal power.

$$Y_A = \frac{E_{DC}}{P_o} \tag{10}$$

2.6.2 Temperature corrected performance ratio

In [30] and [29], a way of correcting the performance ratio in regards to temperature is presented. This is done by looking at the difference between STC temperature and actual cell temperature and using the temperature coefficient of the solar panel. In order to do a temperature correction, equation 11 is used. This equation uses the difference between module temperature (T_{mc}) and STC temperature of 25°C. This temperature difference is then multiplied with the temperature coefficient of the module (γ). This correction value will be negative when the module temperature is higher than 25°C and vice versa since the temperature coefficient is negative in most cases.

$$T_{corr} = (T_{mc} - 25°C) * \gamma \tag{11}$$

This correction factor is then used in equation 12 together with the performance ratio at STC ($PR_{A,STC}$).

$$PR_{A,T_{corr}} = PR_{A,STC}(1 + T_{corr}) \tag{12}$$

3 Method

This chapter will focus on the methods used and practical work done in this thesis. The chapter is divided into three subchapters, one for the scientific method, one for the experimental setup and one with a focus on the economic aspect of this thesis.

3.1 Experimental Setup

The tested PV modules are installed in an 'open-rack' configuration on a flat roof. The test site is located in the south of Norway, Grimstad, at latitude 58°20°N and altitude about 60 m above sea level. The orientation of the modules is almost directly South [32]. The demo roof is installed in the same rack and connected to the same logging system as used in [32]. Fig. 16 shows the installed demo-roof in the aluminum rack on top of UiA.

Figure 16: Shows the location of the experimental setup

The components used in the experimental setup is listed in table 2. Due to wear and tear over the years, some of the components had to be replaced for the experimental work in this thesis. After examining the system, it was discovered that it was necessary to replace some of the outdoor logging equipment. A new IP67 waterproof box was installed along with one new transducer and three new temperature sensors. The new IP67 box can bee seen in Fig. 17.

Table 2: Components used in the experimental setup

Component	Type
BIPV roof tiles	Solarziegel TCRDO 900
Pt100 temperature sensor	JUMO Pt100
IP66/67 waterproof box	Polycarbonate IP66/IP67
Transducer	Phoenix Contact MINI MCR-SL-TC-UI
Electronic load	TDI Dynaload MCL488
Data-acquisition board	NI PCIe-6363 NI PCIe-7851R
LabVIEW program	[32]

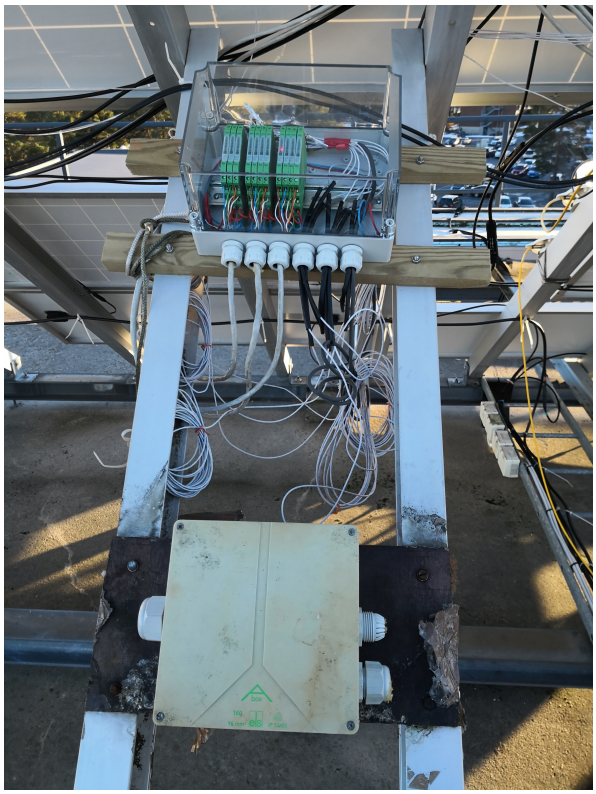

Figure 17: Shows the new transparent IP67 box compared to the old one

Temperature measurement

The sensors used for temperature measurement is class A Pt100 sensors. The class determines the error of the sensor. The error of each class is listed in Appendix. PT100 sensors are classified as Resistance Temperature Detectors (RTD). What this means is that the resistance of the sensor is change with temperature. A Pt100 sensor is made of platinum (Pt) and has a resistance of 100Ω at zero degree Celsius. The reason for choosing this type of sensor is its high accuracy and durability. The change in resistance in an RTD is approximately linear. This makes calibration easier. One of the disadvantages of RTD's is the lead resistance. The lead resistance is the added resistance in the wires connected to the sensors. Pt100 sensors often come with a 2-wire connection. The disadvantage of having only two wires is that the resistance in the wires will add to measured resistance and can thereby influence the measured value. By soldering on two extra wires, the additional resistance added by the wires will be neglected. This has been done to all the sensors used. The sensors are connected to the transducers listed in table 2. The transducers are connected to a power source and sends a small current through the sensors in order to read the values and thereby determining the temperature of the modules. The transducers can be manually programmed by switching the dual in-line package (DIP) switches on each transducer board. A DIP switch is a manual electrical switch. This determines if the output signal is a voltage or current, temperature range, and connecting method. The sensor type that has been used can be seen in Fig. 18.

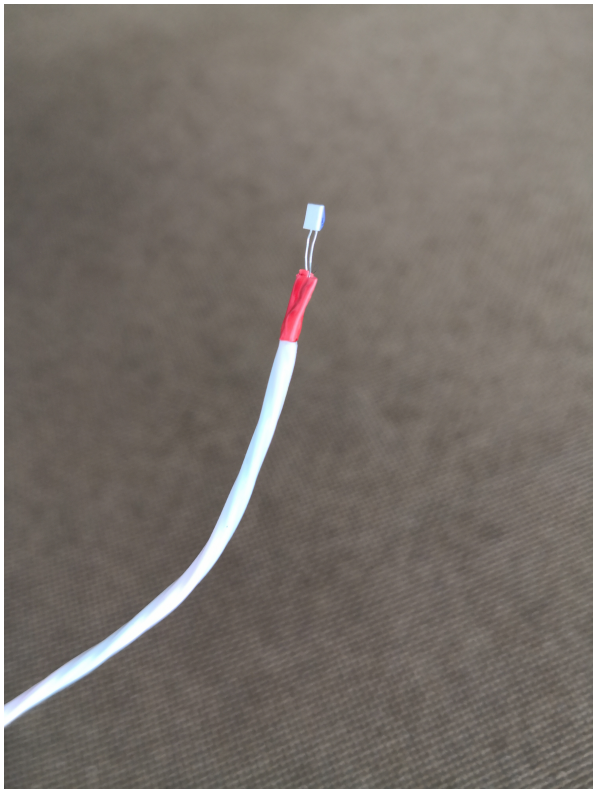

Figure 18: Shows the Pt100 temperature sensor used to measure module temperature

3.2 Demo roof

The demo roof is built to simulate the conditions of a pitched roof with a cold attic. The construction consists of 16 modules and three temperature sensors. A picture of the construction can be seen in Fig. 19. The reason for building the demo roof is to simulate realistic conditions for the BIPV roof tiles, especially in regards to temperature.

(a) Shows the demo roof

(b) Shows the demo roof from the side

Figure 19: Shows the demo roof

The construction is based on a building regulation that describes the bulding of a pitched roof with cold attic [33], and the installation manual made by Skarpnes [34]. The BIPV roof tiles are the same as the roof tiles in [34], therefor the same procedure is used. Since the construction had to be placed inside of the aluminum rack, some improvised solutions after consultation with carpenters and experts in the field were done in order to make the demo roof as realistic as possible. On the backside of the demo roof is a closed room. This room simulates the cold attic with ventilation.

Fig. 20 shows the structure beneath the roof tiles and the simulated cold attic room at the back. The back plate used is a sutaksplate. This plate functions as a wind and waterproof membrane. The plate is screwed to the aluminum rack with five screws on each side. The dimension of the vertical laths and horizontal battens used is 30x48 mm and the distance between each row of battens is 343 mm as in [34]. Each of the roof tiles is screwed into the battens for extra security. The room on the back side is built up of a sutaksplate on the backside and wall boards to seal off the sides. Building foam was used to seal any unwanted holes in the construction.

(a) Demo roof with only one row of roof tiles (b) Cold attic room

Figure 20: Shows pictures from the building process

The system parameters are listed in table 3. All the roof tiles are connected in parallel. This is due to the low current per roof tiles and to protect the logging equipment against high voltage. This type of connection also allows for carpenters to do the work since the voltage does not exceed 60 V. Four Pt100 temperature sensors are placed on the demo roof; one in the bottom middle row, one in the middle of the third row and one in the middle of the top row. The last sensor is placed in the cold attic room on the backside.

Table 3: Shows system parameters for the test setup

Solarziegel TCRDO 900		
	BIPV module	Test String
Number of modules	1	16
Voc	47 V	47 V
Isc	0.265 A	4.24 A
Pmax	9 Wp	144 Wp
Vmpp	37 V	37 V
Impp	0.245 A	3.92 A

3.2.1 BIPV modules

The tiles used in this thesis is produced and put together by Autarq in Germany while the solar cells are produced by BIG SUN Energy Technology Inc. in Taiwan. Fig 21 shows the modules used. The modules consist of 78 small monocrystalline silicon cells with an STC efficiency of 20.1%. The module design is based on Skarpnes' Domino roof tile. In order to get a more aesthetically pleasing look so-called "Dummy modules" are used. A dummy module is in this case just a regular roof tile. The modules are designed like this to make the modules blend naturally in with the dummy modules on the roof. This roof tile can be is seen in [34]. Each stone has two cables coming out of the back of modules. These are used to either parallel or series connect the BIPV roof tiles. The advantage of this connection type is its flexibility. By combining the BIPV modules with the dummy modules, one can customize the strings in regards to obstacles on the roof. An example can bee chimneys and spots with shadow.

(a) BIPV roof tile front (b) BIPV roof tile front back

Figure 21: Shows the BIPV roof tile used

3.3 Data Logging

This chapter will focus on the data collection and handling of the data logged by the custom made LabVIEW program. The sampling frequency is one second, while the recording frequency is one minute. The irradiance is measured using a temperature-compensated mcSi PV-based sensor (SolData 80spc) in combination with an isolation amplifier [32]. The logging of irradiance is limited by a fixed value of minimum 30 W/m^2 so all the irradiance below this limit is discarded. The parameters being logged are then stored in a text file. The parameters in the text file are date, irradiance, ambient temperature, Short circuit current, open circuit voltage, module temperature, power and voltage at the maximum power point for all the modules. The text file is then imported into MATLAB. The logging system can be seen in Fig. 22 and Fig. 23.

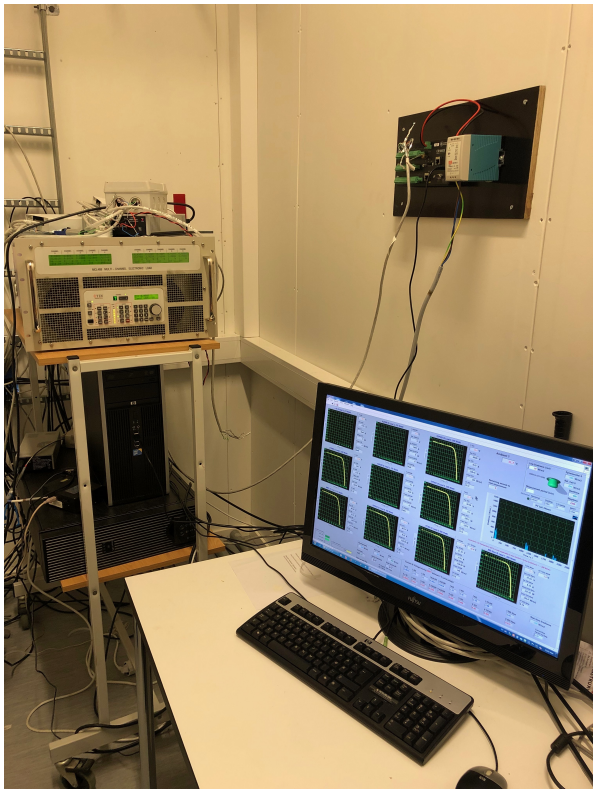

Figure 22: Shows the dynaload and computer used for logging

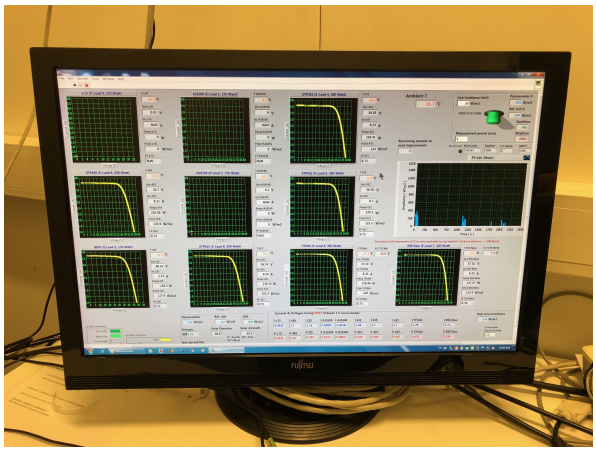

Figure 23: Shows the LabVIEW program used for logging

Since there is only one temperature slot per module in the LabVIEW program, a separate logging system is used for logging data from the three temperature sensors placed on the backside of the BIPV modules. The logger that is used is a Campbell 1000X data logger. The data logger has the same sampling and recording frequency as the LabVIEW program. The logger can be seen in Fig. 24.

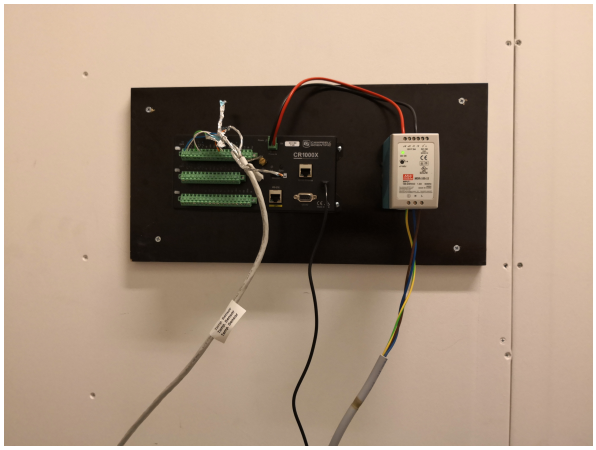

Figure 24: Shows the data logger used for logging data from the temperature sensors.

3.3.1 Data Handling and Filtering

This section will focus on the handling and filtering of the data acquired from the LabVIEW logging program. The first data processed was irradiance data. As mentioned previously, a reference cell and an irradiance sensor are used to measure the irradiance. There are some errors in the data from the reference cell, therefore, only the data from the irradiance sensor is used. This difference between the two datasets can be seen in Fig. 25. Fig. 25 shows that the reference cell shows negative values in periods. This was also the case for several other days.

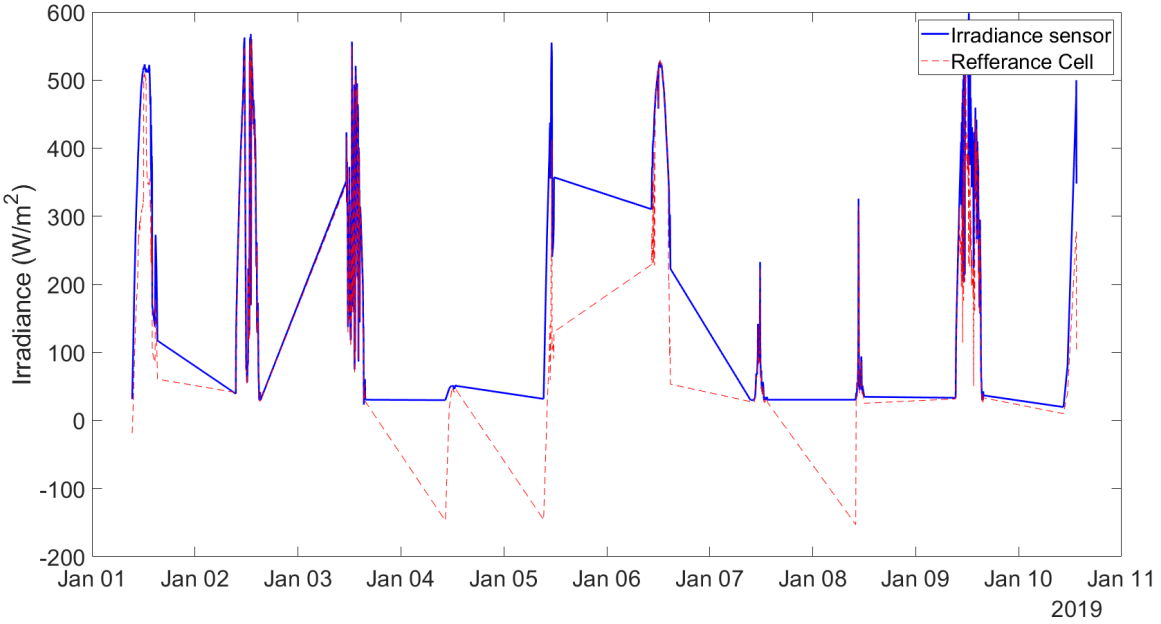

Figure 25: Shows downtime of the system and the difference in data from reference cell and irradiance sensor

The raw data from the LabVIEW program can be seen in Fig. 26. The figure shows the correlation between irradiance and power production from November to May. Periods of down time can also be seen in Fig. 26. The down time between November 2018 and February 2019 is due to the practical work that was done between December and February. Because of this down time,it has been necessary to process and filter the data. The down time in April is due to the computer used for logging was shut down. The BIPV system was connected to the logging system on November 28th. Fig. 26 shows the uncertainties in the data from November to February due to sporadic disconnection. Because of these uncertainties, only data from March to May is used to ensure valid results.

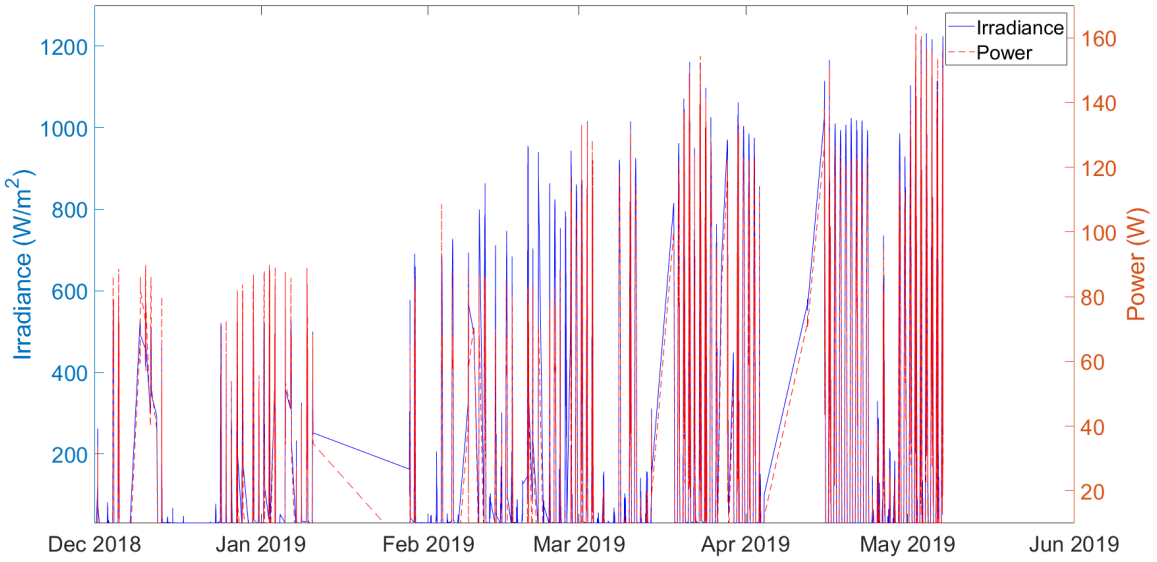

Figure 26: Shows the irradiance and power data from 28th of November 2018 to 7th of May 2019

Temperature data from three of the temperature sensors used on the demo roof cannot be used due to an unknown error, which is currently being investigated. Therefore only data from the top sensor is used for the results presented in this thesis. The error in the temperature data can be seen in Fig. 27 where the red curve is the working sensor. The data logger was connected on April 3rd. The temperature data from the demo roof prior to this date is unreliable due to temporary disconnection and rewiring. The data temperature data from the data logger can be seen in Fig. 27. Here it is clear that both the bottom and middle sensor is not working properly, and therefore only the data from the top sensor is used in this thesis.

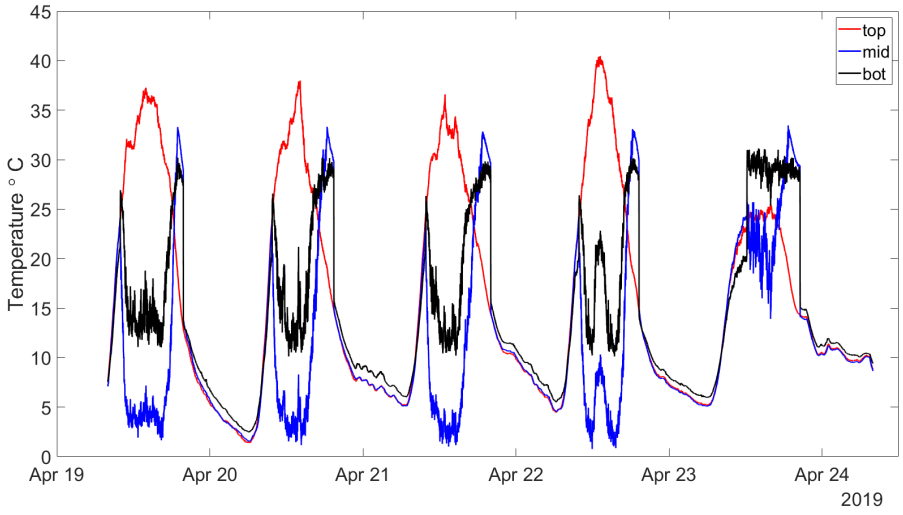

Figure 27: Shows the error in two of the three temperature sensors used on the demoroof

3.4 Performance Analysis

3.4.1 Efficiency and PR evaluation

As the string is not connected to any inverter, only DC data is available. The data that has been processed and used in this thesis is the power production data from the string. This data has been filtered and processed using MATLAB. The filtered data was then used to calculate system efficiency using Eq. 5. Since only the DC values are available, only the performance ratio of the array is calculated. This is done by using Eq. 9. The data used to calculate the Array yield Y_A is the daily energy in kWh as E_{DC} and the rated system power as P_o. The reference yield is the difference in the measured daily in-plane irradiance (H) in kWh/m^2 where H is the measured irradiance and reference irradiance (G) of 1000 W/m^2. This gives a unitless number which is the performance ratio of the array. As temperature is a important factor in regards to PV, a temperature corrected performance ratio has also been calculated.To calculate the temperature corrected PR, the difference between the average daily module temperature and STC temperature were multiplied with the temperature coefficient of the modules. The temperature coefficient used is listed in the datasheet. Since γ is negative, T_{corr} from Eq. 11 will be positive if the module temperature is lower than the STC temperature and vice versa.

3.4.2 IV Analysis

To analyse the actual IV curve of the string, a IV curve traces was used. The instrument used is a I-V500W. This instrument is used to collect precise IV curves. A Pt100 temperature sensor and a reference cell can be connected to the unit for irradiance and temperature measurements. This is so that the measured I-V curves are automatically adjusted to STC to make comparison with datasheet values easier. The instrument used can be seen in Fig. 28. This was also used as a way of validating the data logged by the LabVIEW program.

Figure 28: Shows the IV-curve tracer used for IV analysis [35]

3.4.3 Temperature Analysis

Temperature analysis has been an important focuses in this thesis. The reason for this is the concern in regards to module temperature of BIPV modules. BIPV technologies is as mentioned previously integrated into the building structure and has therefor not the same natural cooling as BAPV modules. This can result in a higher module temperature and lower power production. The BIPV roof tiles used in this thesis is made of concrete. The modules has been mounted in realistic conditions in order to get more realistic temperature readings. Three temperature sensors were mounted on the backside of the demo roof, one in the bottom, middle and top row as well as one in the simulated cold attic room on the backside. Due to errors, only the top sensor is working properly and therefor only the data from this sensor is used. To further inspect the temperature distribution in the string, a IR camera was used. The IR camera used is a Fluke Ti400 and can be seen in Fig. 29. The IR camera was also used as a way of validating the logged temperature data.

Figure 29: Shows the infrared camera used for IR analysis [36]

3.5 Economical cases

This section will focus on the economical aspect of this thesis. In order to do so, two different methods has been used. Firstly, the levelized cost of energy (LCOE) has been calculated and then the investment payback time. LCOE is a common way of comparing different energy sources such as PV or wind to find out which is the most cost effective. The LCOE is describing how much the energy that is produced costs. To do so, the total lifetime costs of the system is divided by the yearly energy produced. The complexity of the LCOE calculation is determined by the amount of information available. The more factors included into the model, the more accurate results. Such factors can be inflation, discount rate, degradation rate, investment costs and operating costs. The LCOE model used in this thesis is based on [37] and is presented in Equation 13.

$$LCOE = \frac{It + \sum_{t=0}^{T}((Ot + Mt + Ft)/(1+r)^t}{\sum_{t=0}^{T}(St(1-d)^t/(1+r)^t} \tag{13}$$

Where:
It = Initial investment/cost including installation, work etc. [NOK]
t = year
T = Lifetime of system [Year]
Ot = Operating cost for t [NOK]
Mt = Maintenance cost for t [NOK]
Ft = Interest expenditures for t [NOK]
r = Discount rate [%]
St = Annual rated energy production [kWh/year]
d = degredation rate [%]

LCOE was calculated for four different cases where each case had different installed capacity but with the same roof area of 150 m^2 and tilt angle of 40 °. The simulated location is UiA, Grimstad. The cases used was 3 kWp, 6 kWp, 9 kWp and 12 kWp. It is estimated that the inverter is changed once during the simulated time period of 25 years. The inverter used by Sun-Net is [38]. Since the maximum power per inverter is 6000 W, the cases with 9 and 12 kWp capacity needs two inverters. The prices and investment costs has been based on Sun-Net's price calculator [39]. As several of the parameters used to calculate the LCOE will vary from project to project, a series of assumptions were needed. According to [40], the discount rate in Norway will vary from 3.5% for low risk project to 6% for medium risk projects. Therefor LCOE was calculated for 3.5, 4, 4.5, 5, 5.5 and 6% to see the effect of changing discount rate. One aspect that will affect the LCOE is if the initial investment is equity or if there is a need for loan. If the initial investment is only based on equity, Ft in Eq. 13 is zero. If the Initial investment is a loan, factor such as size of the loan, annual rate and length of loan has to be considered. For the LCOE simulated in this thesis, the size of the loan is set to 100% of the investment cost, annual rate is set to 3% and length of loan is

set to the warranty lifetime of the system of 25 years. The next parameter to consider is the Annual rated energy production. Since the demo roof only has reliable data for three months, simulated values had to be used. After consulting with Sun-Net, PVGIS was used.

4 Results

This chapter is divided into three subchapters; Performance evaluation, temperature analysis, and economical results.

4.1 Performance Analysis

Fig. 30 shows the daily yield compared to the daily specific yield of the array listed in table 3 from 28th of February to 7th of May. The maximum energy produced in one day is 0.96 kWh and the average is 0.42 kWh. The average daily specific yield is 2.5 kWh/kWp while the max value is 6.3 kWh/kWp. This time span also includes downtime periods in March and April.

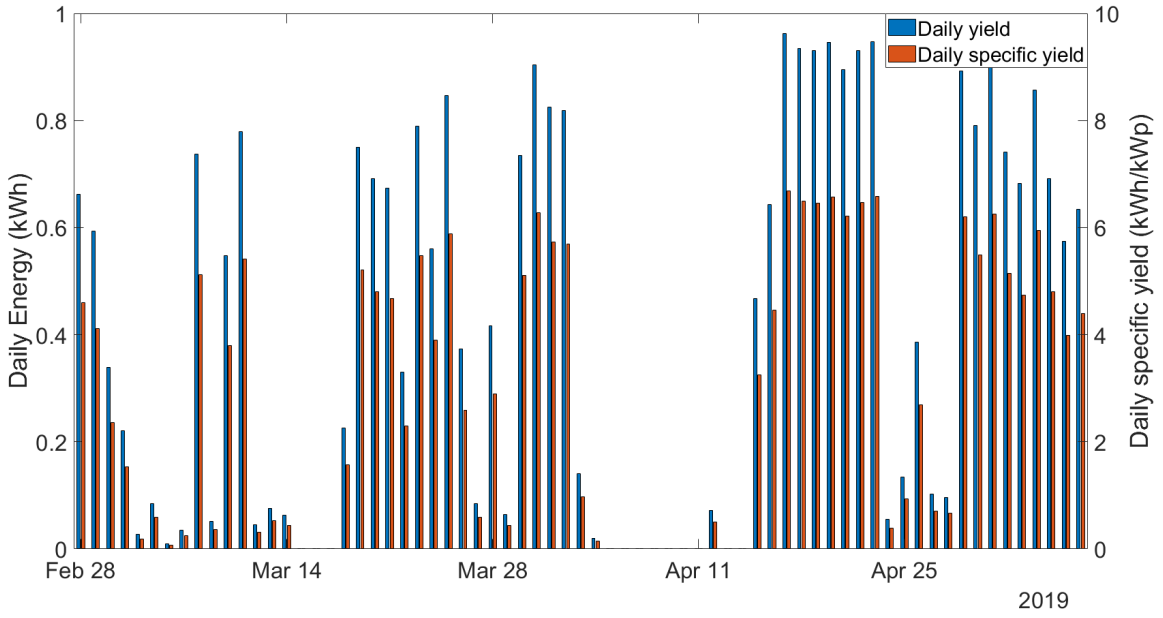

Figure 30: Daily energy and daily specific yield from 28th of February to 7th of may 2019

In Fig. 31 an example of the correlation between power production and irradiance for 23rd of April can be seen. The maximum irradiance is 985 W/m^2 while the maximum power is 118 W. It is clear that the power curve follows the irradiance curve good. The down time is due to using the I-V500W I-V curve tracer.

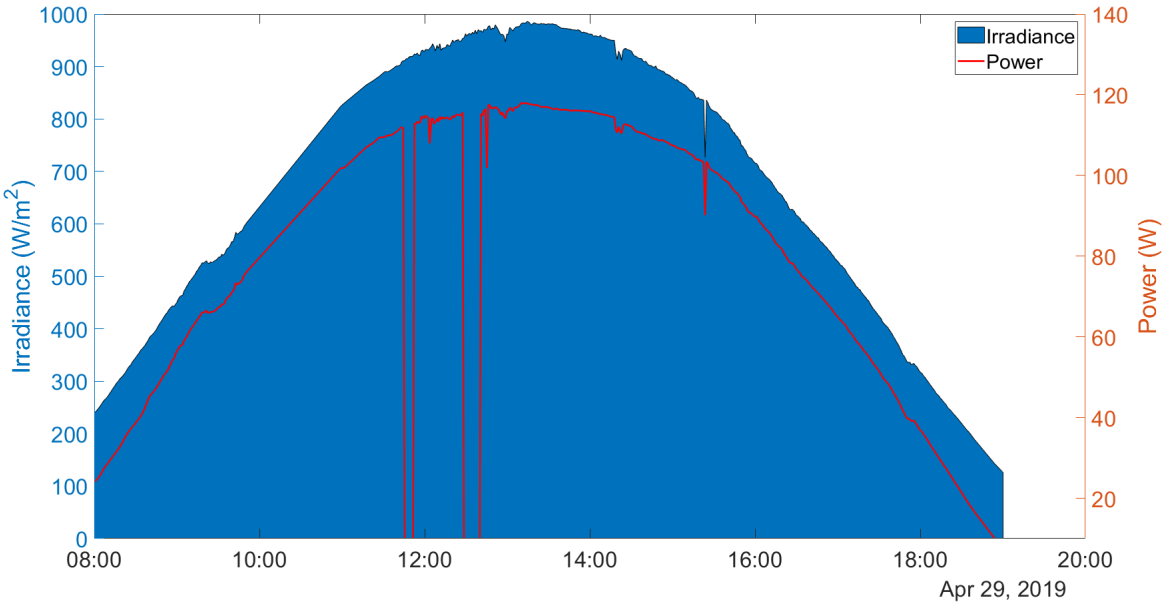

Figure 31: Shows irradiance and power for one day

Fig. 32 shows the measured I-V and P-V curve from the I-V500W I-V curve tracer. This was done on the 29th of April between 11 and 12. This can be seen in Fig. 31.

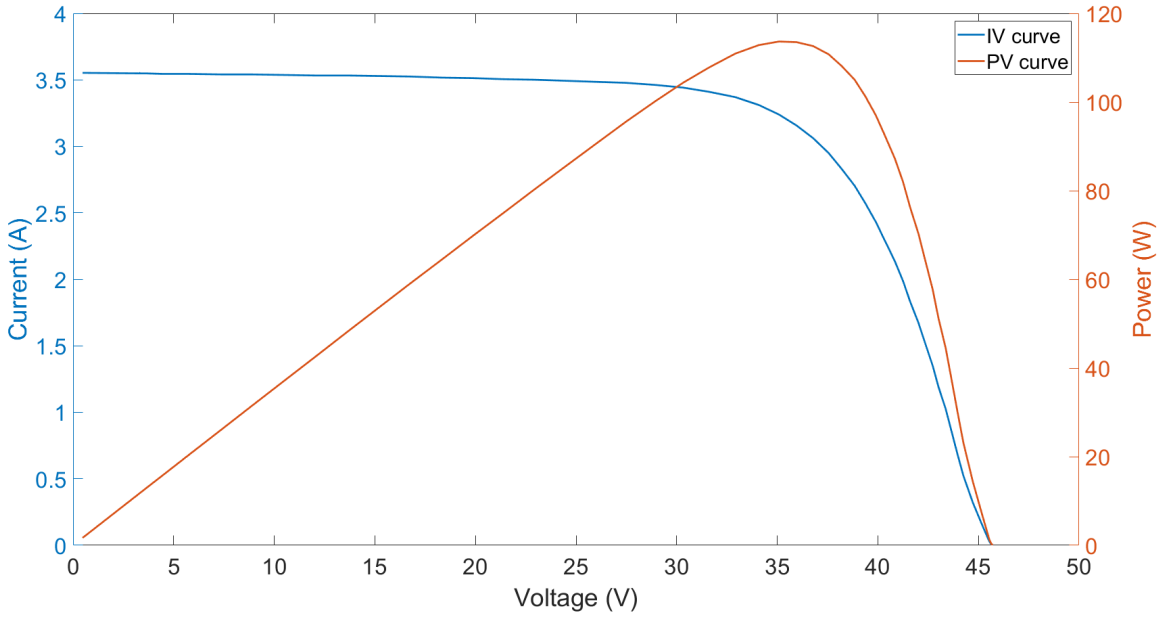

Figure 32: Shows measured I-V and PV curve

The measured values are compared to datasheet values in Table 4. The test was done under approximately STC conditions. The results in Table 4 shows that the measured results are close to the STC results for both the V_{mpp} and V_{oc}. The measured I_{mpp} and I_{sc} is on the other hand 17.3 and 16.3 % lower than the datasheet values. The difference in power is 21 % from the datasheet to measured value. The difference in FF calculated to be 3 % and was calculated using Eq. 3. The STC efficiency is calculated using datasheet values and is not the same as the cell efficiency mentioned previously.

Table 4: Compares datasheet values and measured values

	Datasheet values (STC)	Measured values
Irradiance	1000 W/m^2	955.90 W/m^2
Temperature	25 °C	16.98 °C
Voc	47 V	45.72 V
Isc	4.24 A	3.55 A
Pmax	144 Wp	113.65 W
Vmpp	37 V	35.08 V
Impp	3.92 A	3.24 A
η_{sys}	11%	9.34%
FF	0.73	0.70

4.1.1 Efficiency

Fig 33 shows the efficiency per day within the analysed time period. The average array efficiency for the time period presented in Fig. 33 is 9.6 % with a maximum efficiency of 10.4 %.

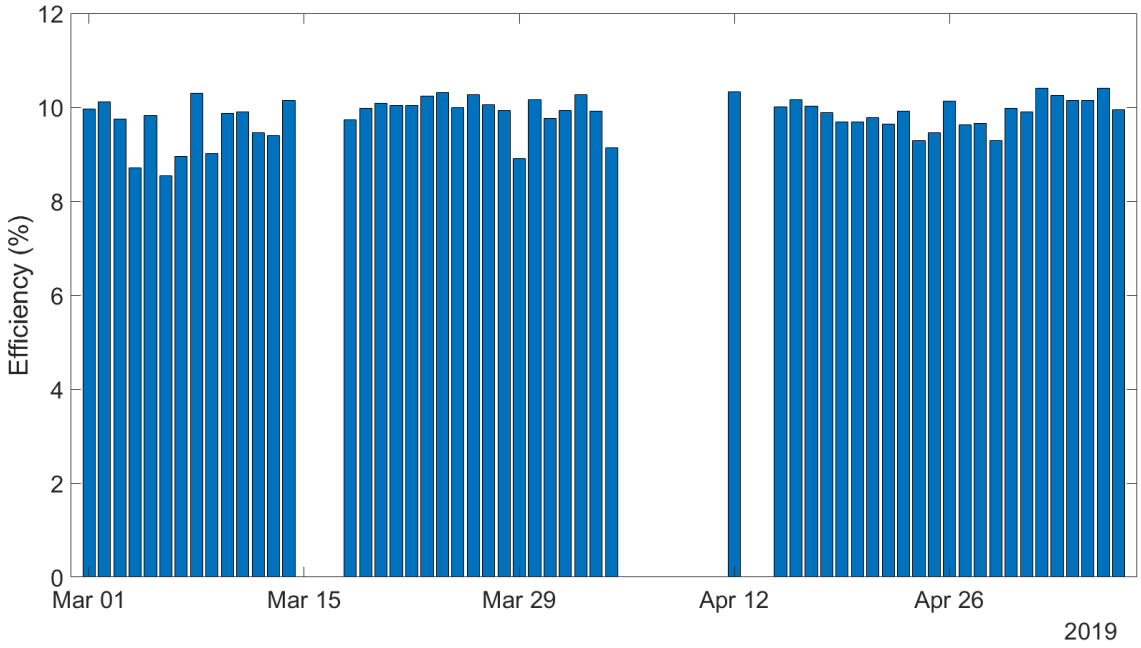

Figure 33: Shows efficiency for several days

To look further into the array efficiency, efficiency was analysed for two different days and compared with module temperature. The first case is a clear day and the second case is a cloudy day.

These two cases can be seen in Fig. 34 and Fig. 35 respectively. The data used is per minute and is analysed for one day.

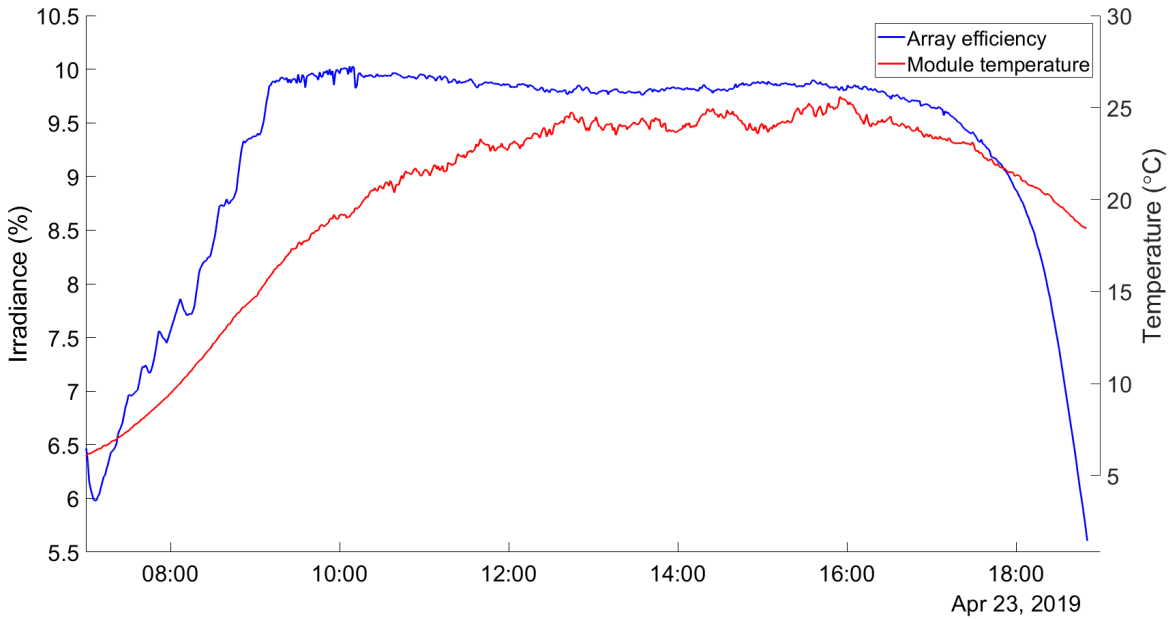

Figure 34: Shows efficiency and cell temperature for a clear day (23rd of April 2019).

The efficiency in the second case has a lot more fluctuation and is on average lower than the first case. The first case presents a much more stable efficiency throughout the day. None of the cases is particularly affected by the change in module temperature.

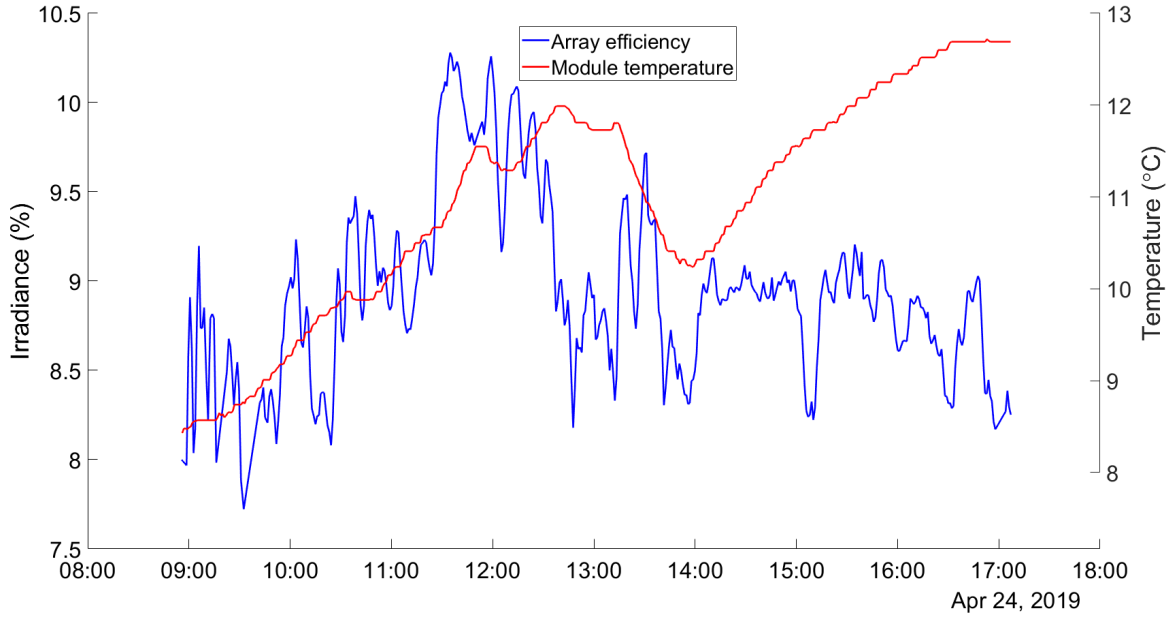

Figure 35: Shows efficiency and cell temperature for a cloudy day

4.1.2 Performance ratio

Fig. 36 shows the PR and temperature corrected PR from April 15th to May 3rd. The max and min PR without temperature correction in this time period is 0.72 and 0.65 respectively, while the average PR_A is 0.68. The max and min temperature corrected PR is 0.77 and 0.66 respectively, and while the average $PR_{A,Tcorr}$ with temperature correction is 0.72.

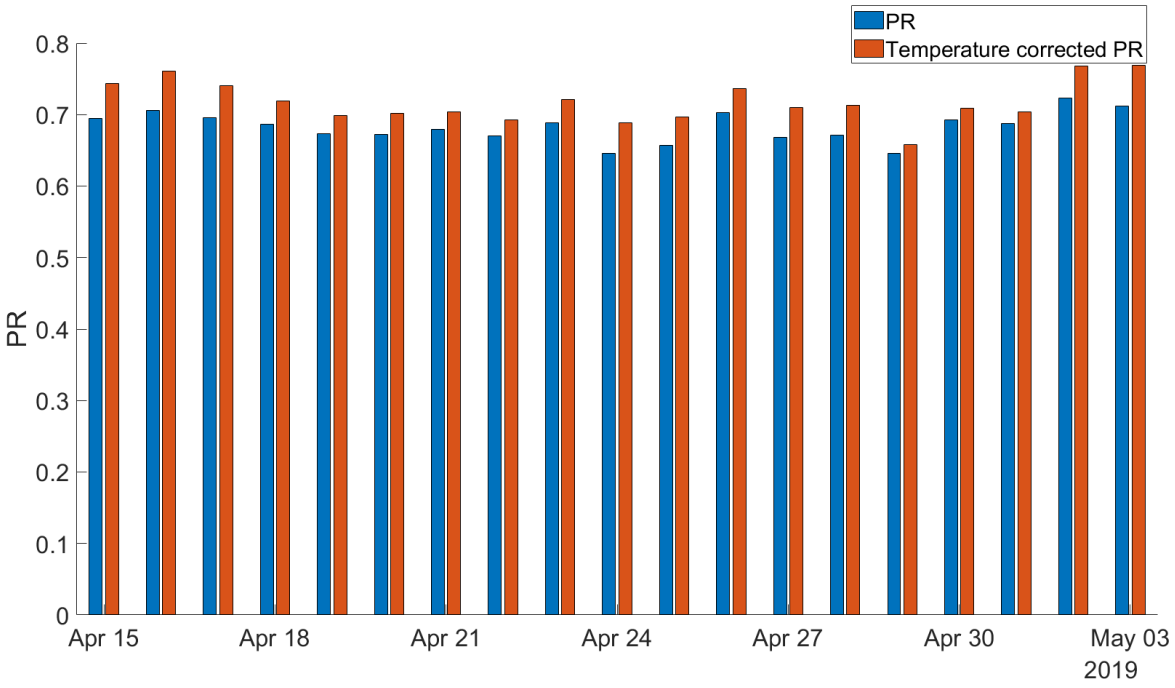

Figure 36: Performance ratio and temperature corrected performance ratio

4.2 Temperature Analysis

This section will focus on the Temperature analysis of the BIPV module and string. The data used as the module temperature is the temperature data from the top sensor on the demo roof. Fig. 37 shows the correlation between irradiance, module temperature, and ambient air temperature for the time period April 16 to May 2. At days with high irradiance (>600 W/m^2), the module temperature can reach around 40 °C, but for days with low irradiance, the module temperature follows the ambient air temperature which in this case is around 10-15 °C during daytime.

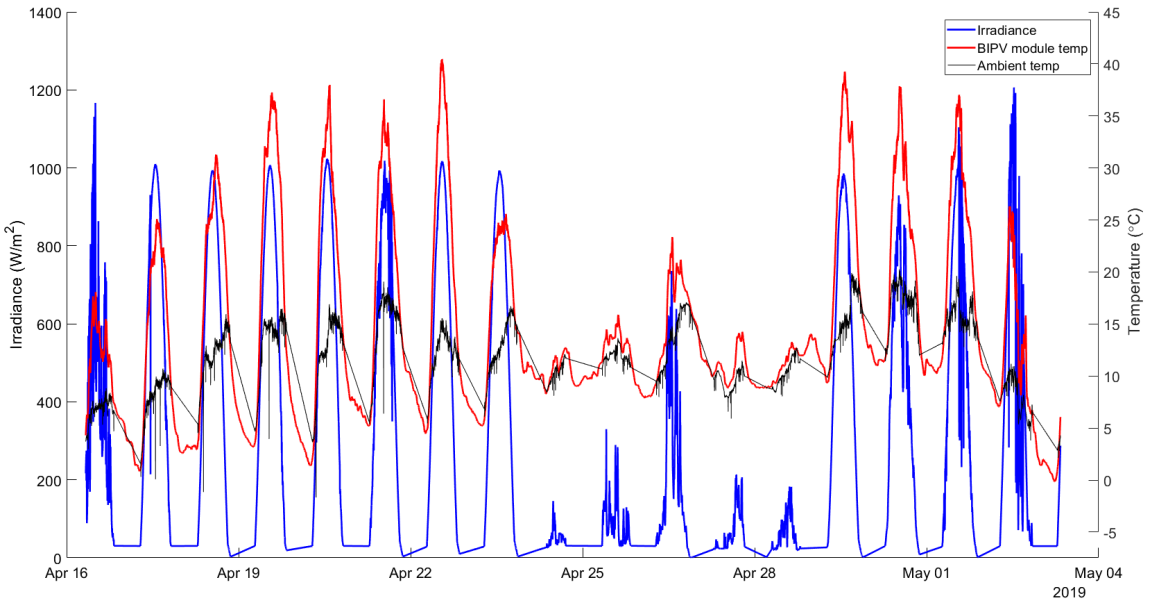

Figure 37: Shows irradiance vs module and ambient temperature

One can see that the BIPV temperature has small-scale fluctuation compared to the ambient air temperature.

One of the concerns of this thesis was the module temperature. In order to evaluate the temperature effect on the BIPV modules, a comparison between the BIPV module temperature and a regular multi crystalline module (Suntech STP422) has been done. The module that is used for comparison is mounted in a open rack in the existing setup.

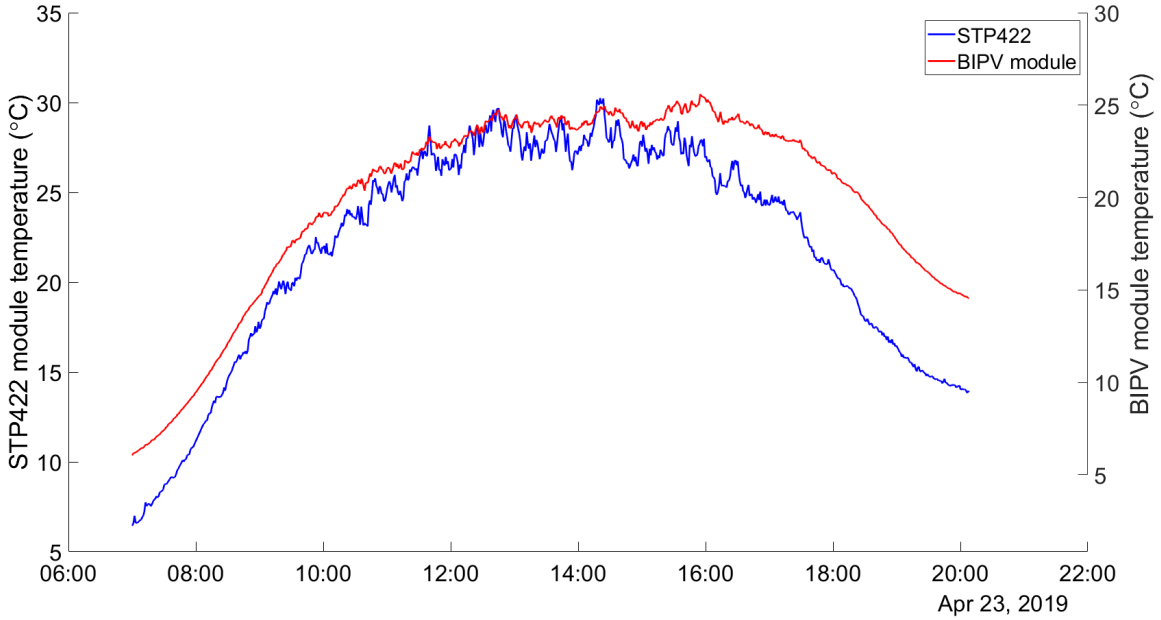

Figure 38: Comparison between module temperature of Suntech STP422 and BIPV

The results from Fig. 38 shows the same effect as in Fig. 37. The BIPV module temperature has much less fluctuation than for the STP422 module. The difference in maximum temperature between the two modules is roughly 4 °C in the middle of the day. At the end of the day, the BIPV module uses significantly longer time to cool down.

4.2.1 IR analysis

Fig. 39 shows the temperature of the top two rows while Fig. 40 shows the temperature of the bottom two rows. The pictures was taken within one minute of each other at 29th of April. The irradiance at this point were between 900-1000 W/m^2.

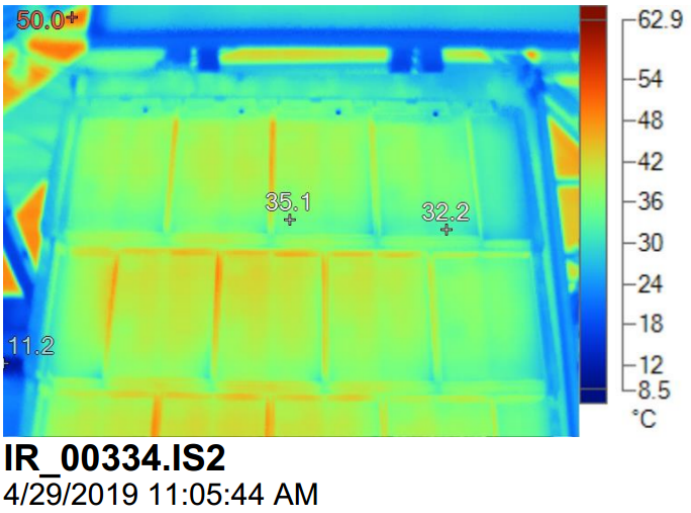

Figure 39: Shows IR picture of top row of demo roof

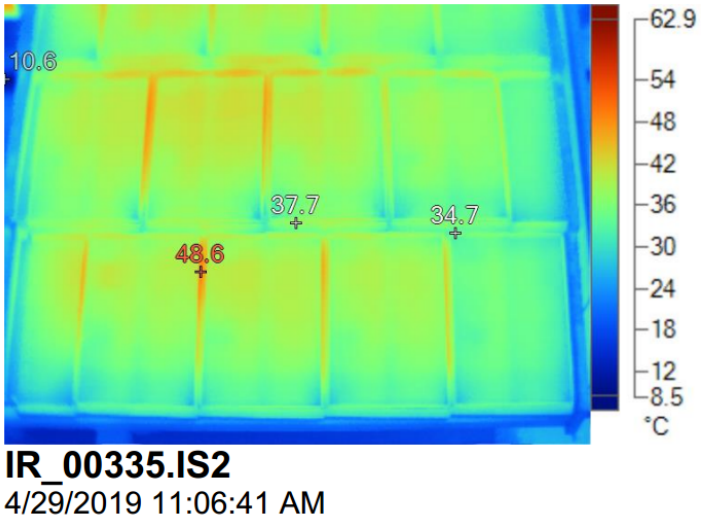

Figure 40: Shows bottom row of demoroof

Fig. 40 shows that the module temperature at the top row is 32-36 °C. This fits with the temperature from Fig. 37 for the same day. Th temperature distribuiton of each stone shows that the moduels are hotter on the middle and top than on the bottom and as well in between the modules.

4.3 Economic results

The economical results that is presented will be for different cases. Each case is based on the price calculator made by Sun-Net and the annual energy output is estimated using PVGIS. Table 5 shows the different parameters for the different cases. Each case is for the building of a new roof.

Table 5: Shows the different cases for the Economical results

Case	Installed capacity (kWp)	Roof Area (m^2)	Investment cost (NOK)	Estimated annual energy output (kWh/year)
1	3	150	102 716	3040
2	6	150	166 590	6040
3	9	150	217 515	9100
4	12	150	282 302	12200

The calculated LCOE values in Fig. 41 is done for case 4. This figure shows how the change in discount rate changes the outcome of the LCOE calculation. This has been done for case 4 with and without loan. The lowest LCOE value is 1.58 NOK/kWh, this is for 3% discount rate and no loan. The highest LCOE value without loan is 1.95 NOK/kWh. The lowest LCOE values with loan is 12.21 NOK/kWh while the highest with a discount rate of 6% is 12.47 NOK/kWh.

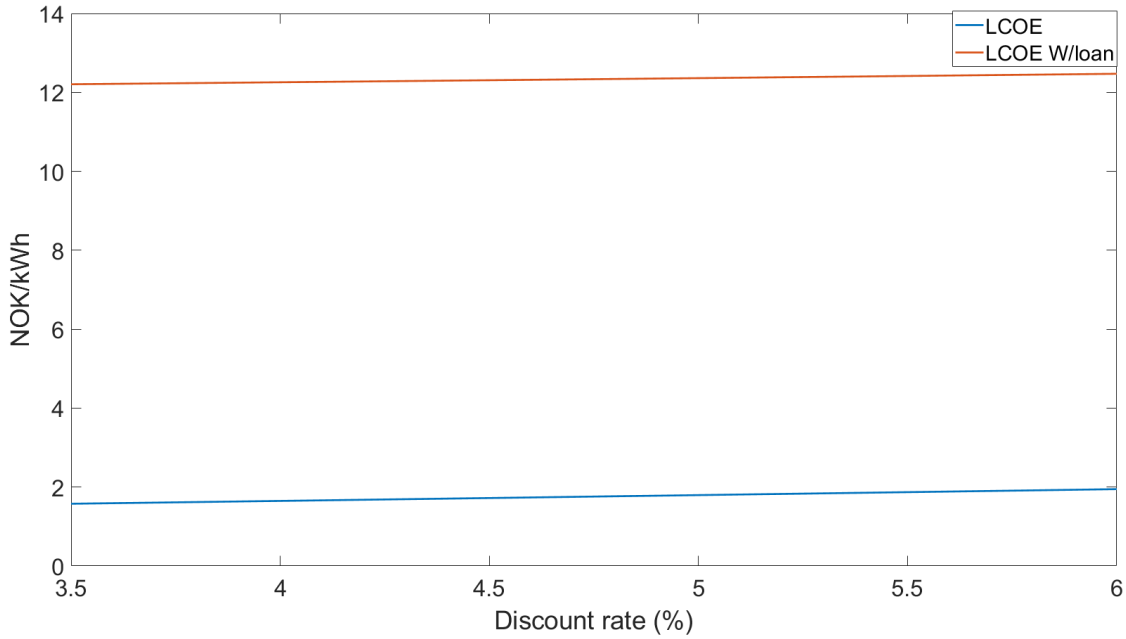

Figure 41: Shows how different discount rates changes the outcome of LCOE calculation with and without loan

Fig. 42 shows the LCOE for the four different cases with a fixed discount rate of 3.5%. This has been done with and without loan. Table 6 shows the results from the LCOE calculations presented in Fig. 42. This shows that case 4 has the lowest LCOE both with and without loan.

Table 6: Shows the results from LCOE calculation for each case with and without loan

Case	LCOE (NOK/kWh)	LCOE W/Loan (NOK/kWh)
1	2.38	17.9
2	1.86	14.52
3	1.68	12.65
4	1.58	12.21

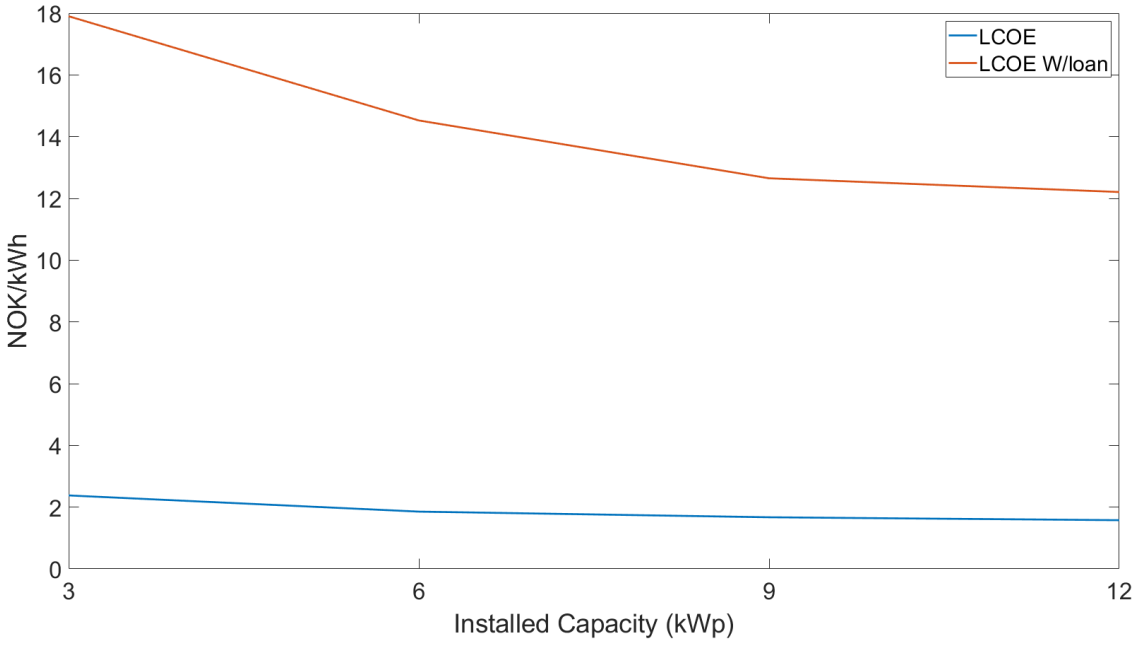

Figure 42: Shows LCOE for four different capacities

The down-payment is calculated by taking the amount of energy produced per year multiplied with the cost of electricity and then subtracting that from the initial investment costs. The results for downpayment can be seen in Fig. 43. Only case 3 and 4 will be able to reach zero within the waranty lifetime of the modules.

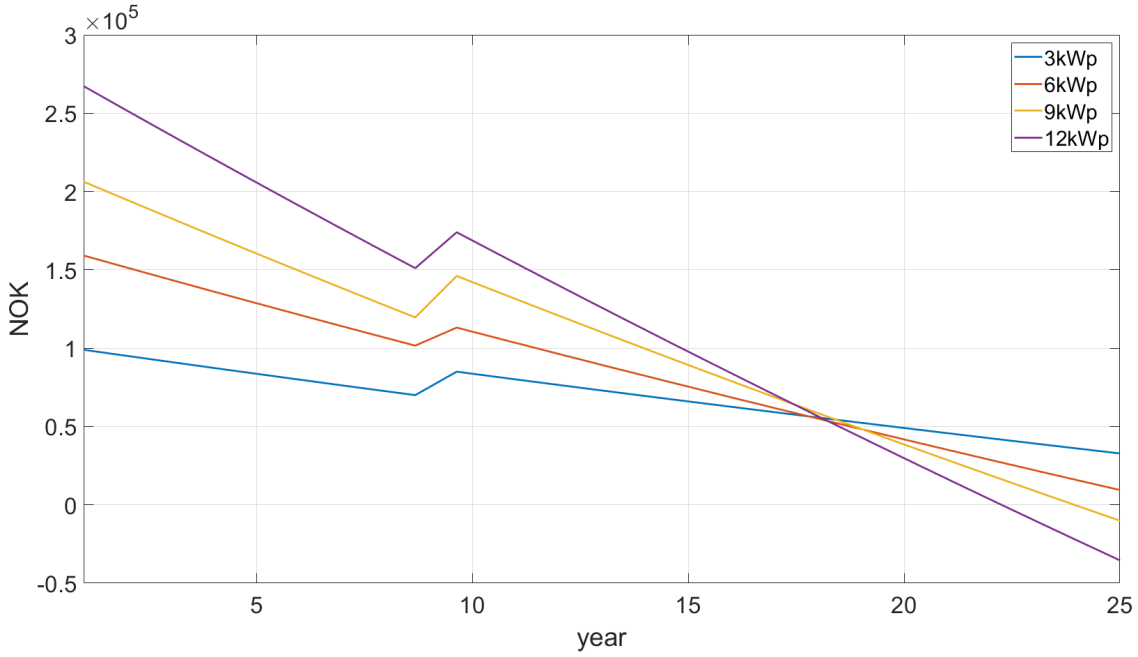

Figure 43: Shows downpayment for different capacities

5 Discussion

5.1 Performance Evaluation

Both performance ratio and efficiency are most often calculated on a yearly basis to give more accurate values. This means that the calculated performance ratio and efficiency can be slightly different than if it was done with measured data for a whole year. The array is performing well compared to the datasheet values listed in table 4, but with significantly lower power output. The daily efficiency presented in Fig. 33 shows that the array is performing close to the STC efficiency at days with high irradiance, but has a lower efficiency when there is less irradiance. This can also be seen in Fig. 35. According to [30], a typical PR for a newer PV plant is 0.8. This means that the array is under performing compared to today's PV technology. A reason for this can be the fact that the array area is not completely covered by PV and therefore some of the irradiance that hit the array is not hitting the PV part of the BIPV modules. The temperature corrected performance ratio is slightly higher for all the days shown in Fig. 36 and has a maximum of 0.77.

5.2 Temperature Analysis

After comparing and validating the working sensor with the rest of the sensors used on the other modules, it was concluded that the data from the top sensor on the demo roof was valid. Fig. 37 shows the correlation between module temperature and irradiance. It is clear that the module temperature is directly affected by the irradiance. One concern is the high temperature compared to the ambient air temperature on sunny days. The reason for this big difference in temperature can be explained by looking at the location of each of the two temperature sensors. The sensor that measures the ambient air temperature has less protection against the weather than the temperature sensor mounted on the backside of the BIPV modules. One of the concerns at the start of this thesis was that the modules would reach high temperatures compared to regular modules and also stay warm for a longer time. The results in Fig. 38 shows that these concerns were partially correct. The BIPV modules does not have a higher temperature throughout the day but it stays warm for a longer time than the free-standing multi-crystalline module. The BIPV modules are also built into a frame so that the only cooling is the air stream underneath, going through and exits on the top. Since the other sensors are not working, the comparison between the bottom, middle and top row could not be done.

5.3 Economic Results

Since the technology tested in this thesis is fairly new, there was a concern in regards to the profitability. Before calculating the LCOE values, it was needed to see the effect of the discount rate on the results. This is because it was difficult to determine a fixed discount rate for the projects since the discount rate is dependent on several other factors. From both Fig. 41 and 42 it can be seen that the discount rate has a small effect when there is no loan, but a significantly higher impact on the LCOE when a loan is needed. LCOE for small-scale PV systems on rooftops in Northern Germany is between 9.89 and 11.54 €$_{Cents}$/kWh according to [41], which is roughly 0.97 and 1.13 NOK/kWh. This value is a bit lower for bigger PV systems on rooftops. By comparing this value to the results presented in Table 42, it can be seen that the calculated values are slightly higher than the LCOE from [41]. The calculated LCOE also follows the same trend where the systems with more capacity have a lower LCOE value. The downpayment for the different cases shows that only the two cases with 9 and 12 kWp capacity of the cases is able to reach zero within the warranty lifetime of the modules.

6 Conclusion

Performance analysis, temperature analysis, and economic cases have been done and presented in order to answer the research questions asked at the start of this thesis. The performance analysis section shows that the average system efficiency is 9.6 %, average PR of 0.68 and an average temperature corrected PR of 0.72. This shows that the tested array is underperforming compared to the BAPV technology that is available on the market today. The I-V curve tracer also shows that the measured values are slightly lower than the values listed in the datasheet, especially the output power.

In regards to the temperature analysis, it has been shown that some of the concerns were correct. The BIPV modules stay warm longer than the Suntech STP422 multi-crystalline module but are in fact colder in the middle of the day. It was also shown that the BIPV modules have a more stable temperature curve throughout the day.

The economic results show that the LCOE for the simulated cases is higher than the compared values and only two of the cases were able to to pay back the lifetime costs. This indicates that system price still is too high to be as cost-effective as today's BAPV technology.

The final conclusion is that the BIPV modules still has room for improvement both in regards to both performance and price. When it comes to the effect of temperature, it is shown that if the modules get a sufficient amount of natural cooling, the temperature will not have a significant impact on the performance compared to traditional BAPV modules.

7 Further Work

Recommendations for further work are:

- Continue working on the already existing test setup in order to do tests with yearly data.
- Connect system to inverter to see the difference between DC and AC power output.
- Make separate logging system for BIPV parameters to make it easier to analyse the logged data.
- Make a new setup with the new BIPV roof tile from Sun-Net and compare the data with the BIPV roof tile that was tested in this thesis.

References

[1] Bjørn Jelle. Building integrated photovoltaics: A concise description of the current state of the art and possible research pathways. *Energies*, 9(1):21, 2016.

[2] International energy agency. *Global Energy CO2 Status Report: The latest trends in energy and emissions in 2018*, 2019. Available: `https://www.iea.org/geco/`. Accessed: 04.05.2019.

[3] Lisa Kvalbein, Erik Stensrud Marstein. Muligheter og utfordringer knyttet til bygningsintegrerte solceller (bipv) i norge, 2018.

[4] PVsites. Bipv market and stakeholder analysis and needs, 2016. Online; CEA, Tecnalia, CTCV, Available from: https://www.pvsites.eu/downloads/category/project-results?page=2.

[5] PVeducation. *Atmospheric Effects*, 2019. Available: `www.pveducation.org/pvcdrom/properties-of-sunlight/atmospheric-effects`. Accessed: 06.03.2019.

[6] Christian A Gueymard. The sun's total and spectral irradiance for solar energy applications and solar radiation models. *Solar energy*, 76(4):423–453, 2004.

[7] Wikimedia commons. *Solar Spectrum*, 2019. Available: `https://upload.wikimedia.org/wikipedia/commons/e/e7/Solar_spectrum_en.svg`.

[8] Laszlo Solymar, Donald Walsh, and Richard RA Syms. *Electrical properties of materials*. Oxford university press, 2014.

[9] Stuart R Wenham, Martin A Green, Muriel E Watt, Richard Corkish, and Alistair Sproul. *Applied photovoltaics*. Routledge, 2013.

[10] PVeducation. *pn-junctions*, 2019. Available: `https://www.pveducation.org/pvcdrom/pn-junctions/formation-of-a-pn-junction`. Accessed: 06.03.2019.

[11] Fraunhofer Institute for Solar Energy Systems. *PHOTOVOLTAICS REPORT*, 2019. Available: `https://www.ise.fraunhofer.de/content/dam/ise/de/documents/publications/studies/Photovoltaics-Report.pdf`. Accessed: 10.03.2019.

[12] Martin A Green. Solar cells: operating principles, technology, and system applications. *Englewood Cliffs, NJ, Prentice-Hall, Inc., 1982. 288 p.*, 1982.

[13] PVeducation. *Amorphous silicon*, 2019. Available: `https://pvcdrom.pveducation.org/MANUFACT/A-SI.HTM`. Accessed: 10.03.2019.

[14] AW Czanderna and FJ Pern. Encapsulation of pv modules using ethylene vinyl acetate copolymer as a pottant: A critical review. *Solar energy materials and solar cells*, 43(2):101–181, 1996.

[15] Klaus J Geretschläger, Gernot M Wallner, and Jörg Fischer. Structure and basic properties of photovoltaic module backsheet films. *Solar Energy Materials and Solar Cells*, 144:451–456, 2016.

[16] Wikimedia Commons. *Solar cell equivalent circuit*, 2019. Available: `https://commons.wikimedia.org/wiki/File:Solar_cell_equivalent_circuit.svg`. Accessed: 12.02.2019.

[17] Wikimedia Commons. *I-V Curve and MPP*, 2019. Available: `https://commons.wikimedia.org/wiki/File:I-V_Curve_MPP.png`. Accessed: 23.02.2019.

[18] Adolf Goetzberger and Volker Uwe Hoffmann. *Photovoltaic solar energy generation*, volume 112. Springer Science & Business Media, 2005.

[19] EE Van Dyk and EL Meyer. Analysis of the effect of parasitic resistances on the performance of photovoltaic modules. *Renewable energy*, 29(3):333–344, 2004.

[20] Tom Markvart, Augustin McEvoy, and Luis Castaner. *Practical handbook of photovoltaics: fundamentals and applications*. Elsevier, 2003.

[21] Swapnil Dubey, Jatin Narotam Sarvaiya, and Bharath Seshadri. Temperature dependent photovoltaic (pv) efficiency and its effect on pv production in the world–a review. *Energy Procedia*, 33:311–321, 2013.

[22] Sun-Net. Soltakstein, 2018. Online; Available from: https://sun-net.no/wpside1/wp-content/uploads/2018/10/soltakstein.png accessed October 17, 2018.

[23] European Comitee for Electrotechnical Standarization. Crystalline silicon terrestrial photovoltaic (pv) modules—design qualification and type approval; en 61215; european standard: Brussels, belgium, 2005.

[24] European Comitee for Electrotechnical Standarization. Thin-film terrestrial photovoltaic (pv) modules—design qualification and type approval; en 61646; european standard: Brussels, belgium, 2008.

[25] European Comitee for Electrotechnical Standarization. Photovoltaic (pv) module safety qualification—part 1: Requirements for construction; en 61730-1; european standard: Brussels, belgium, 2007.

[26] European Comitee for Electrotechnical Standarization. Photovoltaic (pv) module safety qualification—part 2: Requirements for construction; en 61730-2; european standard: Brussels, belgium, 2007.

[27] Underwriters Laboratories Inc. Underwriters laboratories inc. ul standard for safety flat-plate photovoltaic modules and panels; ul 1703; ottawa, on, canada, 2002.

[28] PVsites. Standardization needs for bipv, 2016. Online; CEA, Tecnalia, CTCV, Available from: https://pvsites.eu. accessed November 02, 2018.

[29] Achim Woyte, Mauricio Richter, David Moser, Nils Reich, Mike Green, Stefan Mau, and H Beyer. Analytical monitoring of grid-connected photovoltaic systems—good practices for monitoring and performance analysis. *Report IEA PVPS T13-03*, 2014.

[30] Thomas Nordmann, C Luzi, and G Mike. Analysis of long-term performance of pv systems: Different data resolution for different purposes. *Report IEA-PVPS T13-05*, 2014.

[31] Bill Marion, J Adelstein, K ea Boyle, H Hayden, B Hammond, T Fletcher, B Canada, D Narang, A Kimber, L Mitchell, et al. Performance parameters for grid-connected pv systems. In *Conference Record of the Thirty-first IEEE Photovoltaic Specialists Conference, 2005.*, pages 1601–1606. IEEE, 2005.

[32] Georgi Hristov Yordanov. Characterization and analysis of photovoltaic modules and the solar resource based on in-situ measurements in southern norway. *Norwegian University of Science and Technology, Department of Electric Power Engineering, Trondheim*, 2012.

[33] Sivert Uvsløkk. *Tak med kaldt loft. Delrapport fra prosjekt 4 i FoU-programmet Klima2000*, 2005. Available: `www.sintefbok.no`. Accessed: 08.04.2019.

[34] Skarpnes. *Leggeanvisning. Domino taktegl*, 2016. Available: `https://www.skarpnes.com/wp-content/uploads/2015/05/Skarpnes_leggeanvisning_Domino.pdf`. Accessed: 08.04.2019.

[35] HT-Instruments. *I-V Curve Tracer for maintenance and troubleshooting of photovoltaic systems*, 2019. Available: `https://www.ht-instruments.com/en/products/photovoltaic-testers/i-v-curve-tracers/i-v500w/`. Accessed: 16.04.2019.

[36] Fluke. *Flukes Ti400-kamera for termisk bildebehandlingFlukes Ti400-kamera for termisk bildebehandling*, 2019. Available: `https://www.fluke.com/no-no/produkt/termokameraer/ti400`. Accessed: 16.04.2019.

[37] Kadra Branker, MJM Pathak, and Joshua M Pearce. A review of solar photovoltaic levelized cost of electricity. *Renewable and sustainable energy reviews*, 15(9):4470–4482, 2011.

[38] Sparelys. *Solis 3fase IT 230V 6000w m/DC bryter*, 2019. Available:`https://www.sparelys.no/index.php?option=com_virtuemart&Itemid=39&page=shop.product_details&flypage=flypage_ny.tpl&product_id=2807&category_id=216&gclid=CjwKCAjwy7vlBRACEiwAZvdx9pvLe7hp4_q4KEslkMRFxPXOi_p7HhKrUJt3eH5pcO701IMln3EoahoCnyMQAvD_BwE&vmcchk=1&fbclid=IwAR1bumeyQM5fjQWUjf4xZaC-4tKLNUPRyh0569dYBXfUR6wDx3T-mw2v7wc`. Accessed: 024.02.2019.

[39] Sun-Net. Soltak kalkulator, 2019. Online; Available from: https://sun-net.no/soltak-kalkulator/ accessed March 17, 2019.

[40] Finansdepartementet. *R-14/99 99/5661 C Behandling av diskonteringsrente, risiko, kalkulasjonspriser og skattekostnad i samfunnsøkonomiske analyser*, 1999. Available: https://www.regjeringen.no/no/dokumenter/r-1499-995661-c-behandling-av-diskonteri/id108418/?fbclid=IwAR3Tuwx7ibGkbyG6rT_FfGLfpFWlcLm3Sho4Mx-zNOWzTnIVMLMic-hQTQA. Accessed: 26.04.2019.

[41] Fraunhofer Institute for Solar Energy Systems. *LEVELIZED COST OF ELECTRICITY RENEWABLE ENERGY TECHNOLOGIES*, 2018. Available: https://www.ise.fraunhofer.de/content/dam/ise/en/documents/publications/studies/EN2018_Fraunhofer-ISE_LCOE_Renewable_Energy_Technologies.pdf. Accessed: 18.04.2019.

A Appendix

A.1 Datasheet

Solarziegel TCRDO 900

Autarq Solarziegel

Autarq veredelt hochwertige Ziegel mit einem Solarmodul. So wird ihre Solaranlage dezent und hochwertig in ihr Dach integriert. Unsere Solarziegel gibt es passend zu verschiedenen Ziegeln und zu jeder Dachform. Sie werden wie die Originalziegel verlegt und sind genauso wasserdicht. Autarq Solarziegel werden in Deutschland hergestellt.

Sicher und langlebig

Autarq Solaranlagen arbeiten im sicheren Kleinspannungsbereich unterhalb 120 V. Dies ermöglicht eine sichere und einfache Verlegung gemäß Brandschutznorm VDE 0100-712 und verhindert Elektrosmog. Die Brandlast des Daches wird durch die Solarziegel nicht erhöht. Wir verwenden nur erprobte Standardmaterialien mit hoher Lebensdauer.
Alle verwendeten Materialien sind UV- und witterungsbeständig, ungiftig und recyclingfähig.
Unsere Leistungszusage: auch nach 25 Jahren erzeugen Autarq Solarziegel noch mindestens 80 % der elektrischen Ausgangsleistung.

TCRDO 900 – der Solarziegel für das Ziegelprogramm Domino® von Creaton®

Die Wasserführung und Hinterlüftung des bewährten Domino® Systems von Creaton® bleiben erhalten. Die Anordnung der Solarfelder kann sehr flexibel den Wünschen unserer Kunden angepasst werden. Beim Verlegen werden die Solarziegel durch geprüfte Steckverbindungen untereinander verbunden. Alle Verbindungskabel bleiben unter den Ziegeln verborgen und sind gegen Witterungseinflüsse geschützt. Unsere Anlagen werden als Gesamtsystem inclusive Planung und Beratung, Batteriespeicher, Wechselrichter und Monitoring geliefert.

www.autarq.com

Daten TCRDO 900

Elektrische Daten (STC)	
Nennleistung P_{MPP}	9 W
Nennspannung U_{MPP}	37 V
Nennstrom I_{MPP}	0,245 A
Leerlaufspannung U_{OC}	47 V
Kurzschlussstrom I_{SC}	0,265 A
Temperaturkoeffizient	-0,45 %/K
Elektrische Werte bei Standard-Testbedingungen (STC): 1000 W/m²; 25°C; AM 1,5	

Garantieleistung und Zertifizierung	
Produktgarantie	5 Jahre
Leistungszusage	25 Jahre 80 % der elektrischen Leistung
Normen	IEC 61215, IEC 61730
Hagelschutzklasse	5 (extra schwere Hageleinwirkung)
Brandschutz	Kleinspannungssystem erfüllt VDE 0100-712
Brandbeständigkeit	EN 13501-1 Brandschutzklasse B

Materialdaten	
Abmessungen	257 mm x 437 mm
Gewicht	5 kg
mechanische Belastbarkeit	5400 Pa, hagel- und schneesicher, begehbar
Betriebstemperatur	- 40 bis + 85 °C
Steckverbinder	MC3 kompatibel, UV-fest
Ziegelmaterial	Ton
Solarzellen	monokristallin
Frontglas	3,2 mm gehärtetes Solarglas (ESG)
Anschlusskabel	2 x 4 mm² Solarkabel gemäß PV1F Norm

Kenndaten Gesamtsystem	
Leistung pro Ziegelfläche:	110 W/m²
Systemspannung:	max. 120 V Kleinspannung

Autarq Solarziegel TCRDO 900 werden im Verbund mit **Creaton Domino** Ziegeln auf konventionelle Weise zu einem hinterlüfteten Ziegeldach eingedeckt. Die Solarziegel werden durch Steckverbindungen miteinander verbunden. Die jeweils nicht mit Solarziegeln belegten Flächen wie First, Ortgang und andere Sonderziegel werden mit „Creaton Domino“ Ziegeln aus dem Programm des Herstellers belegt und erlauben eine ästhetische Integration der Solaranlage in die Architektur Ihres Gebäudes.

Ziegel / Dach

Ziegelbedarf:	12 Stück/m²
Empfohlene Dachlatten:	40x60mm
Decklänge (Lattenabstand):	350-354mm
Deckbreite:	223-225mm
Dachneigung:	15-60°
Empfohlene Deckung:	im Verband (versetzt)
Farben:	rot, schwarz, anthrazit
Verpackung:	4er Pack

Weitere Daten zum Ziegel Domino und Details zur Belegung entnehmen Sie bitte dem Originaldatenblatt der Firma Creaton (www.creaton.de).

Autarq GmbH, Brüssower Allee 87, D-17291 Prenzlau, Germany
Hotline: 040 4018 7860, E-Mail: info@autarq.com
www.autarq.com

Version 12/2017. Gültigkeit bis 30.06.2018. Technische Änderungen und Irrtümer bleiben vorbehalten.

BIG SUN
— Your Best Energy

Mono Crystalline Silicon Solar Cell

Physical Characteristics

Dimension	156.75 mm x 156.75 mm ± 0.5 mm
Diagonal	210 mm ± 1.0 mm (round chamfers)
Thickness (Si)	200μm ± 30μm
Front	Three silver busbars, anisotropically texturized surface with dark blue silicon nitride anti-reflection coating.
Back	Full-surface aluminum BSF, Silver / Aluminum soldering pads.

Electrical Characteristics

Efficiency Code	2010	2000	1990	1980	1970	1960
Efficiency (%)	20.1	20.0	19.9	19.8	19.7	19.6
Pmax (W)	4.910	4.886	4.862	4.837	4.813	4.788
Vmpp (V)	0.548	0.546	0.545	0.543	0.542	0.540
Impp (A)	8.968	8.961	8.945	8.930	8.913	8.899
Voc (V)	0.646	0.645	0.644	0.644	0.642	0.641
Isc (A)	9.453	9.446	9.430	9.415	9.401	9.394

*Data under standard testing conditions (STC): 1000 W/M^2, AM1.5, 25°C. All figures bear ±5% of tolerance. The measurement of cell is calibrated by Fraunhofer ISE.
Model name = Product code + Efficiency code. Example: B156X1D2A-1970

Typical Temperature Coefficients

Voltage	-0.314%/°C
Current	+0.034%/°C
Power	-0.336%/°C

Spectral Response (SR)

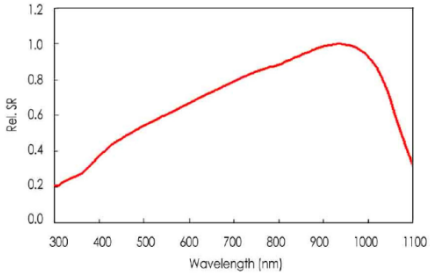

IV Curve of Cell: 1960

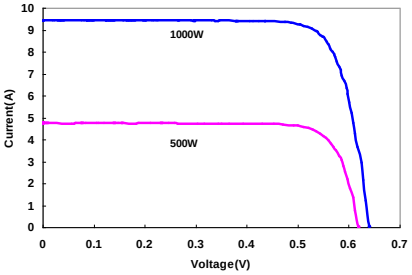

Quality

BIG SUN's Quality system is certified by ISO 9001, Environmental Management System by ISO 14001, Occupational Health and Safety Management System by OHSAS 18001.

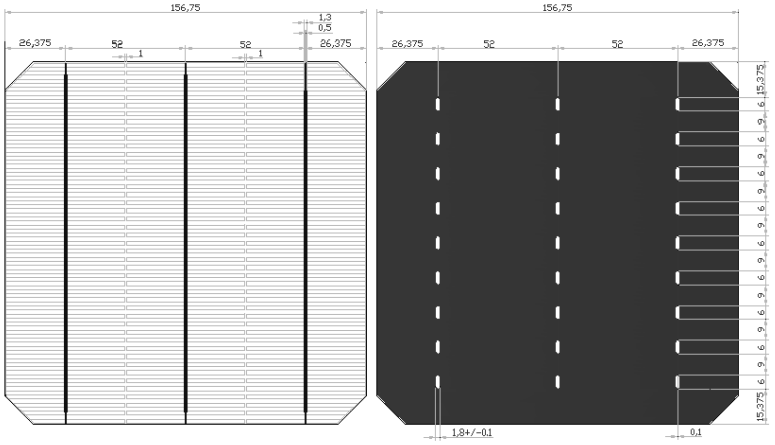

BIG SUN Energy Technology Inc.
No. 458-9, Sinsing Rd., Hukou Township,
Hsinchu County 30353, Taiwan
T: +886 3 598-0288
F: +886 3 598-0299
E: sales@bigsun-energy.com

Subject to specification changes without notification.

CR1000X Specifications

Datalogger

Electrical specifications are valid over a -40 to +70 °C, non-condensing environment, unless otherwise specified. Extended electrical specifications (noted as XT in specifications) are valid over a -55 to +85 °C non-condensing environment. Recalibration is recommended every three years. Critical specifications and system configuration should be confirmed with Campbell Scientific before purchase.

System specifications

Processor: Renesas RX63N (32-bit with hardware FPU, running at 100 MHz)

Memory:

- Total onboard: 128 MB of flash + 4 MB battery-backed SRAM
  - Data storage: 4 MB SRAM + 72 MB flash (extended data storage automatically used for auto-allocated Data Tables not being written to a card)
  - CPU drive: 30 MB flash
  - OS load: 8 MB flash
  - Settings: 1 MB flash
  - Reserved (not accessible): 10 MB flash
- Data storage expansion: Removable microSD flash memory, up to 16 GB

Program Execution: 1 ms to 1 day

Real-Time Clock:

- Battery backed while external power is disconnected
- **Resolution**: 1 ms
- **Accuracy**: ±3 min. per year, optional GPS correction to ±10 µs

Wiring Panel Temperature: Measured using a 10K3A1A BetaTHERM thermistor, located between the two rows of analog input terminals.

Physical specifications

Dimensions: 23.8 x 10.1 x 6.2 cm (9.4 x 4.0 x 2.4 in); additional clearance required for cables and wires.

Weight/Mass: 0.86 kg (1.9 lb)

Case Material: Powder-coated aluminum

Power requirements

Protection: Power inputs are protected against surge, over-voltage, over-current, and reverse power. IEC 61000-4 Class 4 level.

Power In Terminal:

- **Voltage Input**: 10 to 18 VDC
- **Input Current Limit at 12 VDC**:
  - 4.35 A at -40 °C
  - 3 A at 20 °C
  - 1.56 A at 85 °C
- 30 VDC sustained voltage limit without damage.

USB Power: Functions that will be active with USB 5 VDC include sending programs, adjusting data logger settings, and making some measurements. If USB is the only power source, then the CS I/O port and the 5V, 12V, and SW12 terminals will not be operational.

Internal Lithium Battery: AA, 2.4 Ah, 3.6 VDC (Tadiran TL 5903/S) for battery-backed SRAM and clock. 3-year life with no external power source.

Average Current Drain:

Assumes 12 VDC on POWER IN terminals.

- **Idle**: <1 mA
- **Active 1 Hz Scan**: 1 mA
- **Active 20 Hz Scan**: 55 mA
- **Serial** (RS-232/RS-485): Active + 25 mA
- **Ethernet Power Requirements**:
  - **Ethernet 1 Minute**: Active + 1 mA
  - **Ethernet Idle**: Active + 4 mA
  - **Ethernet Link**: Active + 47 mA

Vehicle Power Connection: When primary power is pulled from the vehicle power system, a second power supply OR charge

May 14, 2019

regulator may be required to overcome the voltage drop at vehicle start-up.

Power output specifications

System Power Out Limits (when powered with 12 VDC)

Temperature (°C)	Current Limit[1] (A)
–40°	4.53
20°	3.00
70°	1.83
85°	1.56

[1] Limited by self-resetting thermal fuse

12V and SW12V Power Output Terminals

12V, SW12-1, and SW12-2: Provide unregulated 12 VDC power with voltage equal to the Power Input supply voltage. These are disabled when operating on USB power only.

SW12 current limits	
Temperature (°C)	**Current Limit [1] (mA)**
–40°	1310
0°	1004
20°	900
50°	690
70°	550
80°	470

[1] Thermal fuse hold current.

5 V and 3.3 V

5V: One regulated 5 V output. Supply is shared between the 5V terminal and CS I/O DB9 5 V output.

- **Voltage Output**: Regulated 5 V output (±5%)
- **Current Limit**: 230 mA

C as Power Output

- C Terminals:
  - **Output Resistance (R_o)**: 150 Ω
  - **5 V Logic Level Drive Capacity**: 10 mA @ 3.5 VDC
  - **3.3 V Logic Level Drive Capacity**: 10 mA @ 1.8 VDC

CS I/O Pin 1

5 V Logic Level Max Current: 200 mA

Analog measurements specifications

16 single-ended (SE) or 8 differential (DIFF) terminals individually configurable for voltage, thermocouple, current loop, ratiometric, and period average measurements, using a 24-bit ADC. One channel at a time is measured.

Voltage measurements

Terminals:

- **Differential Configuration**: DIFF 1H/1L – 8H/8L
- **Single-Ended Configuration**: SE1 – SE16

Input Resistance: 20 GΩ typical

Input Limits: ±5 V

Sustained Input Voltage without Damage: ±20 VDC

DC Common Mode Rejection:

- > 120 dB with input reversal
- ≥ 86 dB without input reversal

Normal Mode Rejection: > 70 dB @ 60 Hz

Input Current @ 25 °C: ±1 nA typical

Filter First Notch Frequency (f_{N1}) Range: 0.5 Hz to 31.25 kHz (user specified)

Analog Range and Resolution:

		Differential with Input Reversal		Single-Ended and Differential without Input Reversal	
Notch Frequency (f_{N1}) (Hz)	**Range[1] (mV)**	**RMS (µV)**	**Bits[2]**	**RMS (µV)**	**Bits[2]**
15000	±5000 ±1000 ±200	8.2 1.9 0.75	20 20 19	11.8 2.6 1.0	19 19 18
50/60[3]	±5000 ±1000 ±200	0.6 0.14 0.05	24 23 22	0.88 0.2 0.08	23 23 22
5	±5000 ±1000 ±200	0.18 0.04 0.02	25 25 24	0.28 0.07 0.03	25 24 23

[1] Range overhead of ~5% on all ranges guarantees that full-scale values will not cause over range

[2] Typical effective resolution (ER) in bits; computed from ratio of full-scale range to RMS resolution.

[3] 50/60 corresponds to rejection of 50 and 60 Hz ac power mains noise.

Accuracy (does not include sensor or measurement noise):

- 0 to 40 °C: ±(0.04% of measurement + offset)
- –40 to 70 °C: ±(0.06% of measurement + offset)

Voltage Measurement Accuracy Offsets:

	Typical Offset (µV RMS)	
Range (mV)	Differential with Input Reversal	Single-Ended or Differential without Input Reversal
±5000	±0.5	±2
±1000	±0.25	±1
±200	±0.15	±0.5

Measurement Settling Time: 20 µs to 600 ms; 500 µs default

Multiplexed Measurement Time:

Measurement time = INT(multiplexed measurement time • (reps+1) + 2ms

	Differential with Input Reversal	Single-Ended or Differential without Input Reversal
Example fN1[1] (Hz)	Time[2] (ms)	Time[2] (ms)
15000	2.04	1.02
60	35.24	17.62
50	41.9	20.95
5	401.9	200.95

[1] Notch frequency (1/integration time).

[2] Default settling time of 500 µs used.

Resistance measurements specifications

The data logger makes ratiometric-resistance measurements for four- and six-wire full-bridge circuits and two-, three-, and four-wire half-bridge circuits using voltage excitation. Excitation polarity reversal is available to minimize dc error.

Accuracy:

Assumes input reversal for differential measurements `RevDiff` and excitation reversal `RevEx` for excitation voltage <1000 mV. Does not include bridge resistor errors or sensor and measurement noise.

- **0 to 40 °C**: ±(0.01% of voltage measurement + offset)
- **–40 to 70 °C**: ±(0.015% of voltage measurement + offset)
- **–55 to 85 °C (XT)**: ±(0.02% of voltage measurement + offset)

Period-averaging measurement specifications

Terminals: SE terminals 1-16

Accuracy: ±(0.01% of measurement + resolution), where resolution is 0.13 µs divided by the number of cycles to be measured

Ranges:

- Minimum signal centered around specified period average threshold.
- Maximum signal centered around data logger ground.
- Maximum frequency = 1/(2 * (minimum pulse width)) for 50% duty cycle signals

Gain Code Option	Voltage Gain	Minimum Peak to Peak Signal (mV)	Maximum Peak to Peak Signal (V)	Minimum Pulse Width (µs)	Maximum Frequency (kHz)
0	1	500	10	2.5	200
1	2.5	50	2	10	50
2	12.5	10	2	62	8
3	64	2	2	100	5

Current-loop measurement specifications

The data logger makes current-loop measurements by measuring across a current-sense resistor associated with the RS-485 resistive ground terminal.

Terminals: RG1 and RG2

Maximum Input Voltage: ±16 V

Resistance to Ground: 101 Ω

Current Measurement Shunt Resistance: 10 Ω

Maximum Current Measurement Range: ±80 mA

Absolute Maximum Current: ±160 mA

Resolution: ≤ 20 nA

Accuracy: ±(0.1% of reading + 100 nA) @ -40 to 70 °C

Pulse measurement specifications

Two inputs (P1-P2) individually configurable for switch closure, high-frequency pulse, or low-level AC measurements. See also Digital input/output specifications (p. 4). Each terminal has its own independent 32-bit counter.

> **NOTE:**
> Conflicts can occur when a control port pair is used for different instructions (`TimerInput()`, `PulseCount()`, `SDI12Recorder()`, `WaitDigTrig()`). For example, if C1 is used for `SDI12Recorder()`, C2 cannot be used for `TimerInput()`, `PulseCount()`, or `WaitDigTrig()`.

Maximum Input Voltage: ±20 VDC

Maximum Counts Per Channel: 2^{32}

Maximum Counts Per Scan: 2^{32}

Input Resistance: 5 kΩ

Accuracy: ±(0.02% of reading + 1/scan)

Switch closure input

Terminals: C1-C8

Pull-Up Resistance: 100 kΩ to 5 V

Event: Low (<0.8 V) to High (>2.5 V)

Maximum Input Frequency: 150 Hz

Minimum Switch Closed Time: 5 ms

Minimum Switch Open Time: 6 ms

Maximum Bounce Time: 1 ms open without being counted

High-frequency input

Terminals: C1-C8

Resistance: Configurable in terminal pairs with 100 kΩ pull-up or pull-down

Pull-Up Resistance: 100 kΩ to 5 V

Event: Low (<0.8 V) to High (>2.5 V)

Maximum Input Frequency: 250 kHz

Low-level AC input

Minimum Pull-Down Resistance: 10 kΩ to ground

DC-offset rejection: Internal AC coupling eliminates DC-offset voltages up to ±0.05 VDC

Input Hysteresis: 12 mV at 1 Hz

Low-Level AC Pulse Input Ranges:

Sine wave (mV RMS)	Range (Hz)
20	1.0 to 20
200	0.5 to 200
2000	0.3 to 10,000
5000	0.3 to 20,000

Quadrature input

Terminals: C1-C8 can be configured as digital pairs to monitor the two sensing channels of an encoder.

Maximum Frequency: 2.5 kHz

Resolution: 31.25 µs or 32 kHz

Digital input/output specifications

Terminals configurable for digital input and output (I/O) including status high/low, pulse width modulation, external interrupt, edge timing, switch closure pulse counting, high-frequency pulse counting, UART[1], RS-232[2], RS-485[3], SDM[4], SDI-12[1], I2C[2], and SPI[3] function. Terminals are configurable in pairs for 5 V or 3.3 V logic for some functions.

> **NOTE:**
> Conflicts can occur when a control port pair is used for different instructions (`TimerInput()`, `PulseCount()`, `SDI12Recorder()`, `WaitDigTrig()`). For example, if C1 is used for `SDI12Recorder()`, C2 cannot be used for `TimerInput()`, `PulseCount()`, or `WaitDigTrig()`.

Terminals: C1-C8

Maximum Input Voltage: ±20 V

Logic Levels and Drive Current:

Terminal Pair Configuration	5 V Source	3.3 V Source
Logic low	≤ 1.5 V	≤ 0.8 V
Logic high	≥ 3.5 V	≥ 2.5 V

Edge timing

Terminals: C1-C8

Maximum Input Frequency: ≤ 1 kHz

Resolution: 500 ns

Edge counting

Terminals: C1-C8

Maximum Input Frequency: ≤ 2.3 kHz

Quadrature input

Terminals: C1-C8 can be configured as digital pairs to monitor the two sensing channels of an encoder.

Maximum Frequency: 2.5 kHz

Resolution: 31.25 µs or 32 kHz

Pulse-width modulation

Maximum Period: 36.4 seconds

Resolution:

- **0 – 5 ms**: 83.33 ns
- **5 – 325 ms**: 5.33 µs
- **> 325 ms**: 31.25 µs

Communications specifications

Ethernet Port: RJ45/ jack, 10/100Base Mbps, full and half duplex, Auto-MDIX, magnetic isolation, and TVS surge protection.

Internet Protocols: Ethernet, PPP, RNDIS, ICMP/Ping, Auto-IP (APIPA), IPv4, IPv6, UDP, TCP, TLS, DNS, DHCP, SLAAC, Telnet, HTTP(S), FTP(S), POP3/TLS, NTP, SMTP/TLS, SNMPv3, CS I/O IP

[1]Universal Asynchronous Receiver/Transmitter for asynchronous serial communications.

[2]Recommended Standard 232. A loose standard defining how two computing devices can communicate with each other. The implementation of RS-232 in Campbell Scientific dataloggers to computer communications is quite rigid, but transparent to most users. Features in the data logger that implement RS-232 communication with smart sensors are flexible.

[3]Recommended Standard 485. A standard defining how two computing devices can communicate with each other.

[4]Synchronous Device for Measurement. A processor-based peripheral device or sensor that communicates with the data logger via hardwire over a short distance using a protocol proprietary to Campbell Scientific.

[1]Serial Data Interface at 1200 baud. Communication protocol for transferring data between the data logger and SDI-12 compatible smart sensors.

[2]Inter-Integrated Circuit is a multi-master, multi-slave, packet switched, single-ended, serial computer bus.

[3]Serial Peripheral Interface - a clocked synchronous interface, used for short distance communications, generally between embedded devices.

Additional Protocols: CPI, PakBus, PakBus Encryption, SDM, SDI-12, Modbus RTU / ASCII / TCP, DNP3, custom user definable over serial, UDP, NTCIP, NMEA 0183, I2C, SPI

USB Device: Micro-B device for computer connectivity

CS I/O: 9-pin D-sub connector to interface with Campbell Scientific CS I/O peripherals.

RS-232/CPI: Single RJ45 module port that can operate in one of two modes: RS-232 or CPI. RS-232 connects to computer, sensor, or communications devices serially. CPI interfaces with Campbell Scientific CDM[1] measurement peripherals and sensors.

SDI-12 (C1, C3, C5, C7): Four independent SDI-12 compliant terminals are individually configured and meet SDI-12 Standard v 1.4.

Hardwired: Multi-drop, short haul, RS-232, fiber optic

Satellite: GOES, Argos, Inmarsat Hughes, Irridium

Standards compliance specifications

View EU Declarations of Conformity at www.campbellsci.com/cr1000x.

Shock and Vibration: MIL-STD 810G methods 516.6 and 514.6

EMI and ESD protection:

- **Immunity**: Meets or exceeds following standards:
  - **ESD**: per IEC 61000-4-2; ±8 kV air, ±4 kV contact discharge
  - **RF**: per IEC 61000-4-3; 3 V/m, 80-1000 MHz
  - **EFT**: per IEC 61000-4-4; 1 kV power, 500 V I/O
  - **Surge**: per IEC 61000-4-5; 1 kV power and I/O
  - **Conducted**: per IEC 61000-4-6; 3 V 150 kHz-80 MHz
- Emissions and immunity performance criteria available on request.

Warranty

Standard: Three years against defects in materials and workmanship.

Extended (optional): An additional four years. against defects in materials and workmanship, bringing the total to 7 years.

[1]CPI is a proprietary interface for communications between Campbell Scientific dataloggers and Campbell Scientific CDM peripheral devices. It consists of a physical layer definition and a data protocol. CDM devices are similar to Campbell Scientific SDM devices in concept, but the use of the CPI bus enables higher data-throughput rates and use of longer cables. CDM devices require more power to operate in general than do SDM devices.

CAMPBELL SCIENTIFIC®
WHEN MEASUREMENTS MATTER

Global Sales & Support Network

A worldwide network of companies to help meet your needs

Australia
Location: Garbutt, QLD Australia
Phone: 61.7.4401.7700
Email: info@campbellsci.com.au
Website: www.campbellsci.com.au

Brazil
Location: São Paulo, SP Brazil
Phone: 11.3732.3399
Email: vendas@campbellsci.com.br
Website: www.campbellsci.com.br

Canada
Location: Edmonton, AB Canada
Phone: 780.454.2505
Email: dataloggers@campbellsci.ca
Website: www.campbellsci.ca

China
Location: Beijing, P. R. China
Phone: 86.10.6561.0080
Email: info@campbellsci.com.cn
Website: www.campbellsci.com

Costa Rica
Location: San Pedro, Costa Rica
Phone: 506.2280.1564
Email: info@campbellsci.cc
Website: www.campbellsci.cc

France
Location: Vincennes, France
Phone: 0033.0.1.56.45.15.20
Email: info@campbellsci.fr
Website: www.campbellsci.fr

Germany
Location: Bremen, Germany
Phone: 49.0.421.460974.0
Email: info@campbellsci.de
Website: www.campbellsci.de

South Africa
Location: Stellenbosch, South Africa
Phone: 27.21.8809960
Email: sales@campbellsci.co.za
Website: www.campbellsci.co.za

Southeast Asia
Location: Bangkok, Thailand
Phone: 66.2.719.3399
Email: thitipongc@campbellsci.asia
Website: www.campbellsci.asia

Spain
Location: Barcelona, Spain
Phone: 34.93.2323938
Email: info@campbellsci.es
Website: www.campbellsci.es

UK
Location: Shepshed, Loughborough, UK
Phone: 44.0.1509.601141
Email: sales@campbellsci.co.uk
Website: www.campbellsci.co.uk

USA
Location: Logan, UT USA
Phone: 435.227.9120
Email: info@campbellsci.com
Website: www.campbellsci.com

JUMO GmbH & Co. KG

Delivery address: Mackenrodtstraße 14,
36039 Fulda, Germany
Postal address: 36035 Fulda, Germany
Phone: +49 661 6003-0
Fax: +49 661 6003-607
e-mail: mail@jumo.net
Internet: www.jumo.net

JUMO Instrument Co. Ltd.

JUMO House
Temple Bank, Riverway
Harlow, Essex CM 20 2TT, UK
Phone: +44 1279 635533
Fax: +44 1279 635262
e-mail: sales@jumo.co.uk
Internet: www.jumo.co.uk

JUMO PROCESS CONTROL INC.

885 Fox Chase, Suite 103
Coatesville PA 19320, USA
Phone: 610-380-8002
1-800-554-JUMO
Fax: 610-380-8009
e-mail: info@JumoUSA.com
Internet: www.JumoUSA.com

Platinum-chip temperature sensors with connecting wires to EN 60 751

- **for temperatures from -70 to +600 °C**
- **standardized nominal values and tolerances**
- **resistance values from 20 to 5000Ω**
- **linear characteristic**
- **fast response**
- **highly resistant to shock and vibration**
- **low price level**

PCA style

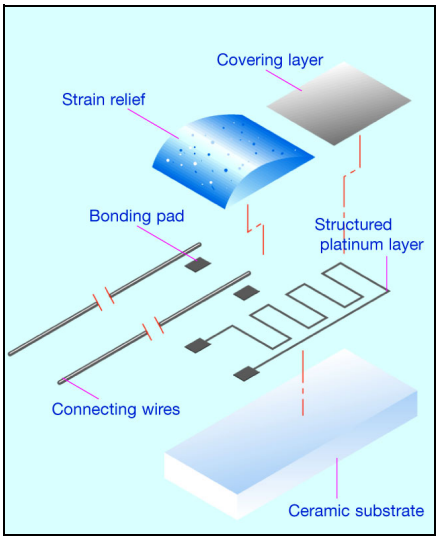

Introduction

Platinum-chip temperature sensors belong to the category of temperature sensors that incorporate thin-film techniques. They are produced at JUMO under clean-room conditions using state-of-the-art technology. A platinum layer, which constitutes the active layer, is sputtered onto a ceramic substrate and subsequently formed into a serpentine structure by a photolithographic procedure. Afterwards, a laser trimming process is used for fine calibration. After calibration, a special glass covering layer is fused onto the platinum serpentine, as a protection against external effects and for insulation. The electrical connection is made through contact areas to which the connecting wires are bonded. Depending on the version, the connecting wires may consist of different materials and may, within certain limits, also have varying lengths and diameters. A further glass layer that is applied to the contact area fixes the connecting wires and additionally provides strain relief.

A large variety of PCA style platinum-chip temperature sensors can be supplied ex-stock as Pt100, Pt500 or Pt1000 temperature sensors. Special nominal values can be produced on request. High-resistance platinum-chip temperature sensors in small sizes are also available. And, thanks to their low mass, very fast response times are achieved. Furthermore, they are outstandingly resistant to shock and vibration when installed and fixed. The operating temperature depends on the particular version, but generally covers -70 to +600°C. However, these platinum-chip temperature sensors can also be used with temperatures far below -70°C, provided that shifts in the nominal value and hysteresis effects, which may occur within certain limits, can be tolerated.

Most temperature applications in the market make use of platinum-chip temperature sensors as the active component for acquiring temperature. Typical application areas can be found in HVAC, medical and laboratory technology, white goods, automobiles and utility vehicles as well as in machinery construction and industrial engineering.

Technical publication

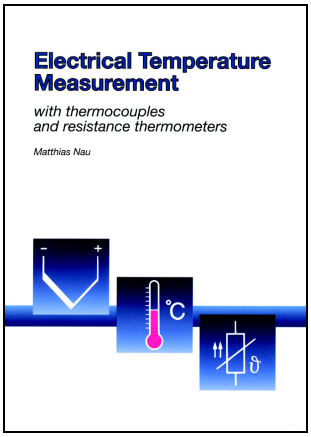

This revised edition takes account of altered standards and recent developments. The new chapter “Measurement uncertainty” incorporates the basic concept of the internationally recognized ISO guideline “Guide to the expression of uncertainty in measurement” (abbreviated: GUM).
In addition, the chapter on explosion protection for thermometers has been updated in view of the European Directive 94/9/EC, which has been in force since 1st July 2003.

February 2003, 164 pages
Publication FAS 146
Sales No. 90/00085081
ISBN 3-935742-07-X

JUMO platinum temperature sensors

Construction and application of platinum temperature sensors	Data Sheet 90.6000
Platinum-glass temperature sensors	Data Sheet 90.6021
Platinum-ceramic temperature sensors	Data Sheet 90.6022
Platinum-foil temperature sensors	Data Sheet 90.6023
Platinum-glass temperature sensors with glass extension	Data Sheet 90.6024
Platinum-chip temperature sensors with connecting wires	Data Sheet 90.6121
Platinum-chip temperature sensors on epoxy card	Data Sheet 90.6122
Platinum-chip temperature sensors with terminal clamps	Data Sheet 90.6123
Platinum-chip temperature sensors in cylindrical style	Data Sheet 90.6124
Platinum-chip temperature sensors in SMD style	Data Sheet 90.6125

01.05/00311575

JUMO GmbH & Co. KG

Delivery address: Mackenrodtstraße 14, 36039 Fulda, Germany
Postal address: 36035 Fulda, Germany
Phone: +49 661 6003-0
Fax: +49 661 6003-607
e-mail: mail@jumo.net
Internet: www.jumo.net

JUMO Instrument Co. Ltd.

JUMO House
Temple Bank, Riverway
Harlow, Essex CM 20 2TT, UK
Phone: +44 1279 635533
Fax: +44 1279 635262
e-mail: sales@jumo.co.uk
Internet: www.jumo.co.uk

JUMO PROCESS CONTROL INC.

885 Fox Chase, Suite 103
Coatesville PA 19320, USA
Phone: 610-380-8002
1-800-554-JUMO
Fax: 610-380-8009
e-mail: info@JumoUSA.com
Internet: www.JumoUSA.com

Platinum-chip temperature sensors with connecting wires to EN 60 751

PCA/L style

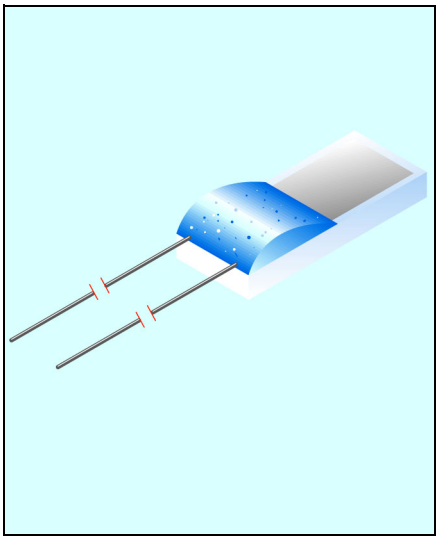

Brief description

Platinum-chip temperature sensors are based on a temperature-dependent resistance whose development and permissible tolerances are defined in the international standard EN 60 751. They combine the favorable properties of a platinum temperature sensor with the advantages of large-scale production. Their distinctive features are standardization and universal interchangeability, as well as high measurement accuracy, excellent long-term stability and good reproducibility of the electrical properties. Furthermore, prices have fallen considerably in recent years, since these sensors are designed to meet large-quantity requirements. With regard to the price, platinum-chip temperature sensors are therefore a genuine alternative to thermistors, which are based on semiconductors.

Platinum-chip temperature sensors, L version, are mainly used in the fabrication of various probes with connecting cables. They are particularly suitable for electrical connection through soft-soldered joints. The connecting wires are made from pure silver and are ideal for this purpose.

The application temperature ranges from -70 to +250 °C. However, the maximum temperature is +350 °C, which opens up additional application possibilities.

Temperature sensors in blister belt packaging or packed in bags

Temperature sensor						Connecting wire				Sales No. for tolerance class		
Type	R_0/Ω	W	L	H	S	Material	Dim.	L1	R_L in mΩ/mm	1/3 DIN B	A	B
PCA 1.2005.1L	1x100	2.0	5	1.3	0.64	Ag	0.2 x 0.3	10	0.3	90/00063358T 90/00415828B	90/00417995T 90/00415827B	90/00063260T 90/00415826B
PCA 1.2005.5L	1x500	2.0	5	1.3	0.64	Ag	0.2 x 0.3	10	0.3	90/00063359T 90/00415831B	90/00417996T 90/00415830B	90/00063261T 90/00415829B
PCA 1.2010.1L	1x100	2.0	10	1.3	0.64	Ag	0.2 x 0.3	10	0.3	90/00047408T 90/00415819B	90/00062559T 90/00415818B	90/00044789T 90/00415817B
PCA 1.2010.1L	1x100	2.0	10	1.3	0.64	Ag	0.2 x 0.3	30	0.3	on request -	on request -	90/00323380T -
PCA 1.2010.5L	1x500	2.0	10	1.3	0.64	Ag	0.2 x 0.3	10	0.3	90/00049133T 90/00415822B	on request 90/00415821B	90/00048147T 90/00415820B
PCA 1.2010.10L	1x1000	2.0	10	1.3	0.64	Ag	0.2 x 0.3	10	0.3	90/00062567T 90/00415825B	90/00062566T 90/00415824B	90/00062565T 90/00415823B
PCA 1.2010.50L	1x5000	2.0	10	1.3	0.64	Ag	0.2 x 0.3	10	0.3	on request on request	on request on request	90/00430080T 90/00430081B

Dim. tolerances: ΔB = ±0.2 / ΔL = ±0.5 / ΔH = ±0.2 / ΔS = ±0.1 / ΔDim. = approx. dim. / ΔL1 = ±0.5
Dimensions mm.

For a definition of the tolerance classes, see Data Sheet 90.6000
T = bag, B = blister belt

Dimensional drawing

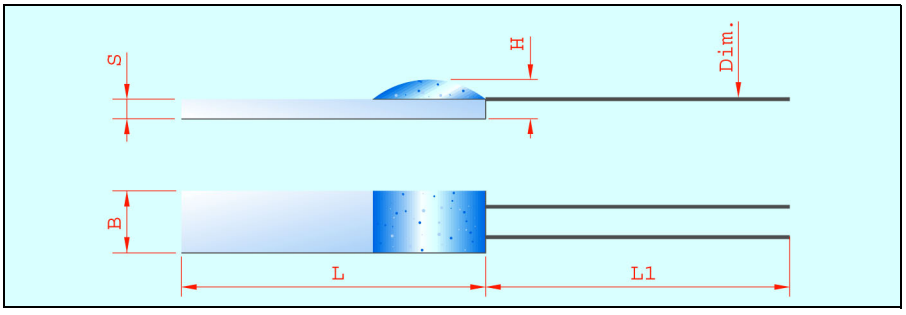

JUMO GmbH & Co. KG

Delivery address: Mackenrodtstraße 14, 36039 Fulda, Germany
Postal address: 36035 Fulda, Germany
Phone: +49 661 6003-0
Fax: +49 661 6003-607
e-mail: mail@jumo.net
Internet: www.jumo.net

JUMO Instrument Co. Ltd.

JUMO House
Temple Bank, Riverway
Harlow, Essex CM 20 2TT, UK
Phone: +44 1279 635533
Fax: +44 1279 635262
e-mail: sales@jumo.co.uk
Internet: www.jumo.co.uk

JUMO PROCESS CONTROL INC.

885 Fox Chase, Suite 103
Coatesville PA 19320, USA
Phone: 610-380-8002
1-800-554-JUMO
Fax: 610-380-8009
e-mail: info@JumoUSA.com
Internet: www.JumoUSA.com

Technical data

Standard
EN 60 751

Temperature coefficient
$\alpha = 3.850 \times 10^{-3} °C^{-1}$ (between 0 and 100 °C)

Temperature range
-70 to +250 °C (+350 °C)

Tolerance

Temperature validity range Class 1/3 DIN B:	-50 to +200 °C
Temperature validity range Class A:	-70 to +300 °C
Temperature validity range Class B:	-70 to +350 °C

Measuring current/maximum current

Pt100	recommended: 1.0 mA	maximum: 7 mA
Pt500	recommended: 0.7 mA	maximum: 3 mA
Pt1000	recommended: 0.1 mA	maximum: 1 mA
Pt5000	recommended: 0.1 mA	maximum: 1 mA

Operating conditions
Platinum-chip temperature sensors may not be used unprotected in humid ambient conditions or corrosive atmospheres. They must also not be immersed directly in liquids. The user may have to carry out some checks before operation.

Please also refer to the Installation Instructions B 90.6121.4 "Notes on the application of platinum-chip temperature sensors."

Connecting wires
These temperature sensors feature connecting wires that are made from pure silver. The connecting wires are especially suitable for soft-soldered joints. During further processing, it is essential to ensure that the connections are not subjected to lateral pressures. The horizontal tension on the individual connecting wire must not exceed the maximum value of 5 N. Any unnecessary bending of the connecting wires must be avoided, as this may result in material fatigue and a wire break. Please also refer to section 3 "Connection methods" in our installation instructions. Longer connecting wires up to 300 mm length (in one piece) can optionally be fitted. Alternatively, extensions of any length or insulated stranded wires can, on request, be fitted at a later stage.

Measurement point
The nominal value specified refers to the standard connecting wire length L1. The measurement is acquired 2 mm from the open end of the wire. If the wire length is altered, changes in resistance will occur which may result in the tolerance class not being met.

Long-term stability
max. R_0 drift 0.05 %/year (see Data Sheet 90.6000 for definitions)

Low-temperature application
Taking into account nominal value drifts and hysteresis effects that may occur within certain limits, temperature measurements down to -200 °C are also possible. Further details can be obtained on request.

Insulation resistance
>10 MΩ at room temperature

Vibration strength
see EN 60 751, Section 4.4.2

Self-heating
$\Delta t = I^2 \times R \times E$ (see Data Sheet 90.6000 for definitions)

Packaging
Blister belt/bag

Storage
In the standard belt packaging, JUMO temperature sensors, PCA/L style, can be stored for at least 12 months under normal ambient conditions. It is not permissible to store the sensors in aggressive atmospheres, corrosive media, or in high humidiy. Since the connecting wires for this version are made from pure silver, storability is enhanced by air-tight packaging and dark surroundings. If this is not the case, the silver will tend to get tarnished with time, which may lead to difficulties when making the solder joint.

Self-heating coefficients and response times

Type	Self-heating coefficient E in °C/mW		Response times in seconds			
	in water (v = 0.2 m/sec)	in air (v = 2 m/sec)	in water (v = 0.4 m/sec)		in air (v = 1 m/sec)	
			$t_{0.5}$	$t_{0.9}$	$t_{0.5}$	$t_{0.9}$
PCA 1.2005.1L	0.02	0.2	0.1	0.3	4	16
PCA 1.2005.5L	0.02	0.2	0.1	0.3	4	16
PCA 1.2010.1L	0.02	0.2	0.3	0.3	7	22
PCA 1.2010.5L	0.01	0.2	0.3	0.5	7	22
PCA 1.2010.10L	0.01	0.2	0.3	0.5	7	22
PCA 1.2010.50L	0.01	0.2	0.3	0.5	7	22

JUMO GmbH & Co. KG

Delivery address: Mackenrodtstraße 14, 36039 Fulda, Germany
Postal address: 36035 Fulda, Germany
Phone: +49 661 6003-0
Fax: +49 661 6003-607
e-mail: mail@jumo.net
Internet: www.jumo.net

JUMO Instrument Co. Ltd.

JUMO House
Temple Bank, Riverway
Harlow, Essex CM 20 2TT, UK
Phone: +44 1279 635533
Fax: +44 1279 635262
e-mail: sales@jumo.co.uk
Internet: www.jumo.co.uk

JUMO PROCESS CONTROL INC.

885 Fox Chase, Suite 103
Coatesville PA 19320, USA
Phone: 610-380-8002
1-800-554-JUMO
Fax: 610-380-8009
e-mail: info@JumoUSA.com
Internet: www.JumoUSA.com

Platinum-chip temperature sensors with connecting wires to EN 60 751

PCA/S style

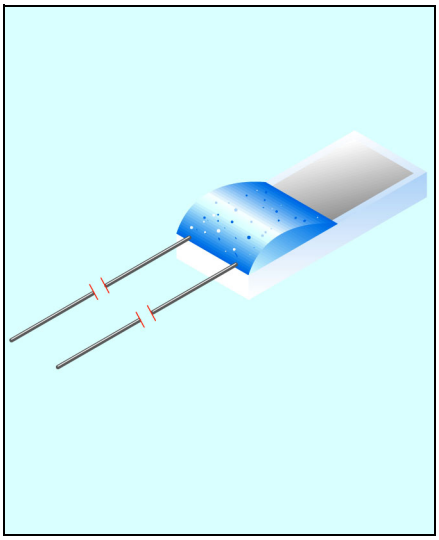

Brief description

Platinum-chip temperature sensors are based on a temperature-dependent resistance whose development and permissible tolerances are defined in the international standard EN 60 751. They combine the favorable properties of a platinum temperature sensor with the advantages of large-scale production. Their distinctive features are standardization and universal interchangeability, as well as high measurement accuracy, excellent long-term stability and good reproducibility of the electrical properties. Furthermore, prices have fallen considerably in recent years, since these sensors are designed to meet large-quantity requirements. With regard to the price, platinum-chip temperature sensors are therefore a genuine alternative to thermistors, which are based on semiconductors.

Platinum-chip temperature sensors, S version, are mainly used for applications at temperatures above 180 °C. They are particularly suitable for electrical connection through weld/crimp or hard-soldered joints. The connecting wires consist of a solid sheathed platinum wire and exhibit high strength. The application temperature ranges from -70 to +400 °C.

Temperature sensors in blister belt packaging or packed in bags

Temperature sensor						Connecting wire				Sales No. for tolerance class		
Type	R_0/Ω	W	L	H	S	Material	D1	L1	R_L in mΩ/mm	1/3 DIN B	A	B
PCA 1.2003.1S	1x100	2.0	2.5	1.3	0.64	Pt-Ni	0.20	10	2.8	90/00358368T 90/00415816B	90/00358365T 90/00415815B	90/00358363T 90/00415811B
PCA 1.2003.1S	1x100	2.0	2.5	1.3	0.64	Pt-Ni	0.20	13	2.8	90/00373811T on request	on request on request	90/00400734T on request
PCA 1.2005.1S	1x100	2.0	5	1.3	0.64	Pt-Ni	0.20	10	2.8	90/00309664T 90/00415804B	90/00089225T 90/00415803B	90/00089206T 90/00415801B
PCA 1.2005.1S	1x100	2.0	5	1.3	0.64	Pt-Ni	0.20	20	2.8	90/00364145T -	on request -	90/00357968T -
PCA 1.2005.5S	1x500	2.0	5	1.3	0.64	Pt-Ni	0.20	10	2.8	90/00309666T 90/00415807B	90/00089226T 90/00415806B	90/00089207T 90/00415805B
PCA 1.2005.5S	1x500	2.0	5	1.3	0.64	Pt-Ni	0.20	20	2.8	90/00364146T -	on request -	90/00357969T -
PCA 1.2005.10S	1x1000	2.0	5	1.3	0.64	Pt-Ni	0.20	10	2.8	90/00358360T 90/00415810B	90/00358359T 90/00415809B	90/00358358T 90/00415808B
PCA 1.2005.10S	1x1000	2.0	5	1.3	0.64	Pt-Ni	0.20	20	2.8	on request -	on request -	90/00358285T -
PCA 1.2010.1S	1x100	2.0	10	1.3	0.64	Pt-Ni	0.20	10	2.8	90/00309674T 90/00415794B	90/00089222T 90/00415793B	90/00089203T 90/00415792B
PCA 1.2010.1S	1x100	2.0	10	1.3	0.64	Pt-Ni	0.20	20	2.8	on request -	on request -	90/00067265T -
PCA 1.2010.5S	1x500	2.0	10	1.3	0.64	Pt-Ni	0.20	10	2.8	90/00309676T 90/00415797B	90/00089223T 90/00415796B	90/00089204T 90/00415795B
PCA 1.2010.10S	1x1000	2.0	10	1.3	0.64	Pt-Ni	0.20	10	2.8	90/00309681T 90/00415800B	90/00089224T 90/00415799B	90/00089205T 90/00415798B
PCA 1.2010.10S	1x1000	2.0	10	1.3	0.64	Pt-Ni	0.25	50	1.8	on request -	on request -	90/00315095T -
PCA 1.2010.20S	1x2000	2.0	10	1.3	0.64	Pt-Ni	0.20	10	2.8	on request on request	on request on request	90/00417435T 90/00417434B
PCA 1.2010.50S	1x5000	2.0	10	1.3	0.64	Pt-Ni	0.20	10	2.8	on request on request	on request on request	90/00430079T 90/00430075B

Dim. tolerances: ΔB = ±0.2 / ΔL = ±0.5 / ΔH = ±0.2 / ΔS = ±0.1 / ΔD1 = ±0.01 / ΔL1 = ±0.5
Dimensions in mm.

For a definition of the tolerance classes, see Data Sheet 90.6000
T = bag, B = blister belt

JUMO GmbH & Co. KG

Delivery address: Mackenrodtstraße 14, 36039 Fulda, Germany
Postal address: 36035 Fulda, Germany
Phone: +49 661 6003-0
Fax: +49 661 6003-607
e-mail: mail@jumo.net
Internet: www.jumo.net

JUMO Instrument Co. Ltd.

JUMO House
Temple Bank, Riverway
Harlow, Essex CM 20 2TT, UK
Phone: +44 1279 635533
Fax: +44 1279 635262
e-mail: sales@jumo.co.uk
Internet: www.jumo.co.uk

JUMO PROCESS CONTROL INC.

885 Fox Chase, Suite 103
Coatesville PA 19320, USA
Phone: 610-380-8002
1-800-554-JUMO
Fax: 610-380-8009
e-mail: info@JumoUSA.com
Internet: www.JumoUSA.com

Dimensional drawing

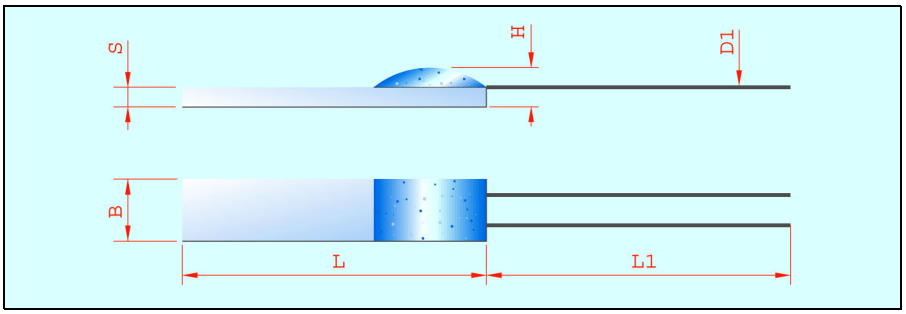

Technical data

Standard	EN 60 751
Temperature coefficient	α = 3.850 x 10^{-3} °C^{-1} (between 0 and 100 °C)
Temperature range	-70 to +400 °C
Tolerance	Temperature validity range Class 1/3 DIN B: -50 to +200 °C Temperature validity range Class A: -70 to +300 °C Temperature validity range Class B: -70 to +400 °C
Measuring current/maximum current	Pt100 recommended: 1.0 mA maximum: 7 mA Pt500 recommended: 0.7 mA maximum: 3 mA Pt1000 recommended: 0.1 mA maximum: 1 mA Pt2000 recommended: 0.1 mA maximum: 1 mA Pt5000 recommended: 0.1 mA maximum: 1 mA
Operating conditions	Platinum-chip temperature sensors may not be used unprotected in humid ambient conditions or corrosive atmospheres. They must also not be immersed directly in liquids. The user may have to carry out some checks before operation. **Please also refer to the Installation Instructions B 90.6121.4 “Notes on the application of platinum-chip temperature sensors.”**
Connecting wires	These temperature sensors feature connecting wires made from sheathed platinum wire with a nickel core. The connecting wires are suitable for crimp/weld and hard-soldered joints. During further processing, it is essential to ensure that the connections are not subjected to lateral pressures. The horizontal tension on the individual connecting wire must not exceed the maximum value of 10 N. Any unnecessary bending of the connecting wires must be avoided, as this may result in material fatigue and a wire break. Please also refer to section 3 “Connection methods” in our installation instructions. Longer connecting wires up to 300 mm length (in one piece) can optionally be fitted. Alternatively, silver wire or insulated stranded wires of whatever length is required can be used as extensions at a later time. Please note, however, that there may be restrictions on the application temperature.
Measurement point	The nominal value specified refers to the standard connecting wire length L1. The measurement is acquired 2mm from the open end of the wire. If the wire length is altered, changes in resistance will occur which may result in the tolerance class not being met.
Long-term stability	max. R_0 drift 0.05 %/year (see Data Sheet 90.6000 for definitions)
Low-temperature application	Taking into account nominal value drifts and hysteresis effects that may occur within certain limits, temperature measurements down to -200 °C are also possible. Further details can be obtained on request.
Insulation resistance	>10 MΩ at room temperature
Vibration strength	see EN 60 751, Section 4.4.2
Self-heating	$\Delta t = I^2 \times R \times E$ (see Data Sheet 90.6000 for definitions)
Packaging	Blister belt/bag
Storage	In the standard belt packaging, JUMO temperature sensors, PCA/S style, can be stored for at least 12 months under normal ambient conditions. It is not permissible to store the sensors in aggressive atmospheres, corrosive media, or in high humidity.

JUMO GmbH & Co. KG

Delivery address: Mackenrodtstraße 14,
36039 Fulda, Germany
Postal address: 36035 Fulda, Germany
Phone: +49 661 6003-0
Fax: +49 661 6003-607
e-mail: mail@jumo.net
Internet: www.jumo.net

JUMO Instrument Co. Ltd.

JUMO House
Temple Bank, Riverway
Harlow, Essex CM 20 2TT, UK
Phone: +44 1279 635533
Fax: +44 1279 635262
e-mail: sales@jumo.co.uk
Internet: www.jumo.co.uk

JUMO PROCESS CONTROL INC.

885 Fox Chase, Suite 103
Coatesville PA 19320, USA
Phone: 610-380-8002
1-800-554-JUMO
Fax: 610-380-8009
e-mail: info@JumoUSA.com
Internet: www.JumoUSA.com

Self-heating coefficients and response times

Type	Self-heating coefficient E in °C/mW		Response times in seconds			
	in water (v = 0.2m/sec)	in air (v = 2m/sec)	in water (v = 0.4m/sec)		in air (v = 1m/sec)	
			$t_{0.5}$	$t_{0.9}$	$t_{0.5}$	$t_{0.9}$
PCA 1.2003.1S	0.02	0.2	0.1	0.3	3	9
PCA 1.2005.1S	0.02	0.2	0.1	0.3	3	9
PCA 1.2005.5S	0.02	0.2	0.1	0.3	3	9
PCA 1.2005.10S	0.02	0.2	0.1	0.3	3	9
PCA 1.2010.1S	0.02	0.2	0.1	0.3	3	9
PCA 1.2010.5S	0.01	0.2	0.2	0.4	3	9
PCA 1.2010.10S	0.01	0.2	0.2	0.4	3	9
PCA 1.2010.20S	0.01	0.2	0.2	0.4	3	9
PCA 1.2010.50S	0.01	0.2	0.2	0.4	3	9

JUMO GmbH & Co. KG

Delivery address: Mackenrodtstraße 14,
36039 Fulda, Germany
Postal address: 36035 Fulda, Germany
Phone: +49 661 6003-0
Fax: +49 661 6003-607
e-mail: mail@jumo.net
Internet: www.jumo.net

JUMO Instrument Co. Ltd.

JUMO House
Temple Bank, Riverway
Harlow, Essex CM 20 2TT, UK
Phone: +44 1279 635533
Fax: +44 1279 635262
e-mail: sales@jumo.co.uk
Internet: www.jumo.co.uk

JUMO PROCESS CONTROL INC.

885 Fox Chase, Suite 103
Coatesville PA 19320, USA
Phone: 610-380-8002
1-800-554-JUMO
Fax: 610-380-8009
e-mail: info@JumoUSA.com
Internet: www.JumoUSA.com

Platinum-chip temperature sensors with connecting wires to EN 60 751

PCA/M style

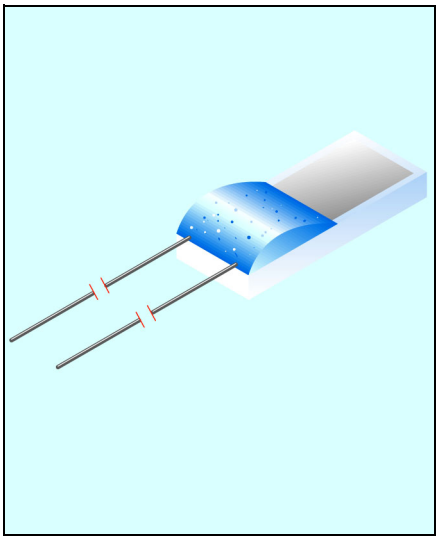

Brief description

Platinum-chip temperature sensors are based on a temperature-dependent resistance whose development and permissible tolerance is defined in the international standard EN 60 751. They combine the favorable properties of a platinum temperature sensor with the advantages of large-scale production. Their distinctive features are standardization and universal interchangeability, as well as high measurement accuracy, excellent long-term stability and good reproducibility of the electrical properties. Furthermore, prices have fallen considerably in recent years, since these sensors are designed to meet large-quantity requirements. With regard to the price, platinum-chip temperature sensors are therefore a genuine alternative to thermistors, which are based on semiconductors.

Platinum-chip temperature sensors, M version, provide the ultimate solution to most application tasks. The temperature sensors feature a particularly wide temperature range, extending from -70 to +550 °C. A large selection of different versions is available ex-stock. Miniaturized versions can also be supplied, which considerably facilitate fabrication for locations where space is at a premium. Of particular advantage is the special covering layer procedure adopted for this version, allowing unprotected use under humid ambient conditions. Typical application examples can be found in HVAC engineering, and in industrial humidity measurement.

Temperature sensors in blister belt packaging or packed in bags

Temperature sensor						Connecting wire				Sales No. for tolerance class		
Type	R_0/Ω	W	L	H	S	Material	D1	L1	R_L in mΩ/mm	1/3 DIN B	A	B
PCA 1.1505.1M	1x100	1.5	5	1.0	0.38	Pt-Ni	0.20	10	2.8	90/00409843T 90/00417179B	90/00409841T 90/00417177B	90/00409840T 90/00417178B
PCA 1.1505.1M	1x100	1.5	5	1.0	0.38	Pt-Ni	0.20	15	2.8	90/00430392T 90/00430396B	90/00430393T 90/00430394B	90/00430391T 90/00430395B
PCA 1.1505.5M	1x500	1.5	5	1.0	0.38	Pt-Ni	0.20	10	2.8	90/00409847T 90/00417185B	90/00409845T 90/00417183B	90/00409844T 90/00417184B
PCA 1.1505.10M	1x1000	1.5	5	1.0	0.38	Pt-Ni	0.20	10	2.8	90/00409850T 90/00417182B	90/00409849T 90/00417180B	90/00409848T 90/00417181B
PCA 1.1505.10M	1x1000	1.5	5	1.0	0.38	Pt-Ni	0.20	15	2.8	on request on request	on request on request	90/00425409T on request
PCA 1.2003.1M	1x100	2.0	2.5	1.3	0.64	Pt-Ni	0.20	13	2.8	90/00412342T 90/00415833B	90/00412341T 90/00415834B	90/00412318T 90/00415832B
PCA 1.2005.1M	1x100	2.0	5	1.3	0.64	Pt-Ni	0.20	10	2.8	90/00387454T 90/00415836B	90/00387455T 90/00415837B	90/00387456T 90/00415835B
PCA 1.2005.5M	1x500	2.0	5	1.3	0.64	Pt-Ni	0.20	10	2.8	90/00387453T 90/00415839B	90/00387449T 90/00415840B	90/00387465T 90/00415838B
PCA 1.2005.10M	1x1000	2.0	10	1.3	0.64	Pt-Ni	0.20	10	2.8	90/00412308T 90/00415842B	90/00412311T 90/00415843B	90/00412307T 90/00415841B
PCA 1.2010.1M	1x100	2.0	10	1.3	0.64	Pt-Ni	0.20	10	2.8	90/00412338T 90/00415845B	90/00412337T 90/00415846B	90/00412339T 90/00415844B
PCA 1.2010.5M	1x500	2.0	10	1.3	0.64	Pt-Ni	0.20	10	2.8	on request on request	on request on request	on request on request
PCA 1.2010.10M	1x1000	2.0	10	1.3	0.64	Pt-Ni	0.20	10	2.8	90/00387458T 90/00415848B	90/00387459T 90/00415849B	90/00387460T 90/00415847B

Dim. tolerances: ΔB = ±0.2 / ΔL = ±0.5 / ΔH = ±0.2 / ΔS = ±0.1 / ΔD1 = ±0.01 / ΔL1 = ±0.5
Dimensions mm.

For a definition of the tolerance classes, see Data Sheet 90.6000
T = bag, B = blister belt

JUMO GmbH & Co. KG

Delivery address: Mackenrodtstraße 14,
36039 Fulda, Germany
Postal address: 36035 Fulda, Germany
Phone: +49 661 6003-0
Fax: +49 661 6003-607
e-mail: mail@jumo.net
Internet: www.jumo.net

JUMO Instrument Co. Ltd.

JUMO House
Temple Bank, Riverway
Harlow, Essex CM 20 2TT, UK
Phone: +44 1279 635533
Fax: +44 1279 635262
e-mail: sales@jumo.co.uk
Internet: www.jumo.co.uk

JUMO PROCESS CONTROL INC.

885 Fox Chase, Suite 103
Coatesville PA 19320, USA
Phone: 610-380-8002
1-800-554-JUMO
Fax: 610-380-8009
e-mail: info@JumoUSA.com
Internet: www.JumoUSA.com

Dimensional drawing

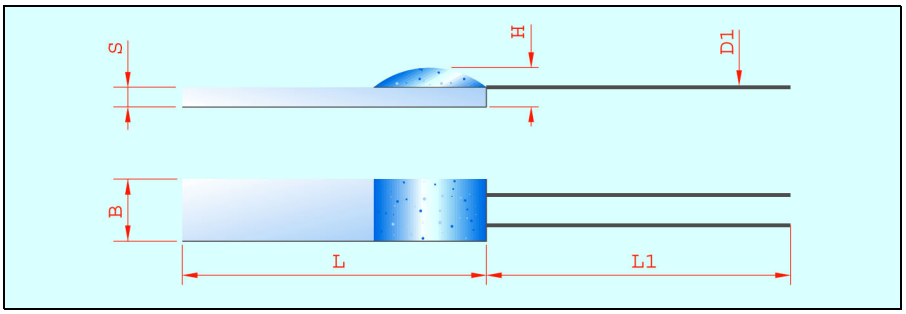

Technical data

Standard	EN 60 751
Temperature coefficient	α = 3.850 x 10^{-3} °C^{-1} (between 0 and 100 °C)
Temperature range	-70 to +550 °C
Tolerance	Temperature validity range Class 1/3 DIN B: -50 to +200 °C Temperature validity range Class A: -70 to +300 °C Temperature validity range Class B: -70 to +550 °C
Measuring current/maximum current	Pt100 recommended: 1.0 mA maximum: 7 mA Pt500 recommended: 0.7 mA maximum: 3 mA Pt1000 recommended: 0.1 mA maximum: 1 mA
Operating conditions	This version of platinum-chip temperature sensors may not be used unprotected in corrosive atmospheres. They must also not be immersed directly in liquids. The user may have to carry out some checks before operation. **Please also refer to the Installation Instructions B 90.6121.4 "Notes on the application of platinum-chip temperature sensors."**
Connecting wires	These temperature sensors feature connecting wires made from sheathed platinum wire with a nickel core. The connecting wires are suitable for crimp/weld and hard-soldered joints. During further processing, it is essential to ensure that the connections are not subjected to lateral pressures. The horizontal tension on the individual connecting wire must not exceed the maximum value of 10 N. Any unnecessary bending of the connecting wires must be avoided as this may result in material fatigue and a wire break. Please also refer to section 3 "Connection methods" in our installation instructions. Longer connecting wires up to 300 mm length (in one piece) can optionally be fitted. Alternatively, silver wire or insulated stranded wires of whatever length is required can be used as extensions at a later time. Please note that there may be restrictions on the application temperature.
Measurement point	The nominal value specified refers to the standard connecting wire length L1. The measurement is acquired 2 mm from the open end of the wire. If the wire length is altered, changes in resistance will occur which may result in the tolerance class not being met.
Long-term stability	max. R_0 drift 0.05 %/year (see Data Sheet 90.6000 for definitions)
Low-temperature application	Taking into account nominal value drifts and hysteresis effects that may occur within certain limits, temperature measurements down to -200 °C are also possible. Further details can be obtained on request.
Insulation resistance	>10 MΩ at room temperature
Vibration strength	see EN 60 751, Section 4.4.2
Self-heating	$\Delta t = I^2 \times R \times E$ (see Data Sheet 90.6000 for definitions)
Packaging	Blister belt/bag
Storage	In the standard belt packaging, JUMO temperature sensors, PCA/M style, can be stored for at least 12 months under normal ambient conditions. It is not permissible to store the sensors in aggressive atmospheres, corrosive media, or in high humidity.

JUMO GmbH & Co. KG

Delivery address: Mackenrodtstraße 14,
36039 Fulda, Germany
Postal address: 36035 Fulda, Germany
Phone: +49 661 6003-0
Fax: +49 661 6003-607
e-mail: mail@jumo.net
Internet: www.jumo.net

JUMO Instrument Co. Ltd.

JUMO House
Temple Bank, Riverway
Harlow, Essex CM 20 2TT, UK
Phone: +44 1279 635533
Fax: +44 1279 635262
e-mail: sales@jumo.co.uk
Internet: www.jumo.co.uk

JUMO PROCESS CONTROL INC.

885 Fox Chase, Suite 103
Coatesville PA 19320, USA
Phone: 610-380-8002
1-800-554-JUMO
Fax: 610-380-8009
e-mail: info@JumoUSA.com
Internet: www.JumoUSA.com

Self-heating coefficients and response times

Type	Self-heating coefficient E in °C/mW		Response times in seconds			
	in water (v = 0.2m/sec)	in air (v = 2m/sec)	in water (v = 0.4m/sec)		in air (v = 1m/sec)	
			$t_{0.5}$	$t_{0.9}$	$t_{0.5}$	$t_{0.9}$
PCA 1.1505.1M	0.02	0.2	0.1	0.3	3	8
PCA 1.1505.5M	0.02	0.2	0.1	0.3	3	8
PCA 1.1505.10M	0.02	0.2	0.1	0.3	3	8
PCA 1.2003.1M	0.02	0.2	0.1	0.3	3	9
PCA 1.2005.1M	0.02	0.2	0.1	0.3	4	16
PCA 1.2005.5M	0.02	0.2	0.1	0.3	4	16
PCA 1.2005.10M	0.02	0.2	0.2	0.3	4	16
PCA 1.2010.1M	0.02	0.2	0.3	0.5	7	22
PCA 1.2010.5M	0.01	0.2	0.3	0.5	7	22
PCA 1.2010.10M	0.01	0.2	0.3	0.5	7	22

JUMO GmbH & Co. KG

Delivery address: Mackenrodtstraße 14,
36039 Fulda, Germany
Postal address: 36035 Fulda, Germany
Phone: +49 661 6003-0
Fax: +49 661 6003-607
e-mail: mail@jumo.net
Internet: www.jumo.net

JUMO Instrument Co. Ltd.

JUMO House
Temple Bank, Riverway
Harlow, Essex CM 20 2TT, UK
Phone: +44 1279 635533
Fax: +44 1279 635262
e-mail: sales@jumo.co.uk
Internet: www.jumo.co.uk

JUMO PROCESS CONTROL INC.

885 Fox Chase, Suite 103
Coatesville PA 19320, USA
Phone: 610-380-8002
1-800-554-JUMO
Fax: 610-380-8009
e-mail: info@JumoUSA.com
Internet: www.JumoUSA.com

Platinum-chip temperature sensors with connecting wires to EN 60 751

PCA/H style

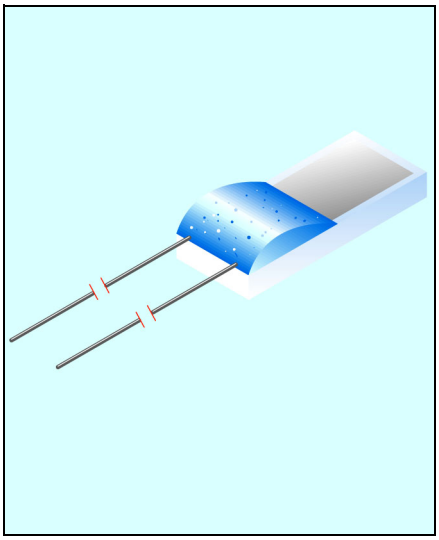

Brief description

Platinum-chip temperature sensors are based on a temperature-dependent resistance whose development and permissible tolerance is defined in the international standard EN 60 751. They combine the favorable properties of a platinum temperature sensor with the advantages of large-scale production. Their distinctive features are standardization and universal interchangeability, as well as high measurement accuracy, excellent long-term stability and good reproducibility of the electrical properties. Furthermore, prices have fallen considerably in recent years, since these sensors are designed to meet large-quantity requirements. With regard to the price, platinum-chip temperature sensors are therefore a genuine alternative to thermistors, which are based on semiconductors.

Platinum-chip temperature sensors, H version, are mainly used for applications at especially high or permanently elevated temperatures. They are particularly suitable for electrical connection through bonding or laser welding procedures, and through hard-soldered joints. The connecting wires are made from pure palladium. The application covers temperatures from -70 to +600 °C.

Temperature sensors in blister belt packaging or packed in bags

Temperature sensor						Connecting wire				Sales No. for tolerance class		
Type	R_0/Ω	W	L	H	S	Material	D1	L1	R_L in mΩ/mm	1/3 DIN B	A	B
PCA 1.2010.1H	1x100	2.0	10	1.2	0.64	Pd	0.25	10	2.3	90/00343070T 90/00415851B	90/00343069T 90/00415852B	90/00053198T 90/00415850B
PCA 1.2010.5H	1x500	2.0	10	1.2	0.64	Pd	0.25	10	2.3	on request on request	on request on request	on request on request
PCA 1.2010.10H	1x1000	2.0	10	1.2	0.64	Pd	0.25	10	2.3	90/00343065T 90/00415855B	90/00343064T 90/00415856B	90/00044796T 90/00415854B

Dim. tolerances: ΔB = ±0.2 / ΔL = ±0.5 / ΔH = ±0.2 / ΔS = ±0.1 / ΔD1 = ±0.01 / ΔL1 = ±0.5
Dimensions in mm.

For a definition of the tolerance classes, see Data Sheet 90.6000
T = bag, B = blister belt

Dimensional drawing

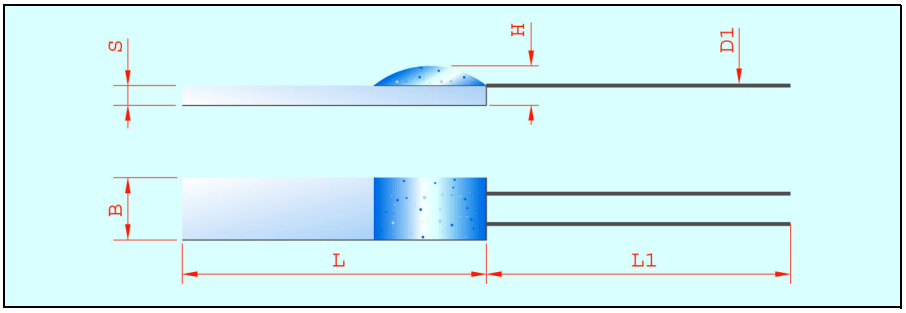

JUMO GmbH & Co. KG

Delivery address: Mackenrodtstraße 14,
36039 Fulda, Germany
Postal address: 36035 Fulda, Germany
Phone: +49 661 6003-0
Fax: +49 661 6003-607
e-mail: mail@jumo.net
Internet: www.jumo.net

JUMO Instrument Co. Ltd.

JUMO House
Temple Bank, Riverway
Harlow, Essex CM 20 2TT, UK
Phone: +44 1279 635533
Fax: +44 1279 635262
e-mail: sales@jumo.co.uk
Internet: www.jumo.co.uk

JUMO PROCESS CONTROL INC.

885 Fox Chase, Suite 103
Coatesville PA 19320, USA
Phone: 610-380-8002
1-800-554-JUMO
Fax: 610-380-8009
e-mail: info@JumoUSA.com
Internet: www.JumoUSA.com

Technical data

Standard	EN 60 751
Temperature coefficient	α = 3.850 x 10^{-3} °C^{-1} (between 0 and 100 °C)
Temperature range	-70 to +600 °C
Tolerance	Temperature validity range Class 1/3 DIN B: -50 to +200 °C Temperature validity range Class A: -70 to +300 °C Temperature validity range Class B: -70 to +600 °C
Measuring current/maximum current	Pt100 recommended: 1.0 mA maximum: 7 mA Pt1000 recommended: 0.1 mA maximum: 1 mA
Operating conditions	Platinum-chip temperature sensors may not be used unprotected in humid ambient conditions or corrosive atmospheres. They must also not be immersed directly in liquids. The user may have to carry out some checks before operation. **Please also refer to the Installation Instructions B 90.6121.4 "Notes on the application of platinum-chip temperature sensors."**
Connecting wires	These temperature sensors feature connecting wires made from pure palladium. The connecting wires are suitable for bonding or laser welding procedures and hard-soldered joints. During further processing, it is essential to ensure that the connections are not subjected to lateral pressures. The horizontal tension on the individual connecting wire must not exceed the maximum value of 6 N. Any unnecessary bending of the connecting wires must be avoided as this may result in material fatigue and a wire break.
Measurement point	The nominal value specified refers to the standard connecting wire length L1. The measurement is acquired 2 mm from the open end of the wire. If the wire length is altered, changes in resistance will occur which may result in the tolerance class not being met.
Long-term stability	max. R_0 drift 0.05 %/year (see Data Sheet 90.6000 for definitions)
Low-temperature application	Taking into account nominal value drifts and hysteresis effects that may occur within certain limits, temperature measurements down to -200 °C are also possible. Further details can be obtained on request.
Insulation resistance	>10 MΩ at room temperature
Vibration strength	see EN 60 751, Section 4.4.2
Self-heating	$\Delta t = I^2 \times R \times E$ (see Data Sheet 90.6000 for definitions)
Packaging	Blister belt/bag
Storage	In the standard belt packaging, JUMO temperature sensors, PCA/H style, can be stored for at least 12 months under normal ambient conditions. It is not permissible to store the sensors in aggressive atmospheres, corrosive media, or in high humidity.

Self-heating coefficients and response times

Type	Self-heating coefficient E in °C/mW		Response times in seconds			
	in water (v = 0.2 m/sec)	in air (v = 2 m/sec)	in water (v = 0.4 m/sec)		in air (v = 1 m/sec)	
			$t_{0.5}$	$t_{0.9}$	$t_{0.5}$	$t_{0.9}$
PCA 1.2010.1H	0.02	0.2	0.3	0.5	7	22
PCA 1.2010.5H	0.02	0.2	0.3	0.5	7	22
PCA 1.2010.10H	0.01	0.2	0.3	0.5	7	22

Datasheet Suntech zonnepaneel
STP225-20/Wd 225 Wp

SUNTECH

Solar powering a green future™

STP225 - 20/Wd
STP220 - 20/Wd

225 Watt
POLY-CRYSTALLINE SOLAR PANEL

Features

- High conversion efficiency based on leading innovative photovoltaic technologies
- High reliability with 0/+5w peak positive power tolerance, ensuring return on investment
- Withstands high wind-pressure and snow load (passed IEC 5400Pa mechanical loading test), and extreme temperature variations

Quality and Safety

- 25-year power output warranty *
- Rigorous quality control meeting the highest international standards
- ISO 9001:2000 (Quality Management System) and ISO 14001:2004 (Environmental Management System) certified factories manufacturing world class products
- IEC61215, IEC61730, conformity to CE

Recommended Applications

- On-grid utility systems
- On-grid commercial systems
- Off-grid ground mounted systems

* Refer to Suntech's warranty document for terms and conditions

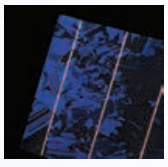

Unique Suntech Back Surface Field (BSF) structure and anti-reflective coating increase cell conversion efficiency.

Thermal isolation between the lamination and latest designed J-box improves panel performance stability. The new J-box also provides perfect interconnection between modules and inverters to ensure the fully utilization of module power output (option with MC4 connector).

Special design on drainage holes and rigid construction prevents frame from deforming or breaking due to freezing weather and other forces.

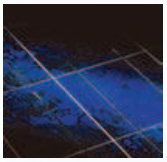

Advanced cell texturing and passivation processes improve module low light irradiance performance and provide more field power output.

Please consult your local dealer for more information.

www.suntech-power.com | E-mail: sales@suntech-power.com

EN-STD-Wd-N01.01-Rev 2009

SolarAccess B.V.
Mr. H.F. de Boerlaan 40 • 7417 DB Deventer
Tel: +31 (0)570 504150 • Fax: +31 (0)570 504159
www.SolarAccess.nl • info@SolarAccess.nl
Ondernemingsnummer: 08135793 • BTW nr: NL8147.24.309.B01

Datasheet Suntech zonnepaneel
STP225-20/Wd 225 Wp

SUNTECH

Solar powering a green future™

STP225 - 20/Wd
STP220 - 20/Wd

Electrical Characteristics

Characteristics	STP225-20/Wd	STP220-20/Wd
Open - Circuit Voltage (Voc)	36.7V	36.6V
Optimum Operating Voltage (Vmp)	29.6V	29.5V
Short - Circuit Current (Isc)	8.15A	8.05A
Optimum Operating Current (Imp)	7.61A	7.46A
Maximum Power at STC (Pmax)	225Wp	220Wp
Module Efficiency	13.6%	13.3%
Operating Temperature	-40°C to +85°C	-40°C to +85°C
Maximum System Voltage	1000V DC	1000V DC
Maximum Series Fuse Rating	20A	20A
Power Tolerance	0 /+5 W	0 /+5 W

STC: Irradiance 1000W/m², Module temperature 25°C, AM=1.5

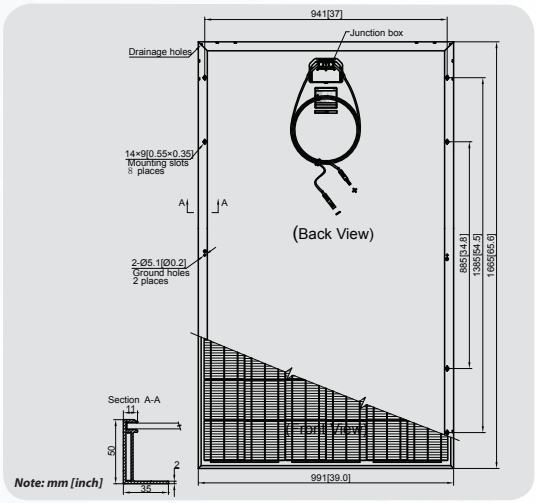

Mechanical Characteristics

Solar Cell	Poly-crystalline 156×156mm (6inch)
No. of Cells	60 (6×10)
Dimensions	1665×991×50mm (65.6×39.0×2.0inch)
Weight	22.5 kg (49.6lbs.)
Front Glass	4mm(0.16inch) tempered glass
Frame	Anodized aluminium alloy
Junction Box	IP67 rated
Output Cables	H+S RADOX® SMART cable 4.0mm² (0.006inch²), symmetrical lengths (-) 1000mm (39.4inch) and (+) 1000mm (39.4inch), RADOX® SOLAR integrated twist locking connectors or MC4 connectors

Temperature Coefficients

Nominal Operating Cell Temperature **(NOCT)**	45±2/°C
Temperature Coefficient of Pmax	-0.47%/°C
Temperature Coefficient of Voc	-0.34%/°C
Temperature Coefficient of Isc	0.045%/°C

Current-Voltage & Power-Voltage Curve (225W)

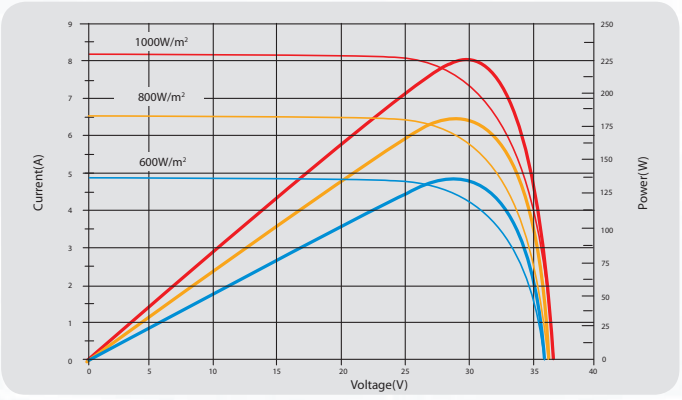

Temperature Dependence of Isc, Voc, Pmax

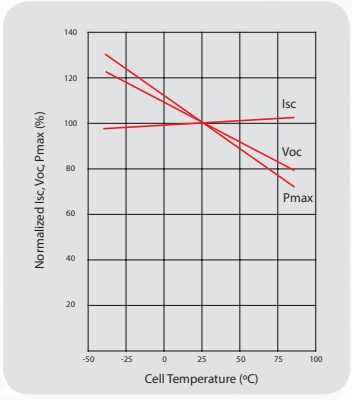

Specifications are subjected to change without further notice

www.suntech-power.com | E-mail: sales@suntech-power.com

EN-STD-Wd-N01.01-Rev 2009

SolarAccess B.V.
Mr. H.F. de Boerlaan 40 • 7417 DB Deventer
Tel: +31 (0)570 504150 • Fax: +31 (0)570 504159
www.SolarAccess.nl • info@SolarAccess.nl
Ondernemingsnummer: 08135793 • BTW nr: NL8147.24.309.B01

MINI MCR-SL-PT100-UI-200

Configurable temperature transducer for PT100

INTERFACE

Data sheet
102478_en_02

1 Description

The MINI MCR-SL-PT100-UI-200... is a configurable 3-way isolated temperature transducer. It is suitable for the connection of PT100 resistance thermometers according to IEC 60751 in 2-, 3-, and 4-wire connection methods. The measuring range can be configured from -50°C to +200°C using a DIP switch.

The standard analog signals 0...20 mA, 4...20 mA, 0...10 V, 0...5 V, 1...5 V, 10...0 V, 20...0 mA, 20...4 mA are available electrically isolated on the output side.

The DIP switches are accessible on the side of the housing and allow the following parameters to be configured:

- Connection method
- Temperature range to be measured
- Output signal
- Type of fault evaluation

The power supply (19.2...30 V DC) can be supplied either via connection terminal blocks "7"/"8" on the modules or in conjunction with the DIN rail connector. Please refer to the section titled "Connection methods" for more information.

Features

- Configurable 3-way temperature transducer
- 2-, 3-, 4-conductor connection method for Pt 100 resistance thermometer
- Measuring range 0°C to 200°C
- Increased accuracy due to smaller temperature measuring range
- Output signal range 0...20 mA, 4...20 mA, 0...10 V, 0...5 V, 1...5 V,10...0 V, 20...0 mA or 20...4 mA
- Approval for Ex-zone 2 (nA)
- Screw or spring-cage connection can be provided
- Can be supplied configured to order or unconfigured

Attention: Correct usage in potentially explosive areas

The module is a category 3 item of electrical equipment. It is absolutely vital to follow the instructions provided here during installation and observe the information in the "Safety regulations and installation notes".

Make sure you always use the latest documentation.
It can be downloaded from the product at www.phoenixcontact.net/catalog.

This data sheet is valid for all products listed on the following page:

2 Table of contents

3 Ordering data

Description	Type	Order No.	Pcs. / Pkt.
MCR temperature transducer, can be configured, for Pt 100 temperature sensors, with screw connection, order configuration	MINI MCR-SL-PT100-UI-200	2864309	1
MCR temperature transducer, can be configured, for Pt 100 temperature sensors, with spring-cage connection, order configuration	MINI MCR-SL-PT100-UI-200-SP	2864192	1
MCR temperature transducer, configurable, for Pt 100 temperature sensors, with screw-connection, not configured	MINI MCR-SL-PT100-UI-200-NC	2864370	1
MCR temperature transducer, configurable, for Pt 100 temperature sensors, with spring-cage connection, not configured	MINI MCR-SL-PT100-UI-200-SP-NC	2864202	1

Accessories	Type	Order No.	Pcs. / Pkt.
DIN rail connector (T-BUS), 5-pos., for bridging the supply voltage, can be snapped onto NS 35/... DIN rails according to EN 60715	ME 6,2 TBUS-2 1,5/5-ST-3,81 GN	2869728	10
MCR power terminal block for supplying several MINI Analog modules via the DIN rail connectors, with screw connection, current consumption up to max. 2 A	MINI MCR-SL-PTB	2864134	1
MCR power terminal block for supplying several MINI-ANALOG modules via the DIN rail connectors, with spring-cage connection, current consumption up to max. 2 A	MINI MCR-SL-PTB-SP	2864147	1
DIN rail power supply unit, primary-switched mode, slim design, output: 24 V DC / 1.5 A	MINI-SYS-PS-100-240AC/24DC/1.5	2866983	1
DIN rail power supply unit, primary-switched mode, slim design, output: 24 V DC / 1.5 A, ATEX approval	MINI-PS-100-240AC/24DC/1.5/EX	2866653	1
Eight MINI analog signal converters with screw connection method can be connected to a control system using a system adapter and system cabling with a minimum of wiring and very low error risk.	MINI MCR-SL-V8-FLK 16-A	2811268	1
Fold up transparent cover for MINI MCR modules with additional labeling option using insert strips and flat Zack marker strip 6.2 mm	MINI MCR DKL	2308111	10
Label for extended marking of MINI MCR modules in connection with the MINI MCR-DKL	MINI MCR-DKL-LABEL	2810272	10

3.1 Order key

(standard configuration entered as example)

Order No.	/	Connection method	/	Measuring range [°C] Start	Measuring range [°C] Finish	/	Output	/	Failure information [1]	/	Factory calibration certificate
2864309	/	3	/	0	100	/	OUT01	/	A	/	NONE

2864309 □ ...-PT100-UI-200

2864736 □ ...-PT100-UI-200-SP

Connection method:
- 2 □ 2-wire
- 3 □ 3-wire
- 4 □ 4-wire

Measuring range [°C] Start: 0, -5, -10, -15, -20, -30, -40, -50

Range (increment): 0 ... 200 (5 K)

Output:
- OUT01 □ 0 ... 20 mA
- OUT02 □ 4 ... 20 mA
- OUT03 □ 0 ... 10 V
- OUT05 □ 0 ... 5 V
- OUT06 □ 1 ... 5 V
- OUT07 □ 20 ... 0 mA
- OUT08 □ 20 ... 4 mA
- OUT09 □ 10 ... 0 V

Failure information: A, B, C, D

Factory calibration certificate:
- NONE □ Without factory calibration
- YES □ With factory calibration certificate (a fee is charged)
- YESPLUS □ Factory calibration certificate with 5 measuring points (a fee is charged)

[1] **Failure information:**

	Measuring range overrange			Cable break		
	0 ... 20 mA	4 ... 20 mA	0 ... 10 V	0 ... 20 mA	4 ... 20 mA	0 ... 10 V
A	20.5 mA	20.5 mA	10.25 V	21 mA	21 mA	10.5 V
B	20.5 mA	20.5 mA	10.25 V	21 mA	21 mA	10.5 V
C	20 mA	20 mA	10 V	21 mA	21 mA	10.5 V
D	20 mA	20 mA	10 V	0 mA	4 mA	0 V

	Measuring range underrange			Short circuit		
	0 ... 20 mA	4 ... 20 mA	0 ... 10 V	0 ... 20 mA	4 ... 20 mA	0 ... 10 V
A	0 mA	4 mA	0 V	0 mA	4 mA	0 V
B	0 mA	3.5 mA	0 V	0 mA	3 mA	0 V
C	0 mA	4 mA	0 V	21 mA	21 mA	10.5 V
D	0 mA	4 mA	0 V	0 mA	4 mA	0 V

4 Technical data

Input	
Sensor type	Pt 100 (IEC 60751/EN 60751)
Sensor input current	1 mA (constant)
Max. permissible overall conductor resistance	10 Ω (Per cable)
Temperature measuring range	-50 °C ... 200 °C
Measuring range span	min. 50 K
Connection method	2, 3, 4-wire
Output	
Voltage output signal	0 V ... 10 V 10 V ... 0 V 0 V ... 5 V 1 V ... 5 V
Max. voltage output signal	Approx. 12.5 V
Non-load voltage	Approx. 12.5 V
Current output signal	0 mA ... 20 mA 4 mA ... 20 mA 20 mA ... 0 mA 20 mA ... 4 mA
Max. current output signal	23 mA
Short circuit current	Approx. 10 mA
Load/output load voltage output	> 10 kΩ
Ripple	< 20 mV_{PP} (at 500 Ω)
Load/output load current output	< 500 Ω (at 20 mA)
Supply	
Nominal supply voltage	24 V DC
Supply voltage range	19.2 V DC ... 30 V DC (to bridge the supply voltage, the DIN rail connector (ME 6,2 TBUS-2 1,5/5-ST-3,81 GN, Order No. 2869728) can be used. It can be snapped onto a 35 mm DIN rail according to EN 60715)
Max. current consumption	< 21 mA (for 24 V DC)
Power consumption	< 500 mW
General data	
Transmission error in the set measuring range	((50 K / Δ Temp)+ 0.05)%
Transmission error in the full measuring range	≤ 0,25 %
Maximum temperature coefficient	< 0.02 %/K
Step response (10-90%)	< 200 ms
Electrical isolation	Basic insulation according to EN 61010
Surge voltage category	II
Mounting position	Any
Degree of protection	IP20
Pollution degree	2
Rated insulation voltage	50 V AC/DC
Test voltage, input/output/supply	1.5 kV (50 Hz, 1 min.)
Dimensions W / H / D	6.2 mm / 93.1 mm / 102.5 mm
Type of housing	PBT green

Connection data	Screw connection	Spring-cage conn.
Conductor cross section, solid	0.14 mm² ... 2.5 mm²	0.2 mm² ... 2.5 mm²
Conductor cross section, stranded	0.2 mm² ... 2.5 mm²	0.2 mm² ... 2.5 mm²
Stripping length	12 mm	8 mm

Ambient conditions	
Ambient temperature (operation)	-20 °C ... 65 °C
Ambient temperature (storage/transport)	-40 °C ... 85 °C

Conformance with EMC directive 2004/108/EC
Noise immunity according to EN 61000-6-2
Noise emission according to EN 61000-6-4

Conformance / approvals	
Conformity	CE compliant
ATEX	Ⓔx II 3 G Ex nA II T4 X
UL, USA / Canada	UL 508 Recognized
UL, USA / Canada	Class I, Div. 2, Groups A, B, C, D T5
Shipbuilding	GL EMC 2 D

5 Safety regulations and installation notes

5.1 Installation notes

- The device is designed for installation in zone 2 potentially explosive areas.
- Installation, operation, and maintenance may only be carried out by qualified electricians. Follow the installation instructions described. When installing and operating the device, the applicable regulations and safety directives (including national safety directives), as well as general technical regulations, must be observed. The technical data is provided in this package slip and on the certificates (conformity assessment, additional approvals where applicable).
- It is not permissible to open or modify the device. Do not repair the device yourself but replace it with an equivalent device. Repairs may only be carried out by the manufacturer. The manufacturer is not liable for damage resulting from violation.
- The IP20 degree of protection (EN 60529) of the device is intended for use in a clean and dry environment. Do not subject the device to any load that exceeds the described limits.
- The device is not designed for use in atmospheres with a danger of dust explosions.

5.2 Installation in the Ex area (zone 2)

- Observe the specified conditions for use in potentially explosive areas.
- The device must be installed in a housing (control or distributor box) which meets the requirements of EN 60079-15 and provides at least IP54 (EN 60529) degree of protection.
- During installation and when connecting the supply and signal circuits, observe the requirements of EN 60079-14. Devices may only be connected to circuits in zone 2 if they are suitable for operation in Ex zone 2 and for the prevailing conditions at the place of use.
- In potentially explosive areas, terminals may only be snapped onto or off the DIN rail connector and wires may only be connected or disconnected when the power is switched off.
- The device must be stopped and immediately removed from the Ex area if it is damaged, has been subjected to an impermissible load, has been stored incorrectly, or if it malfunctions.
- You can download the latest documents for these devices from www.phoenixcontact.net/catalog.

6 Installation

6.1 Connection notes

Attention: Electrostatic discharge!

The device contains components that can be damaged or destroyed by electrostatic discharge. When handling the device, observe the necessary safety precautions against electrostatic discharge (ESD) according to EN 61340-5-1 and EN 61340-5-2.

6.2 Structure

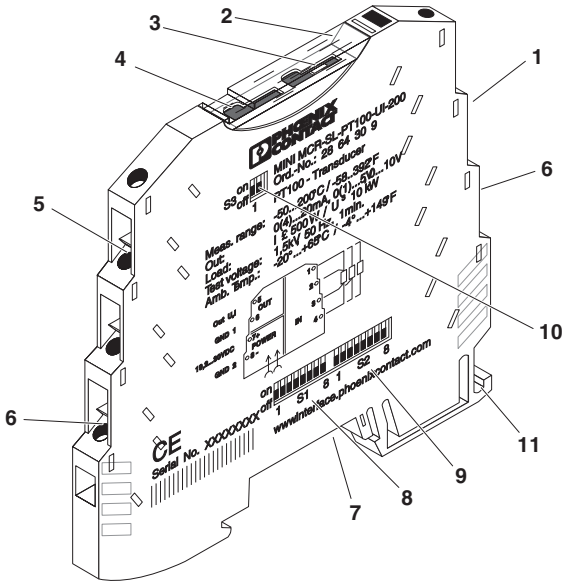

Figure 1 Structure

1. Input: PT100 resistance thermometer
2. Cover
3. Diagnostics LED
4. Groove for ZBF 6 zack marker strip
5. Output: Standard signals
6. Supply voltage
7. Connection option for DIN rail connector
8. DIP switch S1
9. DIP switch S2
10. DIP switch S3
11. Universal snap-on foot for EN DIN rails

6.3 Block diagram

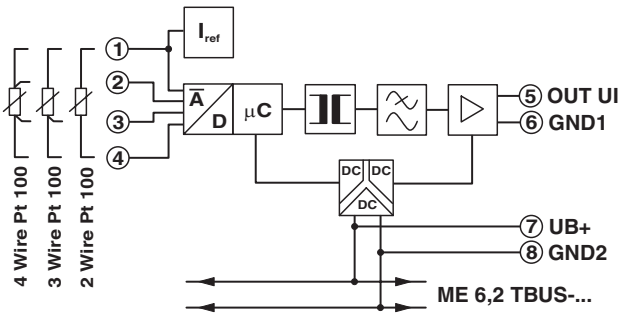

Figure 2 Block diagram

6.4 Power supply

Note:

Never connect the supply voltage directly to the DIN rail connector. It is not permitted to draw power from the DIN rail connector or from individual modules.

Supply via the module

Where the total current consumption of the aligned modules does not exceed 400 mA, the power can be supplied directly at the connection terminal blocks of the module.

A 400 mA fuse should be connected upstream.

Supply via a power terminal block

The MINI MCR-SL-PTB power terminal block (Order No. 2864134) or the MINI MCR-SL-PTB-SP power terminal block (Order No. 2864147), which are the same shape, are used to feed the supply voltage to the DIN rail connector.

A 2 A fuse should be connected upstream.

Supply via a system power supply unit

The system power supply unit with 1.5 A output current connects the DIN rail connector to the supply voltage and can thus be used to supply several modules from the mains.

– MINI-SYS-PS-100-240AC/24DC/1.5 (Order No. 2866983)
– Potentially explosive areas: MINI-PS-100-240AC/24DC/1.5/EX (Order No. 2866653)

6.5 Assembly

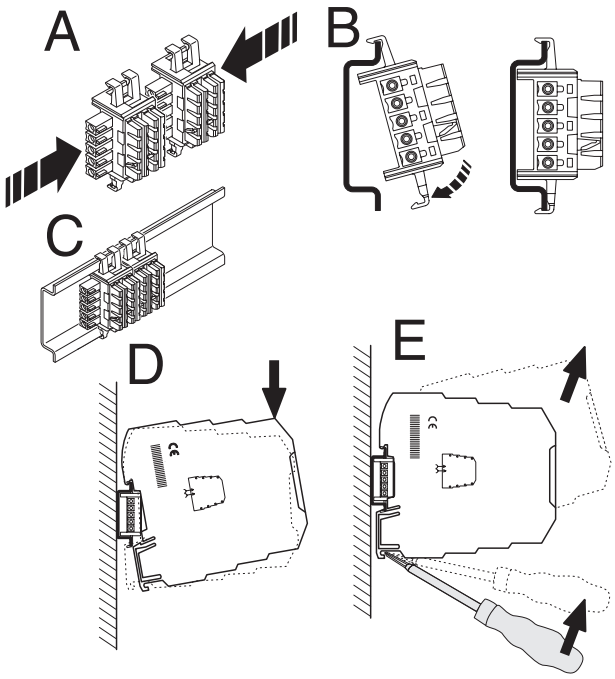

Figure 3 Mounting and removing

– Mount the module on a 35 mm DIN rail according to EN 60715.
– When using the DIN rail connector, first place it into the DIN rail (see A – C). It is used to bridge the power supply. It is also absolutely vital that you snap the module and the DIN rail connector into position in the correct direction: the snap-on foot should be at the bottom and the connector on the left.

6.6 Connecting the wires

The MINI MCR-SL-PT100-UI-200... is available with two types of connection:

– Screw terminal blocks (MINI MCR-SL-PT100-UI-200)
– Spring-cage terminal blocks (MINI MCR-SL-PT100-UI-200-SP)

Screw connection:

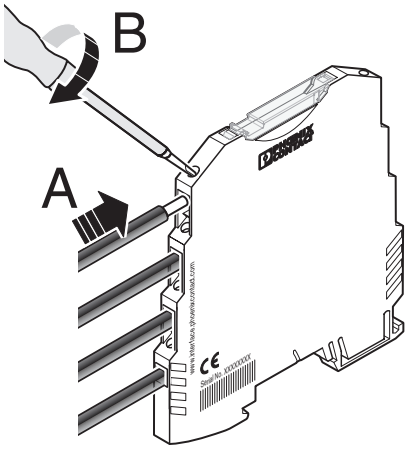

Figure 4 Screw connection

- Insert the wire into the corresponding connection terminal block.
- Use a screwdriver to tighten the screw in the opening above the connection terminal block.

Spring-cage connection:

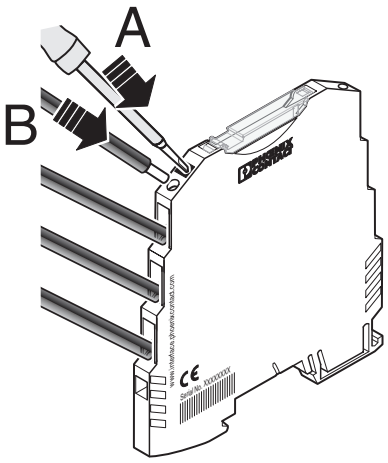

Figure 5 Spring-cage connection

- Insert a screwdriver into the opening above the connection terminal block.
- Insert the wire into the corresponding connection terminal block.

7 Configuration

NC version

If a device has not been configured ("NC type": MINI MCR-SL-PT100-UI-200-NC or MINI MCR-SL-PT100-UI-200-SP-NC), all DIP switches will be set to position 0. The device only has a defined function once the DIP switches have been set.

DIP switch S1

DIP switch S1 is used to specify the connection method, the output signal range, and the measuring range start value.

DIP switch S2

DIP switch S2 is used to specify the measuring range final value and fault evaluation.

DIP switch S3

DIP switch S3 is used to select the voltage or current output.

7.1 Configuration table

DIP S1

1	2	Connection method
		2-wire
•		2-wire
	•	3-wire
•	•	4-wire

3	4	5	Output signal range OUT
			0 ... 20 mA
•			20 ... 0 mA
	•		4 ... 20 mA
•	•		20 ... 4 mA
		•	0 ... 10 V
•		•	10 ... 0 V
	•	•	0 ... 5 V
•	•	•	1 ... 5 V

6	7	8	Start temperature [°C]	[°F]
			0	32
•			-5	23
	•		-10	14
•	•		-15	5
		•	-20	-4
•		•	-30	-22
	•	•	-40	-40
•	•	•	-50	-58

DIP S2

	7	8	Cable break	Measuring range overrange	Measuring range underrange	Short circuit
A			Measuring range final value +5%	Measuring range final value +2.5%	Measuring range start value	Measuring range start value
B	•		Measuring range final value +5%	Measuring range final value +2.5%	Measuring range start value -12.5%	Measuring range start value -25%
C		•	Measuring range final value +5%	Measuring range final value	Measuring range start value	Measuring range final value +5%
D	•	•	Measuring range start value	Measuring range final value	Measuring range start value	Measuring range start value

DIP S3

1	2	OUT
•		0 ... 20 mA, 4 ... 20 mA, 20 ... 0 mA, 20 ... 4 mA
	•	0 ... 10 V, 10 ... 0 V, 0 ... 5 V, 1 ... 5 V

- • ON
- OFF

DIP S2

1	2	3	4	5	6	Final temperature [°C]	[°F]
						0	32
•						5	41
	•					10	50
•	•					15	59
		•				20	68
•		•				25	77
	•	•				30	86
•	•	•				35	95
			•			40	104
•			•			45	113
	•		•			50	122
•	•		•			55	131
		•	•			60	140
•		•	•			65	149
	•	•	•			70	158
•	•	•	•			75	167
				•		80	176
•				•		85	185
	•			•		90	194
•	•			•		95	203
		•		•		100	212
•		•		•		105	221
	•	•		•		110	230
•	•	•		•		115	239
			•	•		120	248
•			•	•		125	257
	•		•	•		130	266
•	•		•	•		135	275
		•	•	•		140	284
•		•	•	•		145	293
	•	•	•	•		150	302
•	•	•	•	•		155	311
					•	160	320
•					•	165	329
	•				•	170	338
•	•				•	175	347
		•			•	180	356
•		•			•	185	365
	•	•			•	190	374
•	•	•			•	195	383
			•		•	200	392

8 Diagnostics LED

The LED which is visible on the front displays the following faults:

– LED flashing: Measuring range span less than 50 K
– LED ON: Open circuit on the sensor side
– LED ON: Short circuit on the sensor side
– LED ON: Measuring range overrange
– LED ON: Measuring range underrange

9 Connection/Application example

2-wire connection method

– For short distances (< 10 m)
– Cable resistances RL1 and RL2 are incorporated in the measurement result directly and falsify the result accordingly.

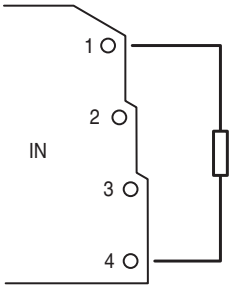

Figure 6 2-wire connection

3-wire connection method

– For long distances between PT100 sensor and MINI analog module
– The value of all cable resistances must be exactly the same (RL1 = RL2 = RL3) in order to balance out the sensor cable resistances.

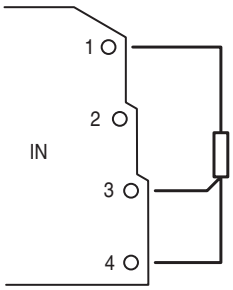

Figure 7 3-wire connection

4-wire connection method

– For longer distances between PT100 sensor and MINI analog module and differing cable resistances (RL1 ≠ RL2 ≠ RL3 ≠ RL4).

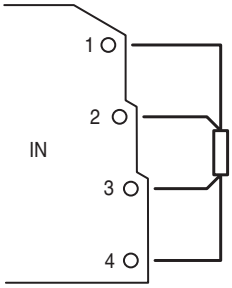

Figure 8 4-wire connection

A.2 MATLAB script

```
[breaklines]
close;
clear;
clc;
%% import data
files = dir('*.txt') ;
N = length(files) ;
Data=[];
for i = 1:N
    thisfile = files(i).name;
    S = readtable(thisfile);
    Data=[Data;S];
end

d=Data(:,1);
d=d{:,:};
d=num2str(d);
d=datetime(d, 'InputFormat','ddMMyyHHmmss'); %hvis det er fra 01-09 så må format være dMMy
[~, sortidx] = sort(d);
Data = Data(sortidx,:);
header={'Time','SolData','IrrUnc','ISFstable','KippZonen','Tamb','IscaSi','VocaSi','VmpaSi
Data.Properties.VariableNames = header;

time=Data.Time;
time=num2str(time);
time=datetime(time, 'InputFormat','ddMMyyHHmmss'); %hvis det er fra 01-09 så må format vær
Data.Time=time;
Data=table2timetable(Data);
Pmaxjanfeb=Data.PmaxA10156;
Data.Pmax(1:11890,:)=Pmaxjanfeb(1:11890,:);
datamin=retime(Data,'Minutely','sum');
Datahr=retime(Data,'Hourly','sum');
Counthr=retime(Data,'Hourly','count');
Dataday=retime(Datahr,'Daily','sum');
Countday=retime(Datahr,'Daily','count');
Datamonth=retime(Dataday,'Monthly','sum');
Countmonth=retime(Data,'Monthly','count');
tempmaxhr=retime(Datahr,'Daily','max');
tempavghr=retime(Datahr,'Daily','mean');
```

```
tempmaxday=retime(Datahr,'Daily','max');
tempavgday=retime(Datahr,'Daily','mean');

%% datasheet values
n=16;
Amod=(224/1000)*(343/1000); %lengde kan være mellom 343 og 354 mm
Pmax_ds=9;
Vmp_ds=37;
Imp_ds=0.245;
Voc_ds=47;
Isc_ds=0.265;
gamma=-0.45/100;
G_ref=1000;
%% importdata from datalogger
Temp=importdata('Tempapril2.mat');
Temp(1,:)=[];
header={'Time','Record','dontuse','topavg','midavg','botavg','topmax','midmax','botmax','t
Temp.Properties.VariableNames = header;
Temp.Time=datetime(Temp.Time,'InputFormat','yyyy-MM-dd HH:mm:ss');
Time=Temp.Time;
Toptemp=Temp.topavg;
Midtemp=Temp.midavg;
Bottemp=Temp.botavg;
Temp=table2timetable(Temp);
Temphr=retime(Temp,'hourly','mean');
Tempdaymax=retime(Temphr,'daily','mean');
Tempdayavg=retime(Temphr,'daily','mean');
countTempday=retime(Temphr,'daily','count');
Timehr=Temphr.Time;
Timeday=Tempdaymax.Time;
Toptemphr=Temphr.topavg;
Toptempdaymax=Tempdaymax.topavg;
Toptempdayavg=Tempdayavg.topavg;
%% labview data per min
Irr=Data.KippZonen;
Isc=Data(:,17);
Voc=Data(:,18);
Vmp=Data(:,19);
Pmaxjanfeb=Data.PmaxA10156;
Pmax=Data.Pmax;
Pmax(1:11890,:)=Pmaxjanfeb(1:11890,:);
```

```
Pmax(11500:11889,:)=NaN;
Tamb=Data.Tamb;
Tjanfeb=Data.TA10156;
T459=Data.T459;
Tamb_bipv=Data(:,51);
%% labview data per hr
timehr=Datahr.Time;
Irrhr=Datahr.KippZonen;
countIrrhr=Counthr.KippZonen;
%Irrhr=Irrhr./countIrrhr;
Ischr=Data(:,17);
Vochr=Data(:,18);
Vmphr=Data(:,19);
Pmaxjanfebhr=Datahr.PmaxA10156;
Pmaxhr=Datahr.Pmax;
Pmaxhr(1:2160,:)=Pmaxjanfebhr(1:2160);
countPmaxhr=Counthr.Pmax;
Pmaxhr1=Pmaxhr./countPmaxhr;
Irrhr1=Irrhr./countIrrhr;
Pmaxhr1=timetable(timehr,Pmaxhr1,Irrhr1);
Pmaxday=retime(Pmaxhr1,'Daily','sum');
Irrday=Pmaxday.Irrhr1;
Pmaxday=Pmaxday.Pmaxhr1;
Tambhr=Datahr.Tamb;
Tmodulehrtop=Datahr.TCIS;
Tmodulehrtop=Tmodulehrtop./(Counthr.TCIS);
Tmodulehrmid=Datahr.TaSi;
Tmodulehrmid=Tmodulehrmid./(Counthr.TaSi);
Tmodulehrbot=Datahr.TNESTE;
Tmodulehrbot=Tmodulehrbot./(Counthr.TNESTE);
Tmodulehrback=Datahr.TGPV;
Tmodulehrback=Tmodulehrback./(Counthr.TGPV);
countTambhr=Counthr.Tamb;
Tambhrmax=tempmaxhr.Tamb;
Tambhravg=tempavghr.Tamb;
T459hr=Datahr.T459;
T459hr=T459hr./(Counthr.T459);
Tamb_bipvhr=Data(:,51);
%% labview data per day
timeday=Dataday.Time;
%Irrday=Dataday.KippZonen;
```

```
countIrrday=Countday.KippZonen;
Pmaxdayjanfeb=Dataday.PmaxA10156;
%Pmaxday=Dataday.Pmax;
%Pmaxday(1:90,:)=Pmaxdayjanfeb(1:90);
countPmaxday=Countday.Pmax;
Tambdaymax=tempmaxday.Tamb;
Tambdayavg=tempavgday.Tamb;
T459day=Data(:,16);
Tamb_bipvday=Data(:,51);
%% labview data per month
timemonth=Datamonth.Time;
Irrmonth=Datamonth.KippZonen;
Iscmonth=Data(:,17);
Vocmonth=Data(:,18);
Vmpmonth=Data(:,19);
Pmaxmonthjanfeb=Datamonth.PmaxA10156;
Pmaxmonth=Datamonth.Pmax;
%% plot temp
figure(1);
starttemp=find(Time=='19-Apr-2019 08:00:00');
stoptemp=find(Time=='24-Apr-2019 08:00:00');
plot(Time(starttemp:stoptemp),Toptemp(starttemp:stoptemp),'r','Linewidth',2)
hold on
plot(Time(starttemp:stoptemp),Midtemp(starttemp:stoptemp),'b','Linewidth',2)
hold on
plot(Time(starttemp:stoptemp),Bottemp(starttemp:stoptemp),'k','Linewidth',2)
legend('top','mid','bot');
ylabel('Temperature \circ C')
set(gca,'FontSize',25)
set(gcf,'color','w');
%% plot labviewdata
startmin=find(time=='29-Apr-2019 08:00:06');
stopmin=find(time=='29-Apr-2019 19:00:12');
starthr=find(timehr=='01-Mar-2019 06:00:00');
stophr=find(timehr=='30-Apr-2019 20:00:00');
startday=find(timeday=='01-Mar-2019 00:00:00');
stopday=find(timeday=='31-Mar-2019 00:00:00');
eff=Pmax./(Irr*Amod*n);
figure;
plot(time(startmin:stopmin),Irr(startmin:stopmin),'b','LineWidth',2);
hold on
```

```
plot(time(startmin:stopmin),Data.SolData(startmin:stopmin),'r--','LineWidth',0.5);
ylabel('Irradiance (W/m^2)')
set(gcf,'color','w');
set(gca,'FontSize',25)
legend('Irradiance sensor','Refferance Cell')
figure;
yyaxis left
plot(time(startmin:stopmin),Irr(startmin:stopmin),'b');
area(time(startmin:stopmin),Irr(startmin:stopmin));
ylabel('Irradiance (W/m^2)')
hold on
yyaxis right
plot(time(startmin:stopmin),Pmax(startmin:stopmin),'r','LineWidth',2);
legend('Irradiance','Power')
ylabel('Power (W)')
ylim([10 140])
set(gcf,'color','w');
set(gca,'FontSize',25)
maxirrmin=max(Irr(startmin:stopmin))
maxpmin=max(Pmax(startmin:stopmin))
figure;
%yyaxis left
%plot(timehr(starthr:stophr),Irrhr(starthr:stophr));
%area(timehr(starthr:stophr),Irrhr(starthr:stophr));
%ylabel('kWh/m^2')
%hold on
%yyaxis right
bar(timehr(starthr:stophr),Pmaxhr(starthr:stophr)./(countPmaxhr(starthr:stophr).*1000),'r'
set(gca,'FontSize',16);
ylabel('Daily Energy (kWh)')

figure;
a=[Pmaxday(startday:stopday)/1000 zeros(length(Pmaxday(startday:stopday)),1)];
b=[zeros(length(Pmaxday(startday:stopday)),1)    Pmaxday(startday:stopday)/(1000*0.144)];
hAx3=plotyy(timeday(startday:stopday),a,timeday(startday:stopday),b,@bar,@bar);
ylabel(hAx3(1), 'Daily Energy (kWh)');
yticks(hAx3(1), [0, 0.2,0.4,0.6,0.8,1])
ylabel(hAx3(2), 'Daily specific yield (kWh/kWp)');
yticks(hAx3(2), [0, 2,4,6,8,10])
legend('Daily yield','Daily specific yield')
set(hAx3,'FontSize',25);
```

```
set(gcf,'color','w');
maxpday=max(Pmaxday(startday:stopday)/1000)
avgpday=mean(Pmaxday(startday:stopday)/1000)


figure;
bar(timemonth,Pmaxmonth/1000)
set(gca,'FontSize',16)
%% combined plot
start=find(time=='23-Apr-2019 07:00:12');
stop=find(time=='23-Apr-2019 20:08:22');
startT=find(Time=='23-Apr-2019 07:00:00');
stopT=find(Time=='23-Apr-2019 20:08:00');
figure;
hold on
x1 = time(start:stop);
y1 = T459(start:stop);
%y3 = Tamb(start:stop);
line(x1,y1,'Color','b','LineWidth',2)
% xlim([datenum('23-Apr-2019 08:00:00'), datenum('23-Apr-2019 19:00:00')]);
% datetick=get(gca,'xtick');
% set(gca,'xticklabel',cellstr(datestr(datetick))')
set(gca,'FontSize',25)
ax1 = gca; % current axes
ax1.XColor = 'k';
ax1.YColor = 'k';
ax1_pos = ax1.Position; % position of first axes
ylabel('STP422 module temperature (\circC)')
set(gca,'FontSize',25);
set(gcf,'color','w');
ax2 = axes('Position',ax1_pos,...
    'XAxisLocation','top',...
    'YAxisLocation','right',...
    'Color','none');
%x2 = datenum(Time);
x2 = Time(startT:stopT);
ax2.XColor = 'none';
y2 = Toptemp(startT:stopT);
line(x2,y2,'Parent',ax2,'Color','b','LineWidth',2)
line(x2,y2,'Parent',ax2,'Color','r','LineWidth',2)
%line(x1,y3,'Parent',ax2,'Color','k','LineWidth',2)
```

```
legend('STP422','BIPV module');
ylabel('BIPV module temperature (\circC)')
% xlim([datenum('23-Apr-2019 08:00:00'), datenum('23-Apr-2019 19:00:00')]);
% datetick=get(gca,'xtick');
% set(gca,'xticklabel',cellstr(datestr(datetick))')
set(gca,'FontSize',25)
set(gcf,'color','w');
%% performance ratio per min
figure;
startpr=find(time=='06-May-2019 06:00:00');
stoppr=find(time=='06-May-2019 19:00:00');
Pmax_min=Pmax;
Pmax_min=Pmax_min/1000; %for å gå fra Wh til kWh
Pmax_min=Pmax_min/(Amod*n);
Po=Pmax_ds*n/1000;
Irr_min=Irr;
Irr_min=Irr_min/1000; %for å få kWh
Y_Amin=Pmax_min./Po;
Yrmin=Irr_min./(G_ref/1000);
PR_Amin=Y_Amin./Yrmin;
efficiency=Pmaxhr./(Irrhr.*Amod*n);
plot(datenum(time),PR_Amin);
xlim([datenum('01-May-2019 08:00:00'), datenum('01-May-2019 19:00:00')]);
datetick=get(gca,'xtick');
set(gca,'xticklabel',cellstr(datestr(datetick))')
Tcorr=(Toptemphr-25)*gamma;
%PR_A_Tcorr=PR_Ahr.*(1+Tcorr);
%% performance ratio per hr
startprhr=find(timehr=='06-May-2019 06:00:00');
stopprhr=find(timehr=='06-May-2019 19:00:00');
Pmax_day=Pmaxhr;
Pmax_day=Pmax_day/1000; %for å gå fra Wh til kWh
Pmax_day=Pmax_day/(Amod*n);
Po=Pmax_ds*n/1000;
Irr_day=Irrhr;
Irr_day=Irr_day/1000; %for å få kWh
Y_Adhr=Pmax_day./Po;
Yrhr=Irr_day./(G_ref/1000);
PR_Ahr=Y_Adhr./Yrhr;
efficiency=Pmaxhr./(Irrhr.*Amod*n);
figure;
```

```
yyaxis left
bar(timehr(startprhr:stopprhr),PR_Ahr(startprhr:stopprhr));
hold on
yyaxis right
bar(timehr(startprhr:stopprhr),efficiency(startprhr:stopprhr)*100,0.5);
Tcorrhr=(Toptemphr-25)*gamma;
%PR_A_Tcorr=PR_Ahr.*(1+Tcorr);
%% performance ratio per day
startpr2=find(Timeday=='15-Apr-2019 00:00:00');
stoppr2=find(Timeday=='03-May-2019 00:00:00');
startpr3=find(timeday=='15-Apr-2019 00:00:00');
stoppr3=find(timeday=='03-May-2019 00:00:00');
timedaypr=timeday(startpr3:stoppr3);
Pmax_day=Pmaxday;
Pmax_day=Pmax_day;  %for å gå fra Wmin til Wh
Pmax_day=Pmax_day./1000; %for å gå fra Wh til kWh
Pmax_day=Pmax_day;
Irr_day=Irrday;
Irr_day=Irr_day/1000; %for å få kW
Irr_day=Irr_day.*(Amod*n); %for å gå fra kWmin til kWh
Y_Aday=Pmax_day./Po;
Yrday=Irr_day./(G_ref/1000);
PR_Aday=Y_Aday./Yrday;
effday=(Pmaxday./(Irrday*Amod*n));
figure;
bar(timeday(startpr3:stoppr3),effday(startpr3:stoppr3)*100)
ylabel('Efficiency (%)')
set(gca,'FontSize',25);
set(gcf,'color','w');
avgeffday=mean(isnan(effday(startpr3:stoppr3)))
Tcorrday=(Toptempdaymax-25).*gamma;
aaaaa=PR_Aday(startpr3:stoppr3);
aaallla=Tcorrday(startpr2:stoppr2);
aa=timeday(startpr3:stoppr3);
aaa=PR_Aday(startpr3:stoppr3);
aaaa=Toptempdaymax(startpr2:stoppr2);
PR_A_Tcorrday=aaaaa.*(1+aaallla);
PRplot=[aaa PR_A_Tcorrday];
figure;
hold on
%yyaxis left
```

```
bar(aa,PRplot)
ylabel('PR')
legend('PR','Temperature corrected PR')
set(gca,'FontSize',25);
set(gcf,'color','w');
PRavgday=mean(aaa)
pracorrdayavg=mean(PR_A_Tcorrday)
PRmaxday=max(aaa)
PRminday=min(aaa)
pracorrdaymax=max(PR_A_Tcorrday)
pracorrdaymin=min(PR_A_Tcorrday)

close;
clear;
clc;

data=xlsread('BIPV.xls');
data2=importdata('Plant_2_BIPV_IV-500W.xls');

Irr=data2.data(5,1);
Vop=data2.data(10,:);
Iop=data2.data(11,:);
P=Vop.*Iop;
Pmax=max(P);
Voc=max(Vop);
Voc=ones(length(Vop)).*Voc;
Vmpp=34.0837;
Isc=max(Iop);
Impp=3.239;
Impp=ones(length(Vop)).*Impp;
Pmpp=ones(length(Vop)).*Pmax;
Pdot=ones(1,length(Vop));
tabledata=[Vop;Iop;P];

yyaxis left
plot(Vop,Iop,'LineWidth',2);
hold on
ylabel('Current (A)')
yyaxis right
plot(Vop,P,'LineWidth',2)
set(gca,'FontSize',25);
```

```
Voc_ds = 47;
Isc_ds=0.265;
xlabel('Voltage (V)')
ylabel('Power (W)')
set(gcf,'color','w');
legend('IV curve','PV curve')
%I = I_L-Io(exp((V+I*Rs)/(n*k*T/q))-1)-(V+I*Rs)/Rsh;

close;
clear;
clc;

% Pris
installing=25000;
Pp1=3;
Pp2=6;
Pp3=9;
Pp4=12;
Pp=[Pp1 Pp2 Pp3 Pp4];
Alternative1=102716;     %3kWp

Alternative2=166590;     %6kWp

Alternative3=217515;     %9kWp

Alternative4=282302;     %12kWp

Enova=10000+1250*Pp;                %støtteordning fra enova
if Enova > 25000
    Enova = 25000;
else
    Enova=Enova;
end

nok_Wp1=Alternative1/(Pp1*1000);
nok_Wp2=Alternative2/(Pp2*1000);
nok_Wp3=Alternative3/(Pp3*1000);
nok_Wp4=Alternative4/(Pp4*1000);

nok_Wp1_enova=(Alternative1)/(Pp1*1000)
nok_Wp2_enova=(Alternative2)/(Pp2*1000)
```

```
nok_Wp3_enova=(Alternative3)/(Pp3*1000)
nok_Wp4_enova=(Alternative4)/(Pp4*1000)
y_prod=3000;                          %yearly production [kWh]
elec_price=1.234;                     %cost of electricity [NOK/kWh]
n=25;                                              %service life of power plant [years]
t=[0:1:n];
d=0.2/25;                                          %annual degredation rate [%]
y_prod=3000;                          %yearly production [kWh]
elec_price=1.234;                     %cost of electricity [NOK/kWh]
R=0.03;                               %Rent on loan [%]
It=Alternative4;                      %initial investment [NOK/year]
Itdif=[Alternative1;Alternative2;Alternative3;Alternative4];
Mt=ones(1,length(t));                              %maintenance cost [NOK/year]
Ot=ones(1,length(t));
Otdr=ones(1,length(t));                           %operation cost [NOK/year]
Otdr(1,1)=It;
Otdr2=ones(4,length(t));                           %operation cost [NOK/year]
Otdr2(1,1)=Alternative1;
Otdr2(2,1)=Alternative2;
Otdr2(3,1)=Alternative3;
Otdr2(4,1)=Alternative4;
Otdr2(1,10)=18495;
Otdr2(2,10)=18495;
Otdr2(3,10)=18495*2;
Otdr2(4,10)=18495*2;
Mtdr=1;
Ft=Alternative4;                      %interest expenditures [NOK/year]
[P1,In1,Ba1]=compute_mortgage(Alternative1,R,25);
[P2,In2,Ba2]=compute_mortgage(Alternative2,R,25);
[P3,In3,Ba3]=compute_mortgage(Alternative3,R,25);
[P4,In4,Ba4]=compute_mortgage(Alternative4,R,25);
loan1=[In1;In2;In3;In4];
loan1=loan1';
t1 = datetime(2019,01,1);
t2 = datetime(2044,12,1);
T = t1:t2;
T = T';
q = ones(length(T),1);
T = timetable(T,q,q,q,q);
Tm = retime(T,'Monthly','max');
Tm.q(1:length(loan1),:)=loan1(:,1);
```

```
Tm.q_1(1:length(loan1),:)=loan1(:,2);
Tm.q_2(1:length(loan1),:)=loan1(:,3);
Tm.q_3(1:length(loan1),:)=loan1(:,4);
for k = 1:length(Tm.q)
if Tm.q(k) == 1
    Tm.q(k) = 0;
end
if Tm.q_1(k) == 1
    Tm.q_1(k) = 0;
end
if Tm.q_2(k) == 1
    Tm.q_2(k) = 0;
end
if Tm.q_3(k) == 1
    Tm.q_3(k) = 0;
end
end
Ty=retime(Tm,'Yearly','sum');
loan1=Ty.q;
loan1=loan1';

loan2=Ty.q_1;
loan2=loan2';

loan3=Ty.q_2;
loan3=loan3';

loan4=Ty.q_3;
loan4=loan4';
loanvalue1=sum(loan1);
loanvalue2=sum(loan2);
loanvalue3=sum(loan3);
loanvalue4=sum(loan4);
loan=[loan1;loan2;loan3;loan4];
loansum=[loanvalue1;loanvalue2;loanvalue3;loanvalue4];
r=[3.5 4 4.5 5 5.5 6]/100;                              %discount rate [%]
%r=3.5/100;
r1=3.5/100;
St1=3040;                               %yearly rated energy output for t [kWh]
St2=6040;
St3=9100;
```

```
St4=12200;
St=St4;
Stdif=[St1;St2;St3;St4];
capex=[];
Time=Ty.T;
Ic1=ones(1,length(t)).*[Alternative1];
inverter=ones(1,17)*(Alternative1+18459);
Ic1(10:26)=inverter;

Ic2=ones(1,length(t)).*[Alternative2];
inverter2=ones(1,17)*(Alternative2+18459);
Ic2(10:26)=inverter2;

Ic3=ones(1,length(t)).*[Alternative3];
inverter3=ones(1,17)*(Alternative3+18459*2);
Ic3(10:26)=inverter3;

Ic4=ones(1,length(t)).*[Alternative4];
inverter4=ones(1,17)*(Alternative4+18459*2);
Ic4(10:26)=inverter4;
prody=[ones(1,length(t)).*St1;ones(1,length(t)).*St2;ones(1,length(t)).*St3;ones(1,length(
Ic=[Ic1;Ic2;Ic3;Ic4];
%% for different discount rates

 for j = 1:length(r)
     for i = 1:length(t)
        if i == 10
            Otdr(i) = 18495*2;
        end

Aprod(j,i)=(St*(1-d).^t(i))./((1+r(j)).^t(i));

capex(j,i)=(Otdr(i)+Mtdr)./((1+r(j)).^t(i));

Acostworst(j,i)=(Otdr(i)+Mtdr + loanvalue4)./((1+r(j)).^t(i));

 Aprodsum=sum(Aprod,2);
 capexA=sum(capex,2);
 Acostworstsum=sum(Acostworst,2);
    end
 end
```

```
LCOE = (capexA)./Aprodsum;
LCOEw = (Acostworstsum)./Aprodsum;
figure;
plot(r*100,LCOE,'LineWidth',2)
hold on
plot(r*100,LCOEw,'LineWidth',2)
ylabel('NOK/kWh')
xlabel('Discount rate (%)')
legend('LCOE','LCOE W/loan')
set(gca,'FontSize',25)
set(gcf,'color','w');
%% for different alternatives with a fixed discount rate
 for p = 1:length(Stdif)
     for i = 1:length(t)

Aprod2(p,i)=(Stdif(p)*(1-d).^t(i))./((1+r1).^t(i));

capex2(p,i)=(Otdr2(p,i)+Mtdr)./((1+r1).^t(i));

Acostworst2(p,i)=(Otdr2(p,i)+Mtdr + loansum(p))./((1+r1).^t(i));

 Aprodsum2=sum(Aprod2,2);
 capexA2=sum(capex2,2);
 Acostworstsum2=sum(Acostworst2,2);
    end
 end

LCOE2 = (capexA2)./Aprodsum2;
LCOEw2 = (Acostworstsum2)./Aprodsum2;
figure;
plot(Pp,LCOE2,'LineWidth',2)
hold on
plot(Pp,LCOEw2,'LineWidth',2)
ylabel('NOK/kWh')
xlabel('Installed Capacity (kWp)')
xticks([0 3 6 9 12])
legend('LCOE','LCOE W/loan')
set(gca,'FontSize',25)
```

```
set(gcf,'color','w');
%% downpayment
for z = 1:4
    for l = 1:length(t)
    Cost_save(z,l)=elec_price.*prody(z,l).*(1-d).^t(l);        %amount of money saved per
    end
end
DP1=cumsum(Cost_save(1,:));
DP2=cumsum(Cost_save(2,:));
DP3=cumsum(Cost_save(3,:));
DP4=cumsum(Cost_save(4,:));
DP=[DP1;DP2;DP3;DP4];
for z = 1:4
    for l = 1:length(t)
        dp(z,l)=Ic(z,l)-DP(z,l);
    end
end
dp=dp';
Ty = addvars(Ty,dp(:,1),dp(:,2),dp(:,3),dp(:,4));
starty=find(Ty.T=='01-Jan-2019');
stopy=find(Ty.T=='01-Jan-2044');
figure;
time=linspace(1,25,26);
plot(time,Ty.Var5(starty:stopy),'LineWidth',2)
hold on
plot(time,Ty.Var6(starty:stopy),'LineWidth',2)
plot(time,Ty.Var7(starty:stopy),'LineWidth',2)
plot(time,Ty.Var8(starty:stopy),'LineWidth',2)
legend('3kWp','6kWp','9kWp','12kWp')
ylabel('NOK')
xlabel('year')
xlim([1 25])
set(gca,'FontSize',25)
grid;
set(gcf,'color','w');
```